SHARING

SELF-ORGANIZED HETEROGENEOUS ADVANCED RADIO NETWORKS GENERATION

Deliverable D4.2

Intra-system offloading: innovative concepts and performance evaluation

Date of delivery	21/01/2015
Contractual date of delivery	31/12/2014
Project number	C2012/1-8
Editor(s)	Edgar Ramos (ERICSSON)
Author(s)	Edgar Ramos (ERICSSON), Gregory Gougeon, Julien Stephan, Mathieu Brau, Yoann Corre, Yves Lostanlen (SIR), Ana Galindo-Serrano, Sofia Martínez López, Yasir Khan (FT), Javier Valiño (TTI), Mohamad Assaad (SUP)
Dissemination level	PU
Workpackage	4
Version	V1.0
Total number of pages	94

Abstract:

In order to address the rapidly increasing data traffic volumes, one efficient way to enhance the system performance is to densify the network, either by deploying new macro cells, or with the help of heterogeneous network deployments. However, together with the network densification, several new challenges appear, related to for example the inter-cell interference and the overall cost of deployment. This deliverable presents the SHARING innovations and concepts within the area of intra-system offloading. The presented innovations are related to SON-based load balancing and inter-cell interference management, load balancing with the help of large scale antenna systems or middleware deployment, mobility management between macro and low-power nodes, and backhaul offloading via proactive caching of data. As indicated by the results, the presented innovations are indeed able to enhance the system performance both in terms of coverage and capacity, which can be expected to contribute to lower CAPEX and OPEX for the operators.

Keywords:

Offloading, Balancing, Performance, Heterogeneous Networks, RRM, SON, WiFi, Backhaul, Energy-Efficiency, Spectrum, Management, Algorithm

Document Revision History

Version	Date	Author	Summary of main changes
0.1	22/09/2014	Edgar Ramos	Initial draft
0.2-0.12		Several authors	Partner contributions
0.13	17/11/2014	Edgar Ramos	First complete draft
0.14-0.15		Kimmo Hiltunen	Review phase/Second stable draft
1.0	05/01/2015	Kimmo Hiltunen	Final version

TABLE OF CONTENTS

EXECUTIVE SUMMARY

This deliverable provides the description and evaluation of innovation proposals and challenges by the SHARING partners related to work package 4, task 4.1 (Intra-system offloading) for SON and/or heterogeneous network deployments. In addition to the concept descriptions, this deliverable presents some evaluation results, where available.

The concepts presented within the area of SON-based load balancing and interference management are:

- **Load balancing by deploying power optimization in LTE macrocell networks**. A novel centralized recursive self-optimization methodology for LTE load balancing based on pilot power optimization is proposed. The concept uses a statistical surrogate model for the parameter-KPI relations and a pattern search algorithm for high dimensional optimization. The proposed approach is advantageous as the algorithm uses extremely small number of noisy observations to build a high dimensional surrogate and subsequently finds the optimum using few iterations, thus making the approach ideal for operators to implement at the OMC level.
- **Capacity optimization through active antenna systems in LTE macrocell networks.** A centralized self-optimization framework is proposed to be applied for AAS-based constrained capacity optimization in LTE-A. Statistical learning is used to model the RRM-KPI functional relationships and a pattern search algorithm is applied in an iterative manner to optimize the network capacity using different capacity-based objective functions. The optimization is shown to result in best-case network improvements up to 90.43%. Furthermore, the technique is demonstrated to be robust for complex, large parameter space network optimization problems, in terms of faster convergence using very few initial NP-KPI data points.
- **Antenna tilt optimization for interference management in LTE-A heterogeneous network deployments.** A surrogate-based self-optimization framework for improving QoS in heterogeneous LTE-A networks is presented. Optimization is carried out for two objective functions: cell-edge and cell-center optimization. For both the objective functions, AAS-based optimization performs well with possible performance gains results of up to 35% for cell-edge SINR and 45% for cell-center SINR.
- **Enhanced inter-cell interference coordination for interference management in LTE-A networks.** A centralized recursive self-optimization algorithm is presented for a heterogeneous LTE-A network deployment with RE + TDM eICIC. The algorithm is based on the use of a surrogate of the network model and a search and poll algorithm for optimization. The proposed approach is advantageous as the algorithm approaches to the global optimum in the first update thanks to the surrogate, and the network continues to operate at this near optimal parametric setting as the algorithm locally searches the global optimum. This makes the algorithm well suited for self-optimization on an operational network.
- **Mobility load balancing in LTE macrocell networks.** Results on the self-optimization of handover margin for mobility load balancing in LTE networks is presented. The impact of changes to handover margin on base station mean load and other QoS KPIs such as BCR and DCR is provided.

- **Cell virtualization based on large scale antenna system.** The concept of virtual small cells is presented, where large antenna arrays at macrocells are used to focus the energy towards a traffic hotspot. As with traditional heterogeneous networks, this creates areas with enhanced SINR and increases the resource reuse of the system (cell splitting gain). The results show that the introduction of virtual small cells can improve the mobile network throughput when compared with a situation where only macrocells are deployed. For a dense urban scenario with full buffer model, system-level simulations show that the average user throughput is increased by 50%. In addition, virtual small cells are shown to reduce the consumed power by 27% compared to the only-macrocell case, while a deployment with traditional picocells leads to a 7% higher power consumption compared to virtual small cells. However, the downside of virtual small cells compared to picocells is that the system performance becomes worse due to higher path losses between the virtual small cells and the users.
- **Intra-LTE offloading by middleware deployment.** Deploying the proposed IP-based middleware in charge of interchanging information between users and the network, makes it possible to trigger centralized decisions to allocate users in the best base station and, thus, balance the traffic handled by small cells and macrocells. Given the baseline considerations it is possible to assess high potential gains in terms of overall QoS of the network, obtaining theoretical gains of up to 25% in terms of QoS enhancement at user side. These results have been obtained through multiple simulations modelling a system where a 24-hour load period is generated and tested over all possible scenarios.

The concepts presented from the mobility management solutions are:

- **Combined cell performance within HSPA heterogeneous network deployment.** The deployment of combined cells is expected to improve the spatial reuse of the codes used for the transmissions. In order to do this, HSPA standardization changes are required. Also the combined cell deployments are expected to improve the receiving and transmitting diversity of the areas of coverage. This should be translated in improvements in throughput, especially for uplink transmissions. In this work, this claim is supported by the simulation results that also indicate an increase in the area load capacity. Additionally to the diversity gain, the users benefit from a lower probability of signalling failure due to handover procedures that otherwise would be required if the same area whould be covered by a heterogenous network deployment.
- **Uplink/Downlink split within a heterogeneous LTE network.** The simulations show, that using uplink/downlink separation results in gains in uplink transmissions. The gains are measured from the mean FTP rates of the users in scenarios both with and without uplink/downlink separation. The highest gains seem to result from a highly loaded system and relatively high CURE such as 16 – 20 dB. With downlink traffic, the simulations show that using uplink/downlink separation results in decreased performance. This is explained by downlink transmissions not benefitting from the increased capacity in uplink, since the uplink transmissions contain only small size TCP acknowledgements. On the contrary, the increased round trip time caused by the backhaul delay between the secondary and the master eNodeB negatively affects the TCP slow start. This can be seen from the protocol simulation results where small file sizes were used. The delay in the uplink signaling causes delay in the downlink transmissions and therefore decreased performance.

The concept presented within the area of backhaul management solutions is:

- **Backhaul offloading by proactive caching.** In this work a decentralized caching solution to maximize the backhaul offloading in small cell networks is proposed. This is done by exploiting the storage capabilities at the small cell base station in which contents are precached at strategic times to satisfy users' QoS requirements. The caching strategy is evaluated in a variety of scenarios as a function of storage constraints, wireless backhaul links, and content popularity.

Finally, on the evaluation of performance and stragegies of heterogenous network deployments, the following studies are presented:

- **Fundamental performance limits of heterogeneous networks**. The objective of this study is to investigate and analyze the performance of heterogeneous cellular networks as a means to quantify the improvement in terms of coverage and rate by using such topologies. The final results of this study are not yet available in this deliverable.
- **Asymptotic performance analysis and design of wireless networks under heavy traffic.** The study focuses in beamforming and power allocation in a wireless network under heavy traffic limit. The objective is to keep the queue outage probability under a certain threshold while the channel evolves according to an ergodic Markov chain. For that, the allocation is divided into two parts: i) equilibrium part allocated depending on the channel statistics, and ii) drift part which is a function of the backlogged queues of the users at each time. Under this model, it is shown that the scaled queue can be modeled as a reflected diffusion process. This allows to derive a closed form expression of the allocated power and beamforming and a closed form expression of the outage probability.
- **Performance of heterogeneous network deployments in a large-scale real environment.** The main objective of the study is to identify network deployment rules that would allow achieving optimal performance from multiple key indicators taking into account a realistic and well accepted forecast over a period of five years of wireless data traffic demand growth. A first study under ideal backhaul assumption evaluates three different small cell deployment topologies with different inter-site distances. Results show that the highest tested offloading configuration (small cell transmit power of 5 W and CRE of 12 dB) and largest tested ABS duty cycle (25%) leads to the best user QoS. The highest tested small cell densification (ISD equal to 50 m) generally gives the best coverage and highest peak throughputs; and it is the only one supporting the four-year traffic growth tested in the study. All these results tend to demonstrate the interest of deploying small cells to jointly absorb expected traffic increase and reduce downlink energy consumption. A second study focuses on the wireless backhaul design to relay the user data between the small cell layer with ISD equal to 200 m to the core network at Y5. A basic approach consisting of a manual attachement of small cells to hubs and median antenna orientations shows very poor performance, making the wireless backhaul introduce a bottleneck in the network. An automated approach is proposed instead where the selection of the hub candidates, the small cell attachments and the antenna orientations are all together optimized. It results in a much better performing wireless backhaul where 74% of the small cells

can be served with the required downlink throughput, and hubs, which are co-located with the macro eNodeBs, experience an average load of 45%.

1 INTRODUCTION

Traffic in the mobile networks is expected to grow very rapidly in the coming years [Cis14][Eri13]. This traffic growth will be caused both by the evolution of mobile terminals (an increasing penetration of smartphones, tablets and mobile computers) and the increased use of more traffic-heavy services, especially video. It is also expected that the wider introduction of various cloud-based services and machine-to-machine communication will accelerate the traffic growth even further.

In general, there are three possible ways to increase the capacity of a mobile network: increased spectrum, improved spectral efficiency and network densification. From the spectrum point of view, the capacity can be enhanced by deploying additional carriers, or by increasing the carrier bandwidth. The spectral efficiency can be improved both by improving the signal-to-interference-ratio for the link between the transmitter and the receiver and by introducing new techniques to enhance the utilization of the high signal-to-interference ratio conditions. These techniques include for example advanced multi-antenna techniques (for example MIMO and beamforming), higher order modulations and advanced interference management (for example interference cancellation, inter-cell interference coordination and coordinated multipoint transmission and reception). However, although the achievable capacity gains via additional spectrum, and improvements in spectral efficiency are considerable, the substantial growth that is predicted for the mobile broadband revolution will require also actions to densify the mobile networks, i.e., to increase the spatial reuse of the radio resources.

The traditional way to densify mobile networks has been to deploy new macrocells, either by adding new sectors to existing sites, or by deploying new macro sites. The benefit of a densified macro deployment is that the network performance can be improved with a fairly small amount of required new hardware, or new sites. However, as new macro sites are becoming increasingly difficult and often expensive to deploy, at least within urban environments, focus is put on the efforts to find more cost-efficient ways to densify the current networks.

An alternative to deploying new macro sites is to deploy low-power sites within traffic hotspots, i.e., the introduction of heterogeneous network deployments. In case of the heterogeneous network deployment, macro cells will provide wide area coverage, while the small low-power cells deployed within traffic hotspots will take care of the majority of the traffic volume. The downside of heterogeneous network deployments compared to the densified macro deployments is that a considerably larger number of new cells is required to be able to offer the same system performance. Even though the cost of a low-power site is usually lower than the cost of a macro site, the overall situation may turn out to be quite challenging from the total network cost point of view.

The total cost of the network deployment consists of a large number of different components, related to both the capital expenditure (CAPEX) and the operational expenditure (OPEX). Examples of the CAPEX-related components include the base station equipment, site equipment and network roll-out. The OPEX-related components include for example site rental, energy, and operation and maintenance. The total cost of the network deployment can be reduced for example by improving the cell capacity and coverage, by introducing various types of SON functions, and by introducing different kinds of energy saving mechanisms.

SHARING Work Package 4 looks into many of the topics listed above. Task 4.1 investigates ways to perform intra-RAT traffic offloading as efficiently as possible, including topics such as load balancing and interference management, mobility management, and backhaul offloading

This deliverable presents an initial view on new opportunities, challenges and innovative concept candidates for SON and heterogeneous network deployments. Chapters 2 to 4 present concepts from Task 4.1 of SHARING WP4. Furthermore, Chapter 5 discusses the performance and deployment strategies of heterogeneous network deployments within different scenarios.

There are several areas that can be targeted with the innovations related to traffic offloading. The first group would belong to optimization of mobility management parameters in order to adjust the cell sizes and the intended coverage areas. This is useful in particular for the heterogeneous network deployments, where the cells might have overlapping coverage areas aimed to provide enhanced coverage and capacity within specific areas. The network would then decide how to move traffic between the overlapping cells in order to maximize performance, capacity, resource utilization as well as energy efficiency, which are becoming more important nowadays. These factors are applicable also for the introduction of new and less traditional deployments and their interactions and coexistence with legacy systems, where traditional mobility procedures, channel estimation and link adaptation might not be applicable. The second group of innovations aims to handle the capacity and performance requirements by managing the available spectrum in order to reduce the interference between neighbouring transmission points and at the same time maximize the system performance. Finally, the third group of innovations targets the optimization of the use of the backhaul connection.

The heterogeneous nature of the deployments targeted by the innovations has inherent challenges that have to be addressed. The first of those challenges is the power imbalance between the overlapping cell layers. The difference in transmission power between the small cells and the macrocells has an impact on the perceived interference between the cells that affects the power control algorithms, the cell selection procedures and indirectly the control channel quality and channel estimation. Additionally, some of the regularly used algorithms to optimize the mobility parameters in macro environments are not possible to be scaled down for small cell environments, such as calculation of the UE speed and estimation of the UE location. Another challenge related to the power imbalance is the actual detection of the small cells, especially when the cell layers are operating on different carrier frequencies.

Yet another aspect of the heterogeneous network deployments is their flexibility, meaning that some deployments might be used "when required" to assist the network to provide the desired capacity or performance. Due to this flexibility the environment and the performance have to be monitored in different parts of the network in order to provide the decision bases to network controllers to activate or deactivate features and deployment options. The collection of the required KPIs, measurements and activity in the network is itself an additional challenge together with the actual organization and processing of the data that in many cases is distributed and might accumulate large volumes of information and the final execution of the configuration decision, especially challenged in distributed environments. It is important to keep in mind that the decisions to modify the network setup will have a direct impact on the balance between network performance, capacity and energy consumption.

2 SON-BASED LOAD BALANCING AND INTERFERENCE MANAGEMENT

The load balancing and interference management requires the interaction of several metrics and system input in order to provide the necessary level of adjustment of power, antenna orientations, carrier selection, intercell coordination, cell borders and cell coverage, transmission patterns, etc. The complexity required to maintain the measurement systems and the process of the correct response requires intelligent algorithms taking into account variations of inputs and the subsequent output feedback in the system. These self-organized systems can be both of distributed and centralized nature and they have an important impact on the system performance. The following sections will focus on describing the SHARING partners' innovations in this area.

2.1 Load balancing by deploying power optimization in LTE macrocell networks

Commentaire [KH1]: *FT*

2.1.1 Introduction

Optimization of wireless networks is a challenge for operators. In this work we propose a methodology for a self-optimizing Radio Access Network (RAN) which adapts the transmitted pilot power according to the current load of the base stations to carry out load balancing. The methodology uses a surrogate function to model the functional relationships between noisy Key Performance Indicators (KPIs) and Radio Resource Management (RRM) parameters, and subsequently performs optimization of the model using a pattern search algorithm in an iterative manner. The methodology is applied to solve a high dimension self-optimization problem for coverage based load balancing in an LTE-A network.

2.1.2 Solution description

The objective of this scenario is to carry out load balancing based on pilot power optimization. The self-optimization algorithm balances/equalizes the loads of the congested cells and the neighbouring cells thereby improving the Quality of Service (QoS) in the congested cell. The solution follows an iterative self-optimization framework as detailed in Section 2.1.1.2 of [D.4.1] consisting of:

- Model sub-block, which takes in the data point, appends it to the existing data set and updates the Kriging model.
- Optimization sub-block, which uses the real relationships (surrogates) and uses a sequential optimization technique called search and poll algorithm to obtain the optimum pilot power settings

The optimum pilot power settings are then fed into the simulator block to obtain the next data point in an iterative manner.

Optimization objective

Denoting the total transmit power of cell s as P_s (dBm) and the vector of total transmit powers by $\mathrm{x} = [\mathrm{P}_1\ \mathrm{P}_2\ \mathrm{P}_3 \ldots\ \mathrm{P}_\mathrm{M}]^\mathrm{T}$, respectively, the objective function of load balancing can be written as:

$$x^* = \arg\min_x f(x)$$
$$s.t.\ \ P_{min} \le P_s \le P_{max}\ \ \forall s \in G_1 \cup G_2 \quad (1)$$

where $\mathrm{f(x)} = \max[\mathrm{load_1(x)}, \dots, \mathrm{load_s(x)}, \dots \mathrm{load_M(x)}]$, $\mathrm{load_s(x)}$ is the load of cell $s\ \forall s \in G_1 \cup G_2$ and P_{min}, P_{max} are the minimum and the maximum allowable total transmit power values to prevent capacity and coverage issues such as coverage holes and pilot pollution.

2.1.3 Scenario

This performance evaluation is related to SHARING scenario 2.1.2 defined in Section 2.1.2 of [D.2.2]. The self-optimization is carried out for the second busiest hour of the day, i.e., optimum total transmit power settings are found for the traffic values of the second busiest hour as described in Section 2.1.1.3 of [D.4.1]. The optimized network settings are then applied to all the hours of the day.

The scenario is further detailed in Section 2.1.1.3 of [D.4.1]. Simulation parameters are provided as part of the description of scenario 2.1.2 [D.2.2].

2.1.4 Prediction Quality of the Kriging Model

First, the prediction quality of Kriging on the above described pilot power based Load Balancing (LB) problem is evaluated. For this, classical prediction quality metrics, such as the coefficient of determination $\mathrm{R^2} = 1 - \frac{\mathrm{SS_{res}}}{\mathrm{SS_{tot}}}$, the mean squared error $\mathrm{MSE} = \sqrt{\frac{\sum_{i=1}^{n}(\mathrm{y_i} - \mathrm{m_{yi}})^2}{n}}$ and coefficient of variation $\mathrm{CV} = \frac{\mathrm{MSE}}{\bar{y}} \times 100$ has been used as performance indicators, where $\mathrm{SS_{res}} = \sum_{i=1}^{n}(\mathrm{y_i} - \mathrm{m_{yi}})^2$ is the residual sum of squares, $\mathrm{SS_{tot}} = \sum_{i=1}^{n}(\mathrm{y_i} - \bar{y})^2$ is the total sum of squares and $\bar{y} = \frac{1}{n}\sum_{i=1}^{n}\mathrm{y_i}$ is the mean of the observations. $\mathrm{R^2}$ is an indicator of how well the regression model fits a set of data and CV indicates the dispersion of noise around the model.

A quota of 400 out of the possible 7^6 design points (pilot power value combinations) were set aside for model building and prediction. Out of these 400 points, 294 were used as a training set of Latin Hyper-Cube sampled (LHS) design points to build the surrogate model (a reference on LHS). The remaining 106 were used as a validation set to evaluate the prediction quality of the built model.

Table 1 lists the quality indicators for different covariance kernels $\phi(\mathrm{x}, \mathrm{x}')$. The Gaussian kernel has a superior performance having a very high value of R^2 and low CV as compared to exponential and linear kernels. These measures indicate a higher confidence on the initial model for carrying out subsequent iterative optimization.

Table 1. Kriging prediction quality

Covariance kernels $\phi(x, x')$	R^2	MSE	CV
Exponential	0.7763	0.1457	18.42
Gaussian	0.9235	0.0499	10.77
Linear	0.2070	0.5165	34.68

2.1.5 Results

An initial surrogate model is built using 294 LHS design points. It is assumed that the eNodeBs (eNB) are operating at an unoptimized default total transmit power setting of $x \equiv [43,43,43,43,43,43,43]$. Optimization is first carried out for the 2nd busiest hour. A total of 61 function evaluations involving 4 successful 'SEARCHES' and 16 successful 'POLLS' were needed to reach the optimum. The algorithm proposes an optimized total transmit power value combination of $x \equiv [42,42,42,43,43,40,40]$.

Figure 1 indicates the bar plots for base station loads. Figure 2 and Figure 3 indicate the bar plots for File Transfer Time (FTT) and Block Call Rates (BCRs) for all eNBs using the optimized and unoptimized solutions. It is clear that the optimization offloads traffic from eNBs in G_1 (eNB5 and eNB6) to G_2 (eNB1 to eNB4) as is indicated by the corresponding KPIs resulting in load reduction by 24%, FTT reduction by 64% and BCR reduction by 98% in the most loaded eNB (eNB5).

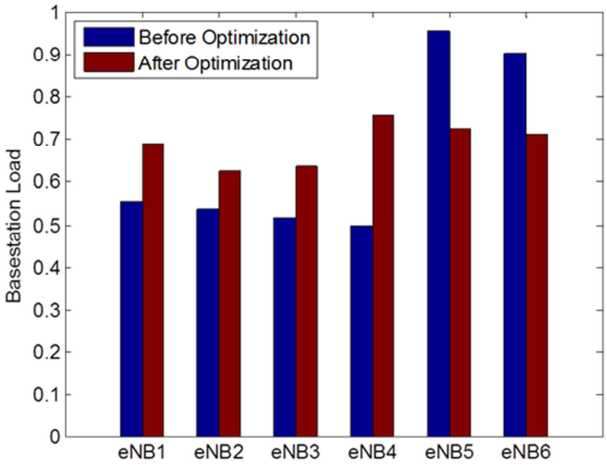

Figure 1. Base station load before and after hourly optimization for the 2nd busiest hour.

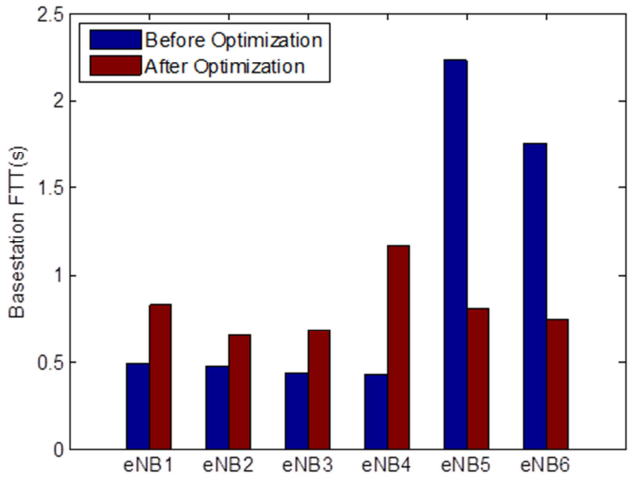

Figure 2. Base station file transfer time before and after hourly optimization for the 2nd busiest hour.

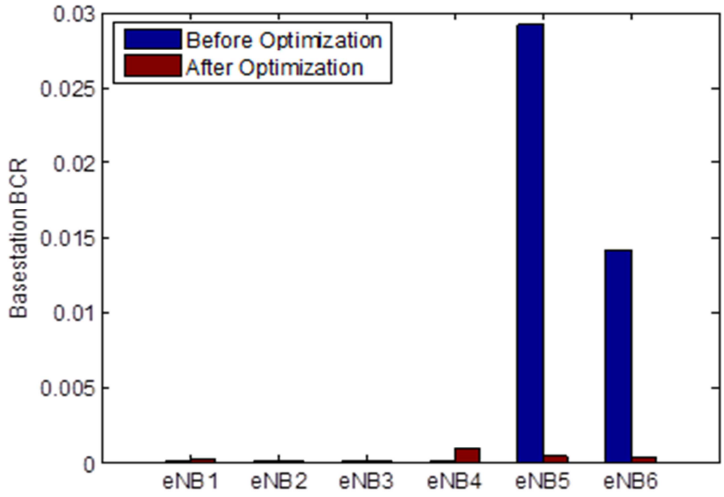

Figure 3. Base station block call rate before and after hourly optimization for the 2nd busiest hour.

Optimized solution obtained from hourly optimization of the 2nd busiest hour was then applied to the network optimization over the day to evaluate the performance impact of the SON algorithm to traffic variations over the entire day. Figure 4 and Figure 5 show the base station load and FTT for an eNB for each of the two zones. As can be seen, the proposed LB algorithm

is able to balance the load over the entire duration of the day by offloading the traffic to base stations with lower loads thereby significantly reducing the FTT.

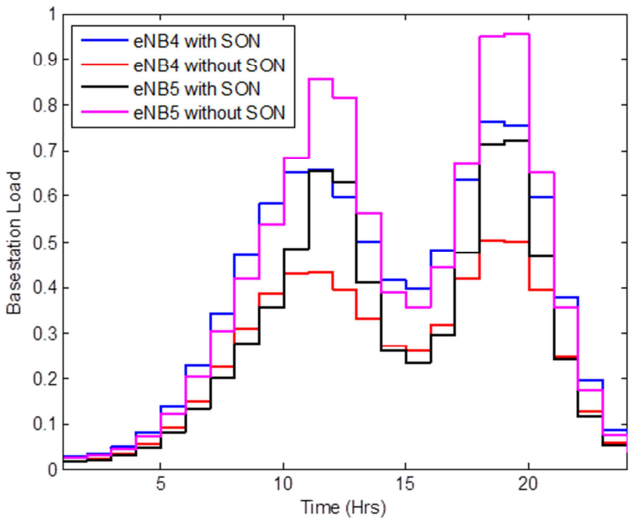

Figure 4. Base station load for daily optimization based on optimized solution from 2nd busiest hour.

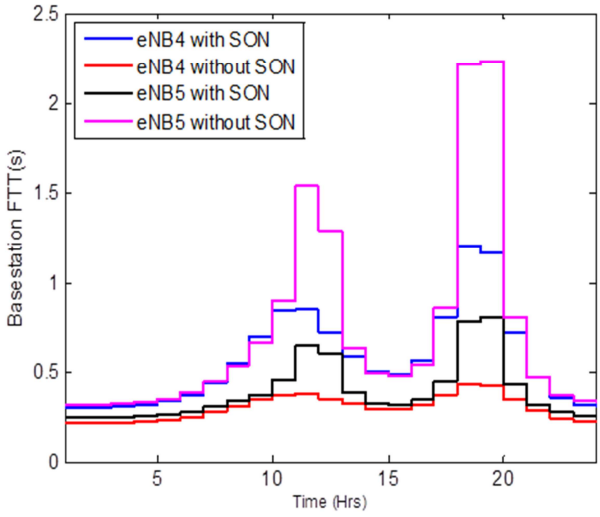

Figure 5. Base station file transfer time for daily optimization based on optimized solution from 2nd busiest hour.

2.1.6 Conclusions

In this work a novel centralized recursive self-optimization methodology for LTE load balancing based on pilot power optimization was presented. The proposed methodology uses a statistical surrogate model for the parameter-KPI relations and a pattern search algorithm for high dimensional optimization. This proposed approach is advantageous as the algorithm uses extremely small number of noisy observations to build a high dimensional surrogate and subsequently finds the optimum using few iterations, thus making the approach ideal for operators to implement at the Operations and Maintenance Center (OMC) level.

2.2 Capacity optimization through Active Antenna Systems in LTE macro cell networks

Commentaire [KH2]: *FT*

2.2.1 Introduction

Network QoS improvements in terms of capacity can be brought about by optimizing antenna tilts. Active Antenna Systems (AAS) have been gaining wide interest recently for their agile ability to electronically adjust the beam in the optimum direction based on operators' QoS interests. In this work we propose to use the surrogate management framework optimization of antenna tilts in LTE-A network and compare optimization results of several capacity-based objectives. Results using a flow level network simulator reveal the need to jointly optimize multi-capacity-objectives in a centralized manner apart from demonstrating the superiority of the iterative self-optimization methodology in terms of faster response, adaptivity and flexiblity.

This performance evaluation and the results are based on the use of a similar iterative self-optimization process as described in Section 2.1.1.1 of [D.4.1]. Here the process aims to optimize the eNodeB antenna tilt settings.

Optimization objective

A typical AAS-based optimization scenario includes adjustments to each of the antenna tilts in M. Here the self-optimization algorithm performs optimization by adjusting each of the antenna tilts and proposes an optimum vector of antenna tilt combination.

Let us denote the antenna tilt of cell s as θ_s (°) and the vector of total transmit powers by $\mathrm{x} = [\theta_1\ \theta_2\ \theta_3 \ldots\ \theta_{|\mathrm{T}|}]^{\mathrm{T}}, \forall \mathrm{s} \in \mathrm{T}$, $|\mathrm{T}|$ being the cardinality of T. The AAS-based self-optimization objective function can be given by:

$$x^* = \arg\min_x f(x)$$
$$s.t.\ \ c(x) \leq Th_c, \theta_{min} \leq \theta_s \leq \theta_{max}\ \ \forall s \in T \qquad (2)$$

where $f(x)$ and $c(x)$ are the objective function to be optimized and the constraint function, respectively, which are both functions of one or more predetermined KPIs defined over T. $\mathrm{c(x)} = [\mathrm{BCR}_1(\mathrm{x}), \mathrm{BCR}_2(\mathrm{x}), \ldots . \mathrm{BCR}_\mathrm{s}(\mathrm{x})], \forall \mathrm{s} \in \mathrm{T}$, where $\mathrm{BCR}_\mathrm{s}(\mathrm{x})$ is the BCR of cell $\mathrm{s}\ \forall \mathrm{s} \in \mathrm{T}$. Th_c is the constraint threshold on BCR. Finally, θ_{min} and θ_{max} are the minimum and maximum allowable antenna tilt values, respectively. The KPIs are as defined in Section 2.1.2.2 of [D.4.1].

2.2.2 Scenario and Results

Simulations are carried out for the downlink and no mobility is assumed. The simulation parameters are defined as part of scenario 2.1.3 [D.2.2] and the scenario with the associated network layout is discussed in Section 2.1.3.3 of [D.4.1].

A surrogate model built using 205 random design points (antenna tilt value combinations) is used for the proposed self-optimization method. For optimization it is assumed that the base stations are operating at an unoptimized default antenna tilt combination of $\{6°, 6°, 6°, 6°, 6°, 6°, 6°\}$. The value of Th_c is fixed at 0.05. Figures below show the bar plots for optimized (white) and unoptimized (black) cell KPIs for different objective function optimizations. The change in aggregated KPIs is shown in Table 2, while the simulation cost to reach the function optimum is shown in Table 3.

Table 2. Percentage change in KPIs for different optimization objectives.

$\mathbf{f(x)}$	**Change in aggregated KPIs (%)**		
	$f_{FTT}(x)$	$f_{5\%}(x)$	$f_{50\%}(x)$
$f_{FTT}(x)$	-3.1445	7.6588	12.8548
$f_{5\%}(x)$	3.1120	67.5727	89.1027
$f_{50\%}(x)$	4.3246	61.8520	90.4332

Table 3. Simulation cost to reach function optimum.

$\mathbf{f(x)}$	**function evaluations (network simulations)**
$f_{FTT}(x)$	39
$f_{5\%}(x)$	13
$f_{50\%}(x)$	26

Figure 6 shows the cell KPIs for $f_{50\%}(x)$ objective (cell-center) optimization. An improvement of 90.4% in $f_{50\%}(x)$ is seen as a result of this optimization (see the results in Table 2). Furthermore, as listed in Table 3, 26 function evaluations were needed to confirm the optimum.

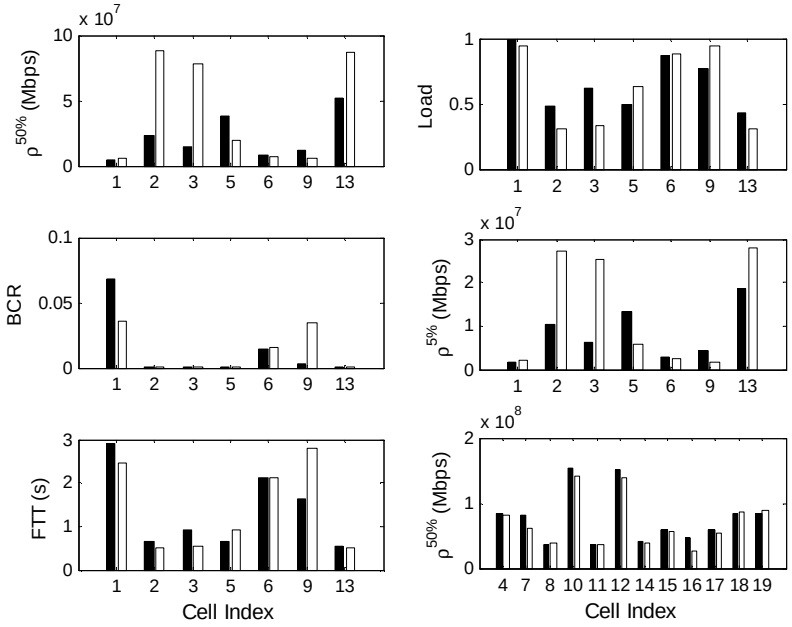

Figure 6. Cell KPIs for $f_{50\%}(x)$ objective (cell-center) optimization.

Figure 7 shows the cell KPIs for $f_{5\%}(x)$ objective (cell-edge) optimization. The gains in the $f_{5\%}(x)$ value are the highest with an improvement of 67.5% after using 13 function evaluations. The BCR in cell 1 is reduced to 5.4%, slightly higher than Th_c but which can be considered tolerable.

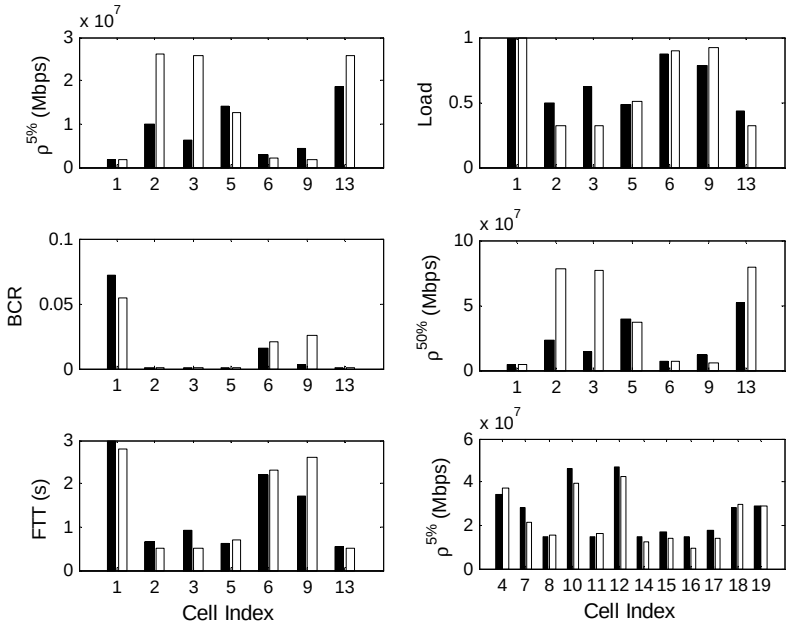

Figure 7. Cell KPIs for $f_{5\%}(x)$ objective (cell-edge) optimization.

Figure 8 shows the cell KPIs for $f_{FTT}(x)$ objective optimization. Optimization uses 39 network evaluations and results in a 3.14% improvement in the $f_{FTT}(x)$ value while some improvements are seen in the other KPIs as shown in Table 2. Observe that the optimization reduces the BCR of cell 1 to a value less than Th_c. BCR of cells 6 and 9 have increased marginally but are well within the tolerable threshold of Th_c.

In both $f_{5\%}(x)$ and $f_{50\%}(x)$ optimization scenarios, slight performance degradations are seen in the observation cells but they are marginal when compared to the improvements achieved in the target cells as is evident from Figure 6 and Figure 7. It is important to note that for the considered urban dense scenario with an inter-site distance of 500 m, optimization of cell-edge or cell median throughput leads to improvements of the same order of magnitude in both metrics as is clear from Table 2.

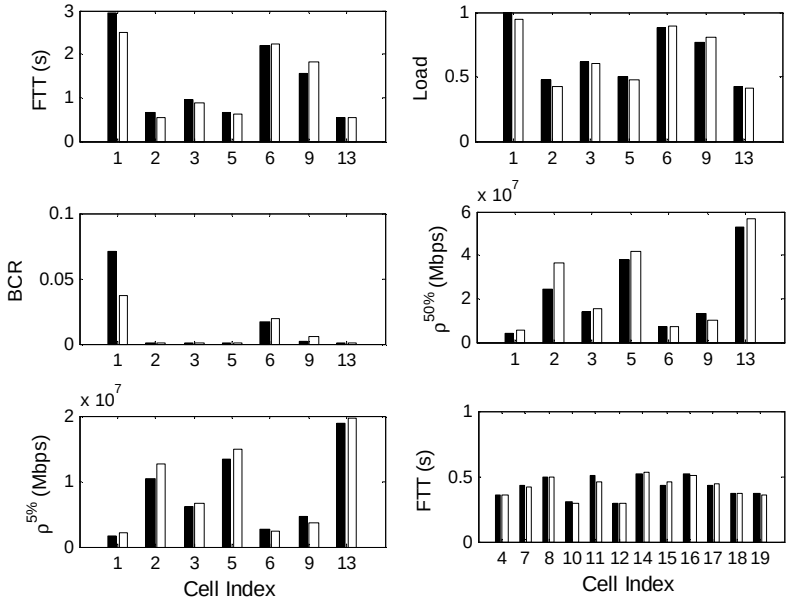

Figure 8. Cell KPIs for $f_{FTT}(x)$ objective optimization.

2.2.3 Conclusions

In this work, a centralized self-optimization framework was applied for AAS-based constrained capacity optimization in LTE-A. Statistical learning is used to model the RRM-KPI functional relationships and a pattern search algorithm was applied in an iterative manner to optimize the network capacity using different capacity-based objective functions. The optimization is shown to improve the network performance up to 90.43%. It is worth noting that a single objective function optimization is not sufficient to achieve the best improvements for all the other objective function values. Thus it is crucial for an operator to deploy an optimization methodology to achieve a balance amongst the competing objectives. This can be well achieved when the operator has a centralized perspective of the network. The results also provide a proof-of-concept for the generic utilization of the novel technique for a wide range of network objective optimizations. The technique demonstrates its robust performance for complex, large parameter space network optimization problems, in terms of faster convergence using very few initial Network Paraneter (NP)-KPI data points**.**

2.3 Antenna tilt optimization for interference management in LTE-A heterogeneous network deployments

Commentaire [KH3]: *FT*

2.3.1 Introduction

This performance evaluation and the obtained results are based on the use of a similar self-optimization process as described in Section 2.1.1.1 of [D.4.1]. In this section, the process aims to find the optimum antenna tilt settings.

Optimization objective

A typical AAS-based optimization scenario includes adjustments to each of the antenna tilts in M. Here the self-optimization algorithm performs optimization by adjusting each of the antenna tilts and proposes an optimum vector of antenna tilt combination.

Let us denote the antenna tilt of cell s as as θ_s (°) and the vector of total transmit powers by $\mathrm{x} = \left[\theta_1\ \theta_2\ \theta_3 \ldots\ \theta_{|\mathrm{M}|}\right]^{\mathrm{T}}, \forall \mathrm{s} \in \mathrm{M}$, $|\mathrm{M}|$ being the cardinality of M. The AAS-based self-optimization objective function can be given by:

$$x^* = \arg\min_x f(x) \quad s.t.\ \ c(x) \leq Th_c, \theta_{min} \leq \theta_s \leq \theta_{max}\ \ \forall s \in M \tag{3}$$

where $f(x)$ and $c(x)$ are the objective function to be optimized and the constraint function, respectively, which are both functions of one or more predetermined KPIs defined over M. $\mathrm{c(x)} = [\mathrm{BCR}_1(\mathrm{x}), \mathrm{BCR}_2(\mathrm{x}), \ldots . \mathrm{BCR}_\mathrm{s}(\mathrm{x})], \forall \mathrm{s} \in \mathrm{M}$, where $\mathrm{BCR_s(x)}$ is the BCR of cell $s\ \forall \mathrm{s} \in \mathrm{M}$. Th_c is the constraint threshold on BCR. Finally, θ_{min} and θ_{max} are the minimum and maximum allowable antenna tilt values.

2.3.2 Scenario

The parameters used in the system simulation are as listed as part of scenario 2.3.2 defined in [D.2.2]. The KPIs are as defined in Section 2.1.3.3 of [D.4.1].

2.3.3 Results

Cell-edge optimization:

Optimization of $\mathrm{f_{5\%}(x)}$ results in performance gains as shown in Figure 9. Optimization provides a clear improvement for all the cell-edge observational KPIs while degradation can be observed for the cell-center KPIs. AAS optimization leads to larger cell-edge QoS improvements for the overall network and also for the macrocells compared to the picocells.

Cell-center optimization:

Optimization of $\mathrm{f_{5\%}(x)}$ results in gains for all observational KPIs as shown in Figure 10. Again it is worth to note that the cell-center improvements for the overall network and for the macrocells are larger than the improvements for the picocells. Also, in contrast to cell-edge optimization performance, the cell-center optimization does not result in any degradation for the observational KPIs.

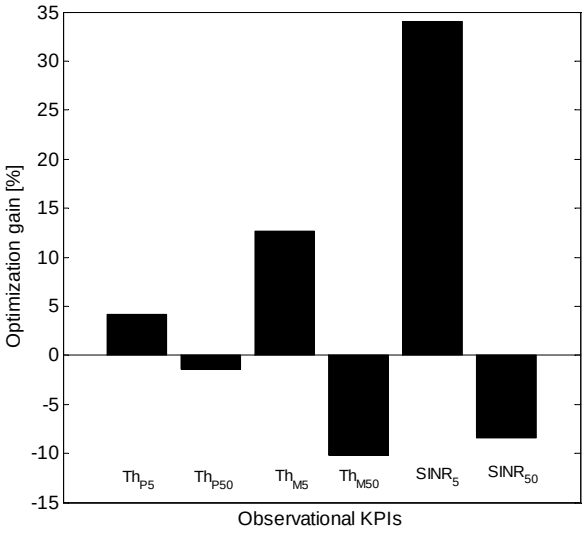

Figure 9. Cell-edge optimization performance.

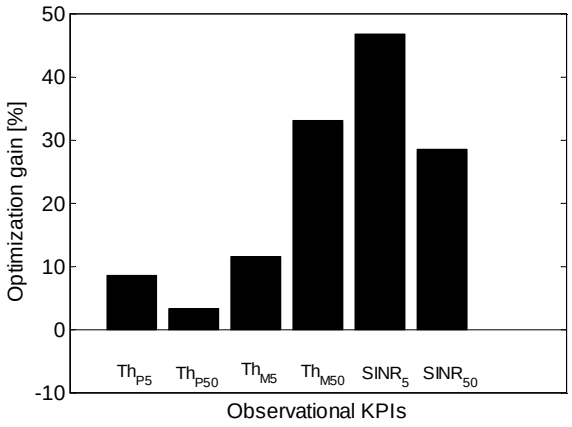

Figure 10. Cell-center optimization performance.

No macrocell blocking is observed for either the cell-edge or the cell-center optimization.

2.3.4 Conclusions

A surrogate based self-optimization framework for improving QoS in LTE-A heterogeneous networks was presented in this work and a capacity improving optimization scenario using enhanced Inter-Cell Interference Coordination (eICIC) was tested using this framework. Optimization was carried out for two objective functions: cell-edge and cell-center

optimization. For both objective functions, the proposed AAS-based optimization performs well with possible performance gains results of up to 35% for cell-edge Signal-to-Interference-plus-Noise Ratio (SINR) and 45% for cell-center SINR.

2.4 Enhanced Inter-Cell Interference Coordination for interference management in LTE-A networks

Commentaire [KH4]: *FT*

2.4.1 Introduction

This performance evaluation and the obtained results are based on the use of an iterative self-optimization process as described in Section 2.1.2. Here, the process is utilized to find the optimum values for both the Cell Range Extension (CRE) (cell selection offset, RE) and the eICIC muting ratio (mR).

Optimization objective

The aim within the eICIC based self-optimization context is to find the optimum $[\mathrm{mR\ RE}]^{\mathrm{T}}$ value by optimizing a pre-determined objective function subject to certain constraints. For the considered TDM eICIC + CRE problem, we define a Joint Performance Metric (JPM) as the weighted sum of the 5%-ile and the 50%-ile of UE SINR:

$$JPM(mR, RE) = (1-\lambda)SINR_{50\%}(mR, RE) + \lambda SINR_{5\%}(mR, RE) \quad (4)$$

where $\lambda\ (0 \le \lambda \le 1)$ is the fairness parameter. $\lambda = 0.5$ can be assumed to have a compromise between cell-center and cell-edge users. The constrained optimization problem is to maximize the above JPM with an upper limit on network BCR. For this, we use the following minimization formulation:

$$\min_{RE,mR}[f(mR, RE)] \quad (5)$$

where $\mathrm{f(mR, RE)} = (1 - \mathrm{JPM_{norm}}) + \mathrm{g(mR, RE)}$, $\mathrm{JPM_{norm}}$ is the normalized JPM:

$$JPM_{norm} = \frac{JPM - \min_{RE,mR}(JPM)}{\max_{RE,mR}(JPM) - \min_{RE,mR}(JPM)} \quad (6)$$

and $\mathrm{g = g(mR, RE) = max_{RE,mR}(0, BCR - BCR_{limit})}$ is the constraint limit on network BCR which is added as a penalty function ($\mathrm{BCR_{limit}}$).

2.4.2 Scenario

The network layout, simulator and scenario are discussed in Section 2.1.4.3 of [D.4.1] and Section 2.3.1 of [D.2.2]. The applied simulation parameters are listed in scenario 2.3.1 [D.2.2].

2.4.3 Results

Figure 11 shows the surface plots of the 5%-ile UE SINR, network BCR and $\mathrm{JPM_{norm}}$ generated for all possible combinations of RE and mR values on the mesh (the mesh size Δ is fixed to $mR = 0.05$, $RE = 1$ dB). The surface plot of the 50%-ile UE SINR is similar to that of the 5%-ile UE SINR and is not shown here. The plot indicates that the cell-edge and mean user quality is the highest when all sub-frames at macro layer are muted and pico layer is operating at medium RE values. However, muting all macro sub-frames raises the BCR of the network as shown in Figure 11.

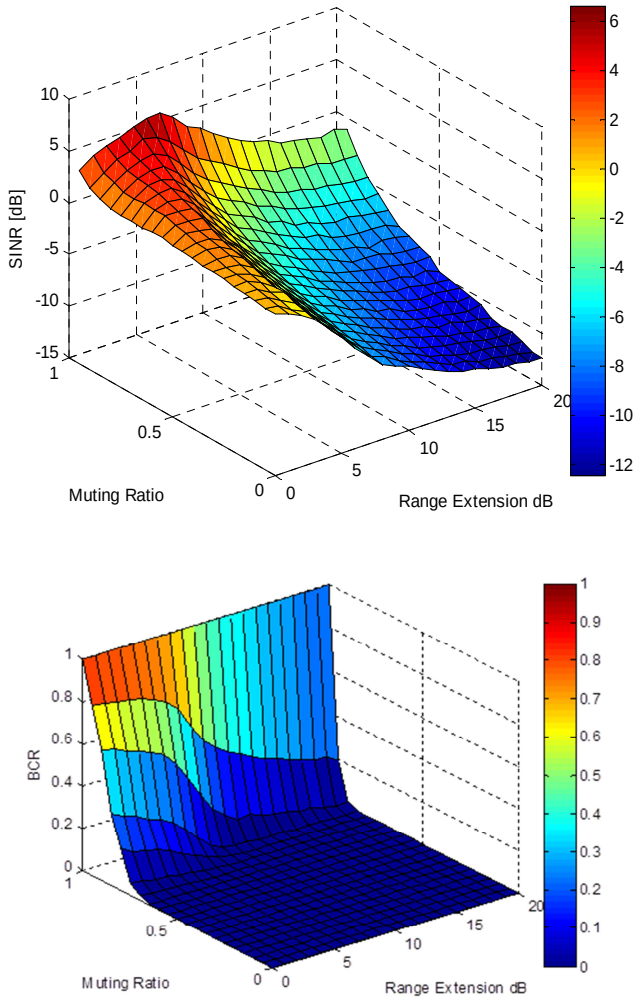

Figure 11. Surface plot of 5%-ile UE SINR and network block call rate.

Figure 12 shows the contour plot of the cost function $([(1 - \mathrm{JPM_{norm}}) + \mathrm{g(mR, RE)}])$ or $\mathrm{f(mR, RE)}$ using 10 initial sampling points defined by LHS and 5 function evaluations carried out by the

search and poll algorithm to reach the global optimum. The search and poll algorithm performed 2 successful 'SEARCH' steps (with a function evaluation and a model update at each) marked by white squares. The third 'SEARCH' was unsuccessful which triggered the 'POLL' step with $[\mathrm{mR} = 0.8, \mathrm{RE} = 5]$ as the poll point. Polling was carried out around this poll point and the solution converged to the global optimum $[\mathrm{mR} = 0.75, \mathrm{RE} = 5]$ (which is also marked by a white square) after 3 function evaluations at the immediate neighbours of the poll point.

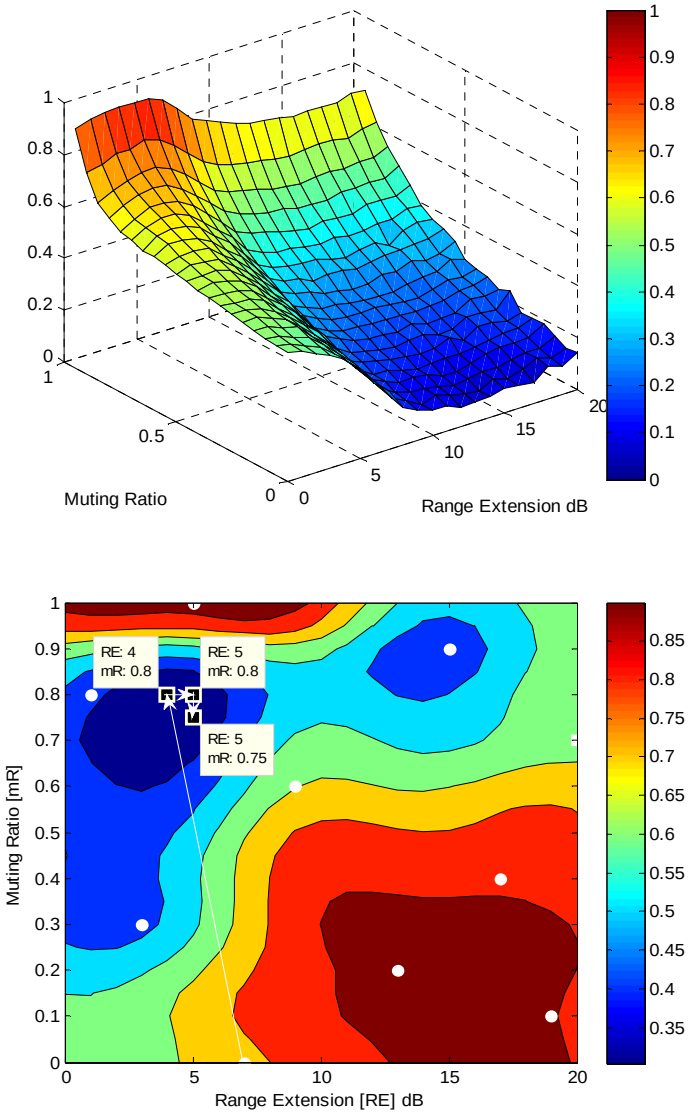

Figure 12. Surface plot normalized JPM and contour plot of cost function prediction with initial sampling plan and optimization update.

Table 4 provides a comparison of network performances for different deployments: macro-only, heterogeneous network deployment (HetNet) without CRE + TDM eICIC, and heterogeneous network deployment with CRE + TDM eICIC operating at the global optimum found by the proposed method. It can be clearly seen that the cell-edge and mean user quality (in terms of SINR and Average Bit Rate, ABR) have improved across the three cases and that the best values are obtained in the optimized scenario. However, this is at the cost of a slight (but tolerable) increase in BCR due to the calls being blocked as a consequence of muting sub-frames at the macro layer. Note that the optimized HetNet setting improves the performance despite a decrease in the available network capacity (in terms of the available Physical Resource Blocks (PRB) that can be assigned to all the users throughout the simulation) with respect to the heterogeneous network without CRE+eICIC.

Table 4. Comparison between network performances with and without pico deployments.

KPIs	Macro	HetNet without CRE+eICIC	HetNet with CRE+eICIC
$\mathrm{SINR}_{5\%\mathrm{ile}}$ [dB]	-0.84	0.62	3.32
$\mathrm{SINR}_{50\%\mathrm{ile}}$ [dB]	4.54	7.07	9.85
$\mathrm{ABR}_{5\%\mathrm{ile}}$ [Mbps]	4.02	11.08	15.18
$\mathrm{ABR}_{50\%\mathrm{ile}}$ [Mbps]	20.57	27.32	35.09
BCR [%]	0	0	2.1
Available network Capacity [PRBs]	45x104	90x104	78.75x104

2.4.4 Conclusions

We presented in this work a centralized recursive self-optimization algorithm for a heterogeneous LTE-A network deployment with RE + TDM eICIC, which uses a surrogate of the network model and a search and poll algorithm for optimization. The proposed approach is advantageous as the algorithm approaches to the global optimum in the first update thanks to the surrogate, and the network continues to operate at this near optimal parametric setting as the algorithm locally searches the global optimum. This makes the algorithm well suited for self-optimization on an operational network.

2.5 Mobility Load Balancing in LTE macrocell networks

Commentaire [KH5]: *FT*

2.5.1 Introduction

This performance evaluation and the obtained results are based on the use of a similar iterative self-optimization process as described in Section 2.1.2. Here, the aim of the process is to find an optimum value for the Handover Margin (HM).

Optimization objective

For the scenario 2.1.1 considered in [D.2.2], let us assume a uniform setting of the HM parameter, i.e., only one $HM_{s,t}$ value, $\forall s \in G_1, t \in G_2 \cap \aleph_s$ (shown by red arrows in the figure). Let us denote this value of $HM_{s,t}$ by x. Then, the objective function of the Mobility Load Balancing (MLB) can be written as:

$$\begin{aligned} x^* &= \arg\min_x f(x) \\ s.t.\ \ BCR^t(x) &\le Th_{BCR},\ \forall t \in G_2 \cap \aleph_s \\ DCR^t(x) &\le Th_{DCR},\ \forall t \in G_2 \cap \aleph_s \end{aligned} \tag{7}$$

where $f(x) = \sum_{\forall s \in G_1, t \in G_2 \cap \aleph_s} [load_s(x) - load_t(x)]^2$, $load_s(x)$ and $load_t(x)$ are the cell loads, $BCR^t(x)$ and $DCR^t(x)$ are the BCR and Drop Call Rate (DCR) of cell t respectively. Th_{BCR} and Th_{DCR} are the upper limit thresholds on the BCR and DCR respectively $\forall s \in G_1, t \in G_2 \cap \aleph_s$.

2.5.2 Scenario and results

The performance evaluation presented in this section is based on scenario 2.1.1 described in [D.2.2]. The network layout and simulation parameters is as discussed in section 2.1.5.3 of [D.4.1]. Most of the results have already been provided in Section 2.1.5 of [D.4.1] and some supplementary results are provided in this section.

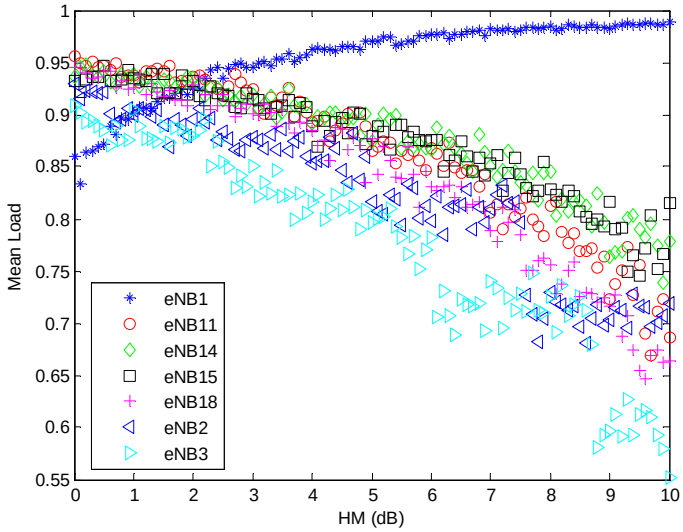

Figure 13. Data points for mean base station load as a function of the handover margin.

Figure 13 provides a variation of mean base station load as a function of the handover margin. It can be seen that with the increase of the handover margin, the load of eNB1 is increasing while the load of eNB11, eNB14, eNB15, eNB18, eNB2 and eNB3 is reducing due to more UEs getting handed over to eNB1 and the postponing of the UE handover from eNB1

towards the neighbouring cells. From the figure it is clear that the load balancing can be achieved at $HM_{s,t} = 2dB$.

Figure 14 and Figure 15 provide a variation of other cell KPIs such as the BCR and DCR as a function of the handover margin. It is clear that the QoS of eNB1 increases while the QoS of all the others in the optimization zone degrades. However a balanced QoS between the base stations is achieved at a value of $HM_{s,t} = 6dB$.

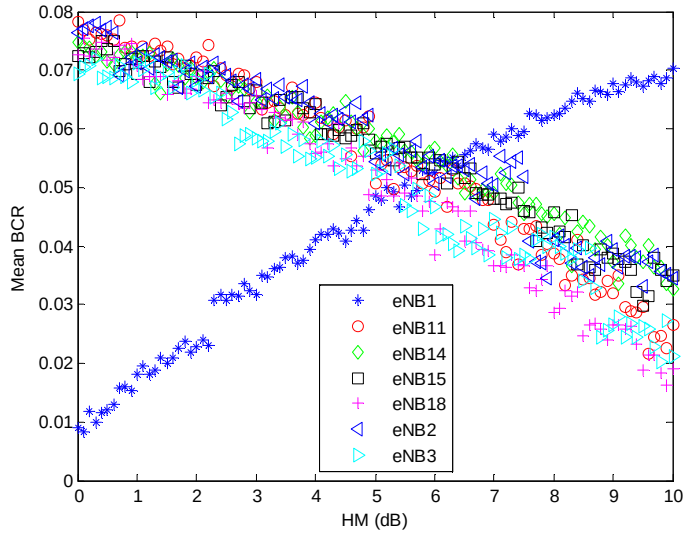

Figure 14. Data points for mean base station BCR as a function of handover margin.

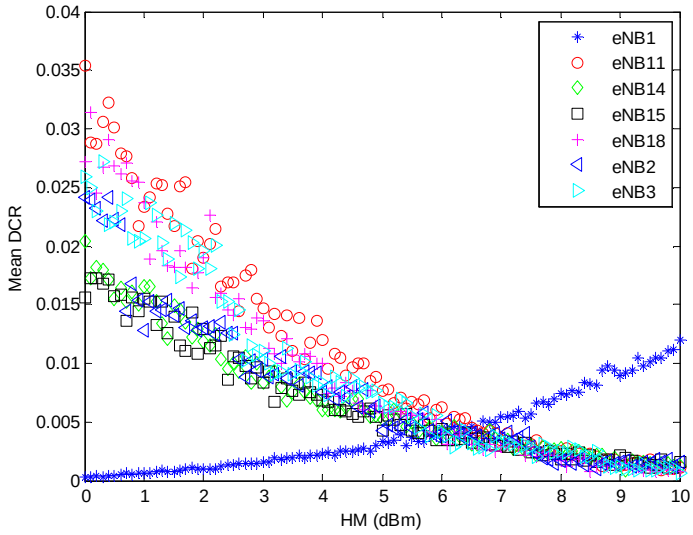

Figure 15. Data points for mean base station DCR as a function of handover margin.

Looking at these plots, it is clear that while a load balancing is achieved at $HM_{s,t} = 2dB$, a better QoS is achieved at higher values of $HM_{s,t}$ thereby encouraging the use of constrained self-optimization mechanism as already demonstrated in [D.4.1].

2.5.3 Conclusions

Results for the self-optimization of handover margin for mobility load balancing in LTE networks was presented in this work in addition to the constrained self-optimization results for load balancing already discussed in Section 2.1.5 of [D.4.1]. The impact of changes to handover margin on base station mean load and other QoS KPIs such as BCR and DCR is provided.

2.6 Cell virtualization based on Large Scale Antenna System

Commentaire [KH6]: *FT*

2.6.1 Introduction

Small cells can provide high Spectral Efficiency (SE) to handle high dense traffic areas and cope with the explosively growing mobile traffic [GATI14]. Typically, the deployment of small cells implies a non-negligible cost in terms of new equipment deployment, site acquisition or leasing, maintenance and increment of the global network energy consumption [MAR10].

Nowadays, research within the field of active antennas is presenting important advances, opening new Energy Efficient (EE) alternatives in the mid-term [HOY11]. One possible scenario is to deploy Large Scale Antenna Systems (LSAS) at the macrocells. The use of this new antenna system would allow creating highly directive beams which are considered as Virtual Small Cells (VSCs). These VSCs can be used to replace the typical macro-picocell deployment consequently reducing the OPEX and CAPEX expenses. Another important characteristic of VSCs is that they could be reconfigurable during the time and thus adapt to the changing traffic conditions. This flexibility is an important advantage compared to the typical macro-picocell deployment.

In Figure 16, we present the solution introduced in our work. Figure 16(a) shows a typical heterogeneous network deployment where picocells cover the existing hotspots, represented by the shaded areas. Figure 16 (b) presents the proposed solution where VSCs replace the typical picocells to cover the existing hotspots. VSCs are therefore managed at the macrocell level, giving place to a completely centralized system free of coordination and backhaul latency constraints. VSCs can work using the same carrier than the macrocell (co-channel operation) allowing an efficient reuse of spectrum, bringing a high SE and considerable aggregated capacity gains.

The general methodology and the solution to shape the VSC beam, particularly the number of antenna elements required, have already been presented in Section 2.2.1 of [D.4.1].

Based on simulations, the performance of three cellular system configurations for a dense urban and a rural scenario are compared, 1) Only-macrocells, 2) macrocell with VSCs covering dense areas and 3) heterogeneous network with picocells covering dense areas.

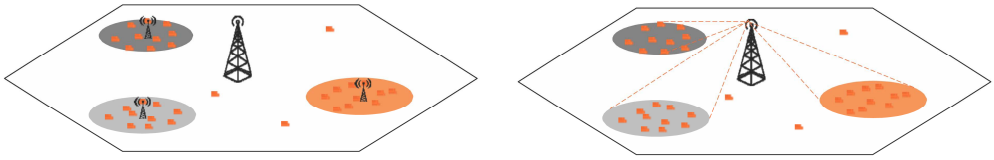

(a) Macrocell-picocells system layout. (b) Macrocell-VSCs system layout.

Figure 16. Considered system layout.

Furthermore, a power consumption analysis of the aforementioned network configurations is presented. The Information and Communication Technology (ICT) industry represents between 2% and 10% of the world power consumption [PLAN07] [CHIA08]. Since the ICTs will become more widely available and used these percentages are expected to grow in the next years [VER08]. In a mobile network, the most energy consuming equipment is the base station, accounting for 60% to 80% of the whole mobile network energy consumption. The use of dense array antenna systems could bring interesting energy savings since they allow the energy to be focalized where and when it is needed. Also, the introduction of the new equipments, which use more efficient electronics make an important difference in the network consumed power.

2.6.2 Simulation tools

In this section we present the two simulation tools used to evaluate the system performance.

System level simulator

In order to assess the network performance provided by VSC, we carried out system-level simulations with a 3GPP LTE (Release 8) simulator. For simulations we assume a full buffer traffic model. Furthermore, the number of users in the cell is constant, equal to 20, and the buffers of the users data flows have always unlimited amount of data to transmit.

Power consumption model

The power model used in this paper has been developed in the framework of the Green-Touch project [GT14]. Since the exponential network growth is not followed by equipment efficiency, the GreenTouch members are working together on different areas to design the technologies that can achieve sustainable networks in the decades to come. In 2013 Green Touch published the Green Meter Research Study [GT13] declaring the possibility of a reduction of the net energy consumption in communication networks up to 90% by 2020. The study does not just quantify the energy benefits of a single technology but rather focuses on the end-to-end network perspective and includes a full range of technologies.

This power model was choosen because of its flexibility and comprehensiveness, i.e., the power consumption estimation includes the hardware characteristics of the BS including cooling, control system, backhauling, among other components. Furthermore, it is straightforward to estimate the consumption of different BS configurations.

2.6.3 Results

In our study we consider two typical scenarios: a dense urban and a rural one, with three tiers. The carrier frequency is assumed to be on 2000 MHz and 800 MHz band for dense urban and rural environments, respectively, and with 10 MHz bandwidth. In both scenarios, the transmitted power is 46 dBm per macrocell sector. We deploy a VSC per macrocell and the total transmitted power is equally splitted between the coverage beam (macrocell) and the VSC beam (43 dBm each).

For each scenario, we compare the following four deployment options:

1. Only-macrocell: This is the baseline case, with no small cells. It is expected to be the lower bound in terms of performance.
2. Macrocell-VSC ideal: VSC beams point to the center of the hotspots. In this scenario there is no limit in the number of antenna elements that can be used to form the beam.
3. Macrocell-VSC real: This scenario is similar to the ideal one but we introduce a realistic constraint on the maximum number on antenna elements that can be used to form the beam. The limit is set at N_{elem}= 10 in both planes. Compared to the ideal option, this constraint may lead to wider beamwidth and reduced directivity of the VSC beam, depending on the VSC location.
4. Macrocell-picocell: This corresponds to the typical deployment of heterogeneous networks, where picocells are deployed at the center of the hotspot. Picocells are configured with a transmission power of 30 dBm for the dense urban case and 37 dBm for the rural one. This scenario is expected to be the upper bound in terms of capacity due to the small distance between transmitters and receivers. However, it is also the most costly deployment option in terms of CAPEX and OPEX, including energy consumption.

2.6.3.1 Network performance results

In this section we present system level simulation results in terms of percentage of UE attachment, SINR, throughput and power consumption.

1) **UE attachment**: Table 5 compares the percentages of UEs attached to each type of cell for each network configuration in both dense urban and rural scenarios. For the macrocell-VSC case, for both ideal and real cases in the dense urban and rural scenarios, the percentage of UEs connected to the VSC is higher than p_{hs} (2/3). This means that when the transmitted power is proportionally splitted between the macrocell and VSC, the VSC covers not only the UEs within the hotspots but also some that are not in this dense traffic area. Transmit power split between coverage beam and VSC beam is a new degree of freedom to optimize heterogeneous networks based on VSC. In other words, VSCs provide the possibility of changing the power transmitted to cover a hotspot, to adapt the size of the VSC to the traffic conditions. Finally, for the macrocell-picocell scenario, it can be noticed that the percentage of UEs connected to the picocells is less than 2/3. This is because hotspots are randomly located and therefore some of them are close to the macrocell, resulting in a shrinked picocell coverage area.

Table 5. UE attachement percentage in dense urban and rural scenarios.

Scenarios	Macrocell-VSC ideal		Macrocell-VSC real		Macrocell-picocell	
	Macrocell (%)	VSC (%)	Macrocell (%)	VSC (%)	Macrocell (%)	Picocell (%)
Dense urban	22	78	20	80	46	54
Rural	12	88	17	83	53	47

2) **SINR and user throughput**: The average SINR of the macrocell-VSC ideal case is 0.9 dB higher than the only-macrocell one but when the limitation in the maximum number of antennas is introduced, i.e., macrocell-VSC real case, the average SINR decreases with 2.5 dB compared to the only-macrocell case. This detriment in the SINR is due to the interference between the VSC and the macrocell.

Despite the SINR degradation for the macrocell-VSC real case, the average user throughput is always enhanced when introducing VSCs compared to only-macrocell case, for both the ideal and the real cases. This is due to the reuse of the resources at the macrocell and VSCs. The gain over the only-macrocells case introduced by the ideal case is of 0.94 Mbps (+103%), for the real case the gain regarding the only-macrocell case is of 0.5 Mbps (+55%). As expected, the macrocell-picocell case outperforms the macrocell-VSC cases. The gain over the only-macrocell case is of 1.4 Mbps (+153%). These results are summarized in Table 6.

Table 6. Average SINR and throughput for dense urban scenario.

Scenarios	Only-macrocell	Macrocell-VSC ideal	Macrocell-VSC real	Macrocell-picocell
Av. SINR (dB)	7.8	8.7	5.3	9.9
Av. Throughput (Mbps)	0.9	1.9	1.4	2.3

Figure 17 presents the Cumulative Distribution Function (CDF) of the SINR for the rural scenario. If we consider SINR less than −6 dB as out of coverage, the only-macrocell case yields 47% of UEs out of coverage. When introducing picocells, the percentage of out-of-coverage UEs drops to 28%. When introducing VSC, the percentage of out-of-coverage UEs drops to 11% and 35% for the ideal and real cases, respectively. Contrarily to the dense urban scenario, which is interference-limited, the rural scenario is a noise-limited one. Therefore, the introduction of VSCs does not imply an increase in the interference, except for VSCs that are very close to the macrocell site. Augmenting the directivity of the VSC beams can lead to larger coverage than the coverage of the conventional picocells. Therefore, with a large number of antenna elements (e.g., macrocell-VSC ideal), the introduction of VSCs outperforms the conventional small cell deployment in terms of coverage.

In conclusion, the introduction of VSC can be used as a throughput booster for the dense urban scenario and as a coverage solution for rural scenarios. Conventional picocells outperform VSC in terms of user throughput in dense urban scenarios if we consider limited number of antennas (limited directivity for the VSC beam), but this comes at the price of increased cost and reduced flexibility. Also note that these results do not take into account the changes in the traffic location that occur along the day. Such simplification artificially

benefits the performance results of traditional heterogeneous networks versus VSCs, which can actually adapt their location to the moving traffic.

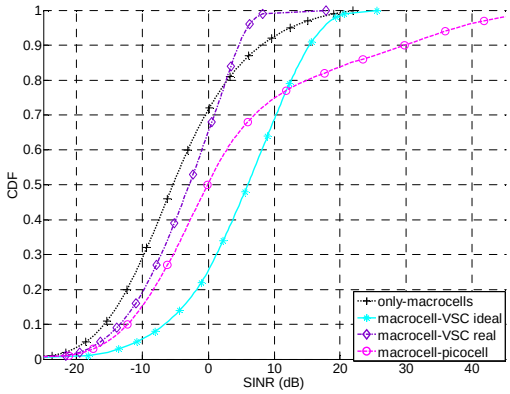

Figure 17. SINR CDF at rural scenario for the four studied network deployments.

2.6.3.2 Power consumption simulation results

The power model tool does not consider Frequency Division Duplex (FDD) when using LSAS, since it has been developed following the MU-MIMO concept [MAR10]. Since our system does not require Channel State Information (CSI) feedback for every antenna element, we do not take into account the energy consumed by the training phase. Therefore, the given results are an accurate approximation of the consumed power by the system.

Here, the results in terms of consumed power and EE are presented. EE is computed as the ratio of the average cell throughput Th_i in (Mbps) given by the system-level simulation tool over the average consumed power per cellP_i in (W) given by the power model simulator [GDOC14].

$$e = \frac{\sum_{i=1}^{N_{cell}} Th_i}{\sum_{i=1}^{N_{cell}} P_i} \frac{[Mbps]}{[W]} \quad (8)$$

Particularly, for the macrocell-picocell scenario, we sum up the macrocell and picocell throughput as well as their consumed power in order to estimate their efficiency. Figure 18 shows the average power consumption of a sector for the dense urban and rural scenarios. Since we are considering Remote Radio Head (RRH) macrocells, i.e., the Radio Frequncy (RF) unit is directly attached to the antenna, so there are no feeder losses (3 dBm), the power at Power Amplifier (PA) could be halved with respect to a typical macrocell. The introduction of the VSCs allow a saving of about 27% and 43% in the dense urban and in the rural scenarios with respect to the only-macrocell and of 36% and 73% with respect to the macrocell-picocell case.

Figure 19 represents the EE, computed as described in equation (8). The macrocell-picocell scenario has a very high efficiency due to the high throughput that the system can provide. VSC system value is 20% lower than macrocell-picocell but it doubles the only-macrocell case

in dense urban environment. For the rural scenario, the efficiency of VSCs is 44% lower than macrocell-picocell case but more than 2.5 times higher than the only-macrocell one.

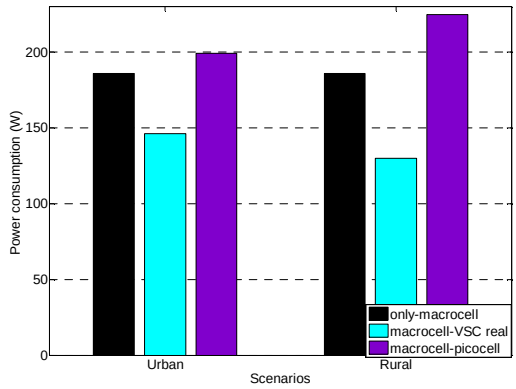

Figure 18. Consumed power per sector for dense urban and rural scenarios.

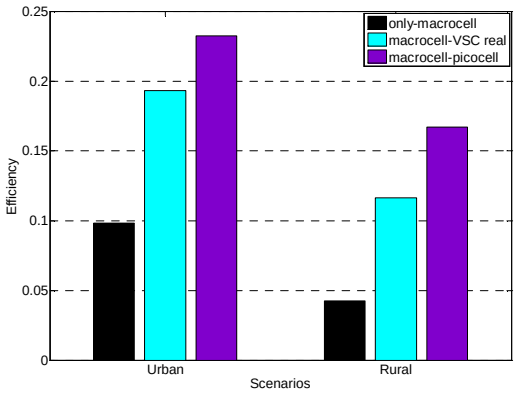

Figure 19. System EE for dense urban and rural scenarios.

While the deployment with VSCs has the lowest power consumption, the macrocell-picocell deployment seems to be the most efficient. This is because the presented results correspond to the full buffer traffic model. Deploying physical small-cell close to the user, with this traffic profile, boosts the average throughput of the system which will not be the case in real traffic conditions. Furthermore, if we consider the embodied energy of a new site, maintenance, the additional backhauling needed, it is clear that the total EE will drop drastically for the heterogeneous network deployment.

As a final remark, it has to be taken into account that VSCs allow to reduce the total radiated power per cell compared to traditional heterogeneous networks since for the VSC case it is equal to 46 dBm meanwhile for the heterogeneous network the total radiated power per cell is 46 dBm for the macrocell plus 30 dBm for the picocell.

2.6.4 Conclusions

This work presents the concept of VSCs, where large antenna arrays at macrocells are used to focus the energy towards a hotspot. As with traditional heterogeneous networks, this creates areas with enhanced SINR and increases the resource reuse of the system (cell splitting gain).

As presented in the system-level simulation results, the introduction of VSCs can improve the mobile network throughput when compared with a situation where only macrocells are deployed. For a dense urban scenario with full buffer traffic model, system-level simulations show that the average user throughput is increased by 50%. In addition, using GreenTouch power model for large scale antenna systems, VSCs save 27% of the consumed power regarding the only-macrocell case whereas picocells introduce a 7% extra power consumption compared to the macrocell-VSC deployment. When comparing VSCs with the heterogeneous network deployment, we see that the system performance suffers some detriments due to the higher path losses between the VSCs and the users. However, the fact of not having to deploy new equipment, saving also in backhauling, leasing and maintenance can largely compensate for the reduced gains in network performance compared to the heterogeneous network deployment. It should also be noted that these results do not take into account the changes in the traffic location that occur along the day. Such simplification artificially benefits the performance results of traditional heterogeneous networks versus VSC. In reality, VSC give more flexibility since their location and size can vary depending on the traffic dynamics.

2.7 Intra-LTE offloading by middleware deployment

Commentaire [KH7]: *TTI*

2.7.1 Introduction

Moving users require satisfying and guaranteeing their needs in terms of coverage and QoS even with the challenging conditions brought by the mobility aspects. Therefore, the network must be able to manage the changes in the serving cells without any prejudice to the customer. That means intelligently managing handover procedures so as to guarantee that each user is served in the most appropriate cell given their characteristics and network requirements. The envisioned solution consists of creating and deploying a middleware capable of helping in these processes, which will perform handovers as high level operations, forcing disconnections and reconnections but not going into the control plane details.

The proposed innovation corresponds to scenario 2.9.1 in [D.2.2]. The scenario being faced in this case is therefore similar to the one shown in Figure 20, where an offloading process is carried out between the LTE cells where the diverse users are moving from and to while carrying out active sessions.

Thus, the proposed innovation implies the creation of the aforementioned middleware, which will be deployed in the base stations and will work on an Internet Protocol (IP) level, capable of managing the cell occupation, given the impossibility of obtaining valid direct information from the users in certain levels.

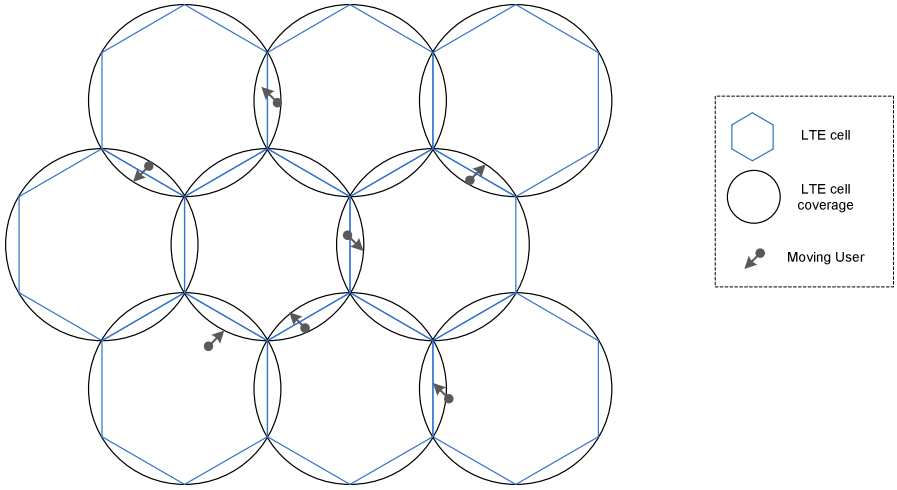

Figure 20. Intra-LTE offloading scenario.

The scenario presents an added difficulty, marked by the mobility of the users, which will derive in the need of maintaining an exchange of information between the lower and upper layers both at local and remote level (offering defined Service Access Points, SAP) and in a global network scale as well. Figure 21 depicts roughly the interactions taking place between the lower entities (for example the case represented by transceivers, base stations or users) and the high level entities managed at core network level.

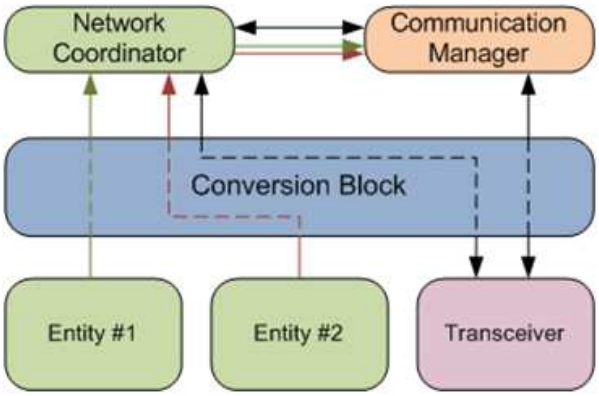

Figure 21. Basic block diagram of the envisaged middleware.

The envisioned middleware will be a functional entity that will receive and manage information from different layers dispatching primitives to their final destination, trying to avoid duplicity of paths. It will also support event-subscription functionalities for higher layers and functional blocks at local and remote level.

In addition, this middleware, which will receive the name of *Conversion Block*, will enable technology-agnostic information management when necessary. The *Conversion Block* presents capacity to analyse and adapt measurements and parameters depending on the RATs below and capability to accommodate the received data to a given Common Data Model (i.e., battery level alarms, overload levels in APs or BSs, SNR border values, etc.).

All in all, the *Conversion Block* will imply a novel and an efficient method to perform intra-LTE duties, as required in the mobility conditions so typical nowadays. Its internal structure will be similar to the one shown in Figure 22, distinguishing two main parts: the ACCESS section, directly connected to the desired entity, and the CORE section, where a dedicated database is deployed and the information processed and conveniently dispatched.

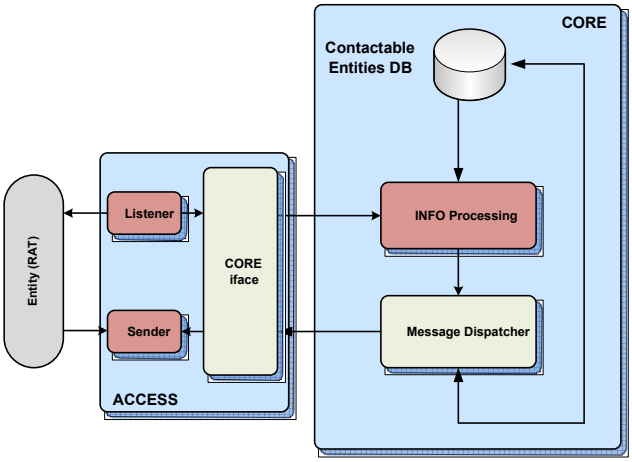

Figure 22. Internal structure of the middleware.

2.7.2 Common data model

The way the information is exchanged is defined via a common data model. Three main primitives, as listed in Table 7 are considered to communicate local and remote entities.

Table 7. Middleware primitive's types.

Primitive Type	Description
Event	Indicates dynamic changes (spectrum, link, quality).
Configuration/Command	Physical configuration, resource allocation, mobility
Information Exchange	Exchange and discover info about user details and information associated, QoS features in communications, etc.

Having the aforementioned types in mind, up to three types of communication modes are considered, see Table 8.

Table 8. Middleware communication modes.

Communication Mode	Description
Request	Handles petitions
Acknowledgement	Notifies an entity its message has been properly received
Indication	Provides information considered as important

The standard IEEE 802.21 is used as reference for the common data model definition. Inside each aforementioned primitive, the following fields explained in Table 9 can be used.

Table 9. Middleware primitives.

Primitive	Semantics
ENTITY_REG	Registers an entity at the middleware. Some information about the entity itself shall be delivered so as to properly identify it.
GET_INFO	Field used to request information regarding an already registered entity.
INFO_DETAILS	Specifies the information required by the entity which initiated the request
EVENT_SUBSCRIPTION	Remote event subscription request managed by middleware.
EVENT	Some value has trespassed a threshold and, thus, a notification is generated.
COMMIT	Once received some information on neighboring access points, a mobile terminal decides the new base station to be connected to and sends a primitive to its current base station. This will manage a new connection process.

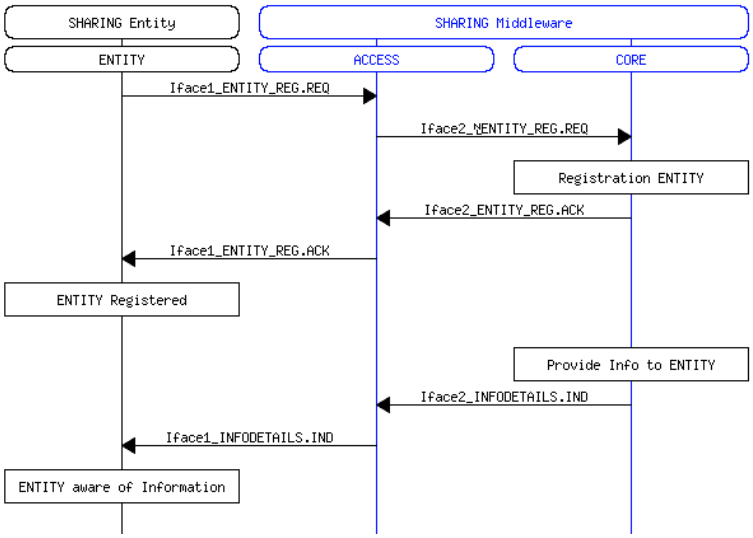

Figure 23. Interactions between the entities and the middleware.

An example of primitive exchange between SHARING entities is depicted at Figure 23. This figure presents a Message Sequence Chart (MSC) where a SHARING entity (namely, user

equipment) registers in the middleware. Once the middleware returns the acknowledgement message, it proceeds to incorporate the entity information into the database. From now on, that entity is accessible and it is able to receive the requested or subscribed information.

2.7.3 Simulator definition and requirements

Section 2.7.2 defines the way the data flows inside the middleware, considering all potential situations regarding the scenario considered. At this point, with the entire common data model already defined, it is time to start developing and defining the simulator tool used to assess the potential gains.

The simulator is built using a two-step simulator.

- In a first step, a simulator is built so as to characterize the cell coverage scenario. The idea consists of being able to determine the power received for each base station within the coverage area at each point. The simulating tool should allow the creation of just LTE scenarios and combined LTE/WiFi layouts so as to consider both intra- and inter-LTE offloading approaches. The output of this first simulation tool will be a coverage matrix for the scenario, saved as a table inside the database.
- Using the coverage matrix previously obtained, a second simulation tool is developed so as to test a daily load pattern and evaluate the potential gains in terms of QoS. This simulation tool assumes that the network is aware of some extra user parameters with respect to the data available in current LTE networks. This information will be transferred using the middleware and primitives previously defined.

The two main entities envisaged to be used in the middleware are users and base stations. In the first case, some extra information, as discussed before, is needed so as to apply the new strategies. The data regarding users is introduced in Table 10, highlighting in red the incremental information introduced. The base station parameters are also summarized in Table 11, but they are similar to the ones used currently. This data from both users and base station will be combined to produce the results.

Table 10. User information.

User Parameters	
X_position	X position in the grid (m)
Y_position	Y position in the grid (m)
X_next	Next X position expected from a random mobility model
Y_next	Next Y position expected from a random mobility model
RSSI	BS and power received at each instant
Interfaces	True if it supports attachment to small cells and false otherwise
Battery	Battery left on the mobile phone
SLA	MBps required by the user
Session	Minutes left of the user session
QoS	QoS experienced at each moment
Selected_EB	EB to which the user is attached in this moment
Priority	Bearer class

Table 11. Base Station (BS) information.

Base Station Parameters	
Name	Unique Identifier of the BS into the layout
Max_Load	Maximum Load in MBps allowed by the cell
CurrentUsers	Current users supported by the BS
CurrentLoad	Current load handled by the BS
CurrentLoadGBR	Current load of just Guaranteed BitRate (GBR) users
X_position	X position in the layout (m)
Y_position	Y position in the layout (m)
Max_users	Maximum number of users allowed
Power_cons	Power output of the BS
Coverage_radius	Coverage radius of the BS (m)
Type	True if it is LTE or false if it is a small cell

In addition to these base station and user parameters, some considerations shall be also introduced so as to assign user priorities and model the behaviour of the network. The system will be designed so as to introduce situations on which the available resources are not enough for all user requirements. This way, as in real networks, types of users must be defined, depending on the throughput/application needs and the associated fee contracted.

So as to provide this hierarchy of users, LTE bearer classes are used, with minor adaptations to fit into the simulator.The system distinguishes between Guaranteed BitRate (GBR) users (whose bandwidth (BW) requirements cannot be neglected) and Non-Guaranteed BitRate (Non-GBR) users (low priority, QoS can be diminished if needed).

In addition, each user can be using different profiles, depending on the type of data demanded. The considered profiles for users (in descending order of throughput requirements) are Gaming, Multimedia Streaming, Videocalls, Mail and Voice calls.

Mixing both user and profile information, a complete detail of bearer classes used by the simulator can be shown at Table 12. The incremental information that has been adopted by the simulator consists on the probability of occurrence of each user type and the resultant priority.

Table 12. Bearer classes.

Service	BW (Mbps)	Class	Priority	Probability
Voice	0.1	GBR (reserved BW)	1	10%
Videocall	0.5		3	5%
Streaming	1.5		4	5%
Gaming	2		2	2%
Voice	0.1	Non-GBR	9	30%
Videocall	0.5		8	10%
Streaming	1.5		5	15%
Mail	0.5		6	20%
Gaming	2		7	3%

Considering all available information depicted in this chapter, the middleware should be now able to perform intelligent user allocations at each instant depending on the context information sent by the users. On the following sections the strategies used to compare the results and the results themselves are presented.

2.7.4 Assumptions and strategies

This section covers the intelligence programmed in the simulator so as to compare between the baseline results (not applying the proposed enhancements) and the results obtained using the new data available.

The base parameter to optimize will be the QoS experienced by users in the network. Pursuing that goal, three strategies are proposed.

Table 13. Bearer classes.

Strategy	Details
Simple	Users are attached to the base station from where more power is received
Intermediate	If the base station with more power is crowded, it looks for another one with less users
Complex	Uses bearer classes to allocate users • Users with GBR are always allocated in the best base station. If they demand high bit rates, in the most powerful one. If they require voice/mail services, in the less crowded one. • Users with non-GBR may be forced to handover if a GBR user comes • All users look for the best choice of base station

The general layout for this simulation considers a grid of 5x5 macro base stations able to handle 250 users and 120 Mbps each. The base station coverage radius is 50 meters and the Inter-Site Distance (ISD) is $\sqrt{3} \cdot 50$ meters.

Depending on the coverage assumptions, two different approached have been followed, resulting in two different scenario layouts:

- In a conservative first approach (Figure 24 and Figure 25), it is considered that the base station radius is strict and further that distance the user cannot receive data from the base station.
- In a more realistic approach (Figure 26 and Figure 27), this coverage radius is extended in a 1.5 factor. The number of base stations reachable form the same point is, thus, increased. The middleware is in this case more flexible as it has more options to allocate users and better balance the load between cells. It is important to note that this assumption does not collide with the LTE frequency reuse strategy. In addition, the user battery shall be also considered, as the user may be forced to handover to distant cells. Just users with more than 40% remaining battery are suitable to use distant cells.

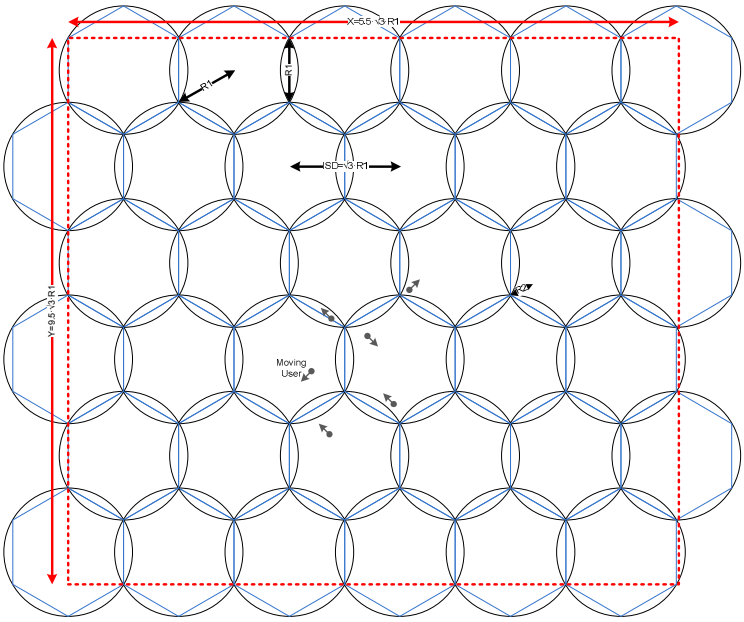

Figure 24. Conservative layout.

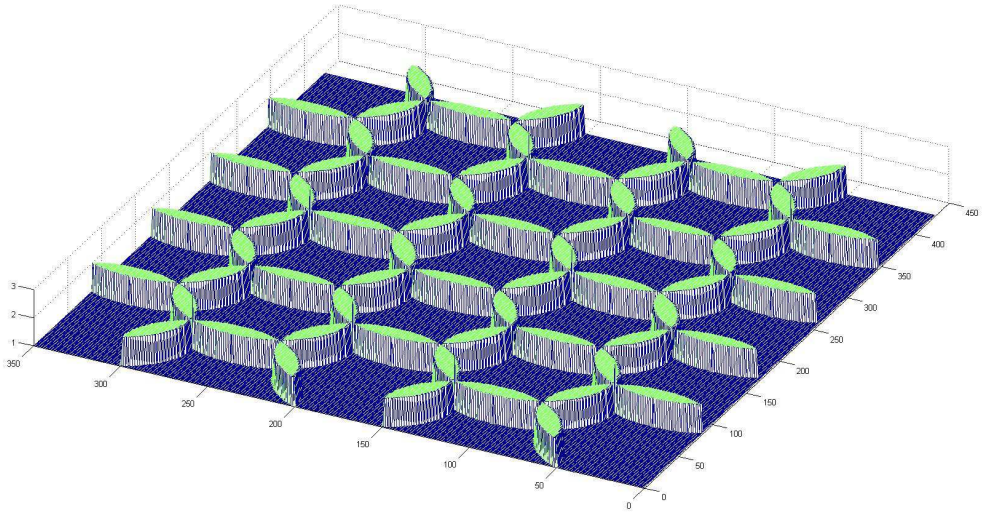

Figure 25. Number of base stations seen at each point with conservative approach.

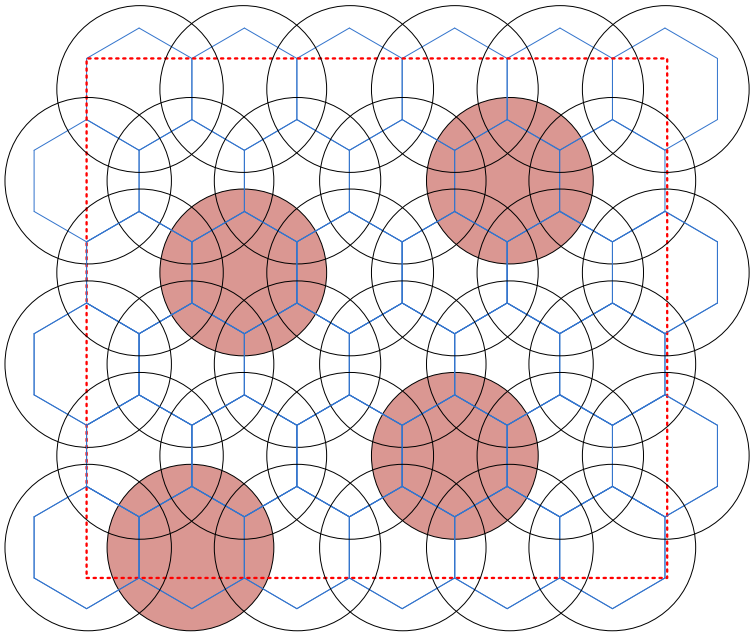

Figure 26. Realistic approach (1.5 coverage radius extended).

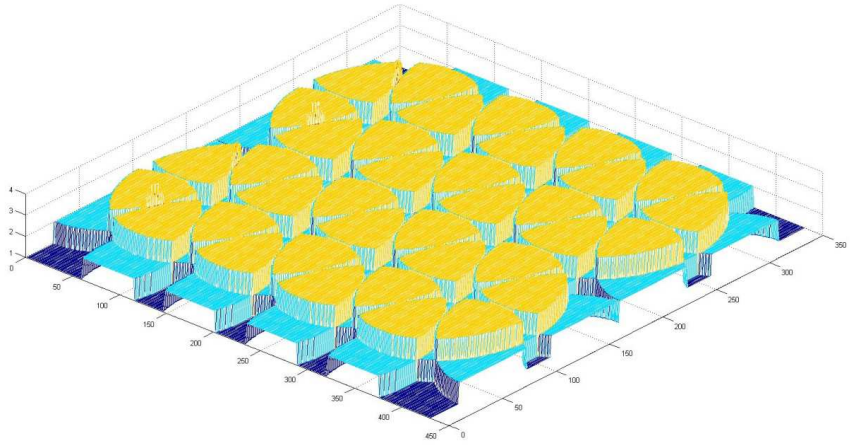

Figure 27. Number of base stations seen at each point with realistic approach.

One important assumption of the simulator is that it is designed to test the QoS of the overall network. In order to be able to determine the potential enhancements, the system has been dimensioned so as to be able to handle all potential users (0% probability of not covering a new user) but with capacity resourced under the peak traffic expected, in an attempt to force

QoS below 100% at least on peak hours. Depending on the strategy selected, the downgrade of QoS will be higher and more lasting as the balance between base stations can be enhanced via the use of the proposed middleware.

Users are programmed to move randomly, but following a coherent path. This way, at each moment, a user has equal probability to stay still, or move 1 step on any direction. Examples of the user movement paths are shown in Figure 28. The maximum number of users is determined by the use of the traffic patterns. In this case, FP7 EARTH project traffic models for urban scenarios are considered as a basis for the simulation, adding extra noise to simulate more realistic traffic situations.

User session lifetime is considered to be random between 1 and 25 minutes. Finally, 30% of capacity resources at each base station is reserved for GBR users (taken into account when using complex strategy). This consideration enables the assumption of not allowing decreases of QoS for GBR users.

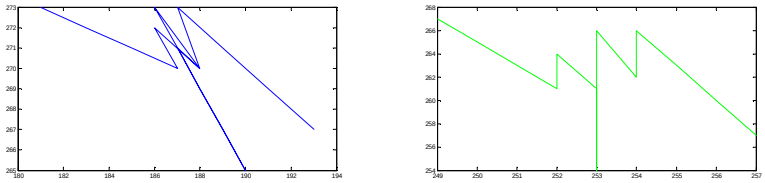

Figure 28. Examples of user movement paths.

2.7.5 Results

The simulator interfaces for both the network planning and the 24-hour period simulator can be seen at Figure 29 and Figure 30.

The final objective of this middleware plus simulator tool definition is to enhance the overall network QoS. This can be achieved due to the fact that the network will be aware of some user related parameters not used currently, and interchanged thanks to the middleware.

Differentiating between layout and strategy used, the following results are presented:

- Any SHARING defined policies, intermediate or complex, obtain better QoS performance with respect to the simple approach (not using the available new data). This can be seen, for instance, comparing between Figure 31, where the simple policy is applied, and Figure 32, in which the complex policy is used, and the resultant number of users experiencing bad QoS (red curve) is decreased significantly. When using the complex policy, 13% peak and 25% mean enhancements can be obtained in terms of overall QoS with respect to simple policy.
- Using the conservative scenario, as it allows less flexibility in terms of cell load balancing, produces always less QoS performance compared with the realistic scenario. As depicted in Figure 32 and Figure 33, using the same policy (complex) but varying the scenario from conservative (Figure 32) to realistic (Figure 33) impacts on the amount of users with bad QoS, obtaining much better results in the latter case.

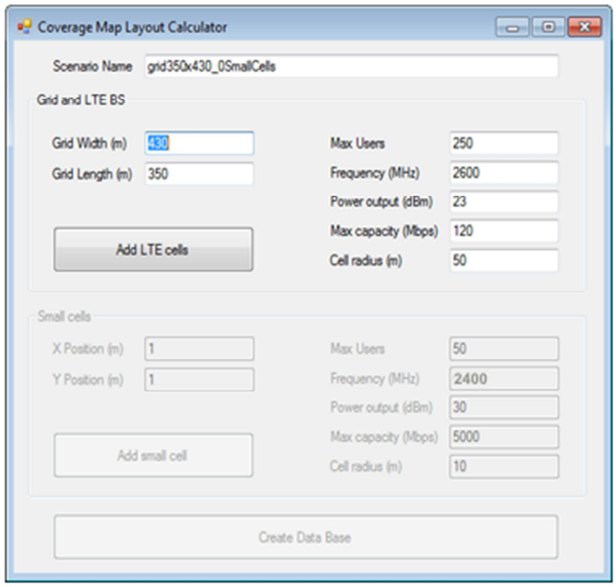

Figure 29. Network planning tool.

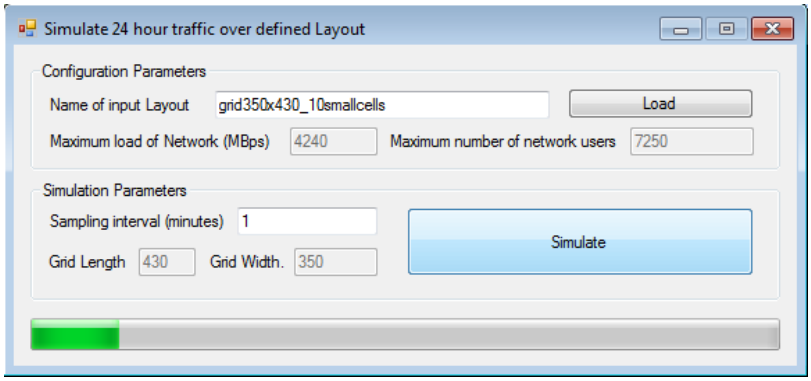

Figure 30. 24-hour simulator interface.

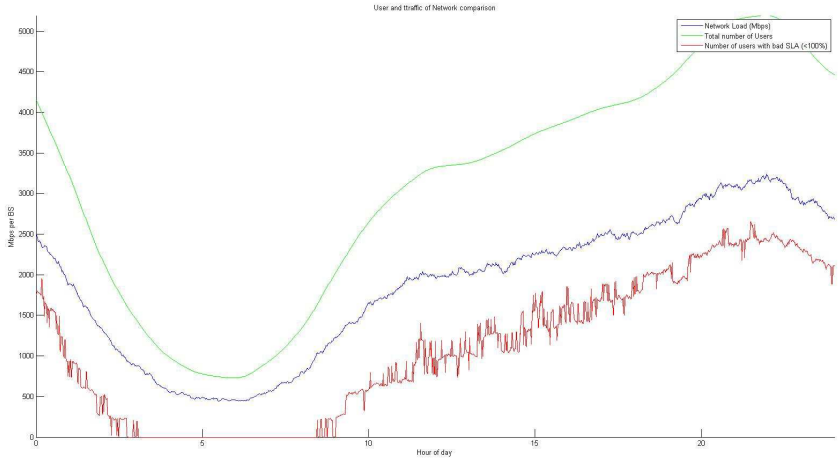

Figure 31. QoS (red curve) of the network using simple policy in conservative scenario.

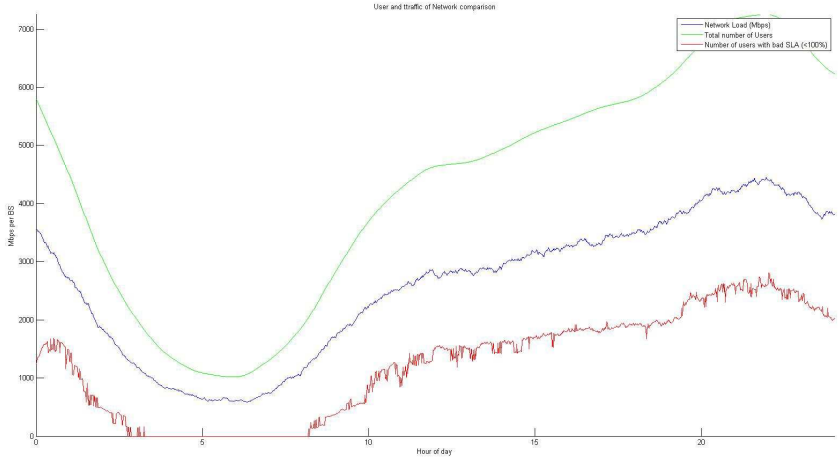

Figure 32. QoS (red curve) of the network using complex policy in conservative scenario.

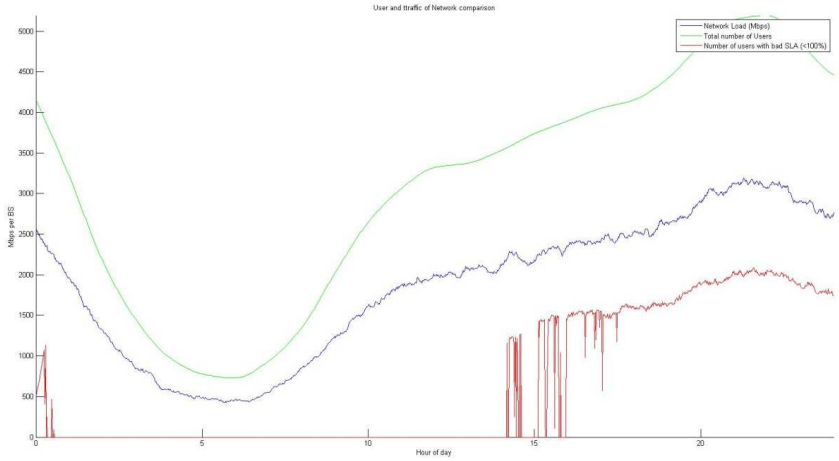

Figure 33. QoS (red curve) of the network using complex policy in realistic scenario.

The results provide consistent and very interesting enhancement results for QoS considerations. Thus, it can be considered as theoretically proven the advantages of the middleware deployment and the sharing of context user data.

2.8 Dynamic Uplink-Downlink optimization in TDD-based small cell networks

Commentaire [KH8]: *UOULU*

We consider a wireless communication system consisting of a set of small cell base stations (SCBSs) $\boldsymbol{B} = \{1, \dots, B\}$. We assume that a User Equipment (UE) arrives at location x within the considered geographical area according to a Poisson arrival process with rate $\lambda(x)$. Each UE requests either a downlink (DL) or uplink (UL) file whose size follows an exponential distribution with mean $1/\mu(x)$. A closed-access policy is assumed in this work, meaning that each SCBS has its own subscribed UEs, and hence no handover is considered. We further assume L_b to be the coverage area of an SCBS b, where a UE at location x is served by an SCBS b if $x \in L_b$. We assume that the system operates in Time Division Duplex (TDD) mode. A time frame consists of a number of N_f subframes. A frame is divided into two portions, uplink portion and downlink portion. Each portion consists of a group of subframes dedicated to serving either uplink or downlink traffic. A switching point w_b is defined as the point in which SCBS b switches from uplink mode to downlink mode. There is a number of $N_f - 1$ possible switching points for a frame length of N_f, then $w_b \in \{1, \dots, W_f\}$, where $W_f = N_f - 1$. For any of these possible switching points, there will be at least one subframe for uplink and for downlink in each frame.

We define the vector $w = [w_1, w_2, \dots, w_B]$ as the vector of switching points for all SCBSs in the system. Varying switching points asynchronously in different cells may cause opposite transmission directions in different cells which leads to cross-link interference (i.e. uplink-to-

downlink interference and downlink-to-uplink interference). Consequently, SINR for uplink and downlink, respectively, for a receiving node at location $x \in L_b$ is given by:

$$\Gamma_b^{UL}(x) = \frac{p_b^{UL} h_{b,b}(x)}{\sigma^2 + \sum_{j \in B_{UL} \setminus \{b\}} p_j^{UL} h_{j,b}(x) + \sum_{k \in B_{DL}} p_k^{DL} h_{k,b}(x)} \quad (9)$$

$$\Gamma_b^{DL}(x) = \frac{p_b^{DL} h_{b,b}(x)}{\sigma^2 + \sum_{j \in B_{UL}} p_j^{UL} h_{j,b}(x) + \sum_{k \in B_{DL} \setminus \{b\}} p_k^{DL} h_{k,b}(x)} \quad (10)$$

where p_b^{UL} (p_b^{DL}) is the uplink (downlink) power from the serving node b, p_j^{UL} (p_j^{DL}) is the uplink (downlink) power from the interfering node j, $h_{m,b}(x)$ is the channel gain, including pathloss, between the transmitting node in SCBS b and the receiving node in location $x \in L_b$, B_{UL} and B_{DL} are the sets of cells operating in uplink and downlink, respectively, and σ^2 is the noise variance. Furthermore, the data rates of a UE at location $x \in L_b$ for uplink and downlink, respectively, are given by:

$$c_b^{UL}(x) = f_b \log_2\left(1 + \Gamma_b^{UL}(x)\right) \quad (11)$$

$$c_b^{DL}(x) = f_b \log_2\left(1 + \Gamma_b^{DL}(x)\right) \quad (12)$$

where f_b is the bandwidth allocated to that UE. The system-load density at location x is defined as

$$\varrho_b^{(l)}(x) \coloneqq \frac{\gamma^{(l)}(x)}{c_b^{(l)}(x)} \quad (13)$$

where $l \in \{UL, DL\}$ and $\gamma^{(l)}(x) = \lambda^{(l)}(x)/c_b^{(l)}(x)$ is the load density at location x. The cell load density for cell b is defined as the time delay needed to serve the uplink and downlink traffic as follows:

$$\rho_b^{(l)}(w_b) = \frac{1}{\delta^{(l)}(w_b)} \int_{x \in L_b} \varrho_b^{(l)}(x) dx \quad (14)$$

where $l \in \{UL, DL\}$, $\delta^{(l)}(w_b)$ is the uplink or downlink duty cycle, which is the fraction of time frames dedicated to either uplink or downlink service within a frame, and is expressed as follows:

$$\delta^{(l)}(w_b) = \begin{cases} \frac{w_b}{W_f} & l = UL \\ \frac{W_f - w_b}{W_f} & l = DL \end{cases} \quad (15)$$

Here, dividing each cell load by its respective uplink or downlink duration is done in order to account for the uplink/downlink effective traffic. Therefore, lower duty cycles lead to higher delays and vice versa. Our objective is to find the vector of switching points w that minimizes

the overall average flow delay by minimizing $\sum_b \frac{\rho_b}{1-\rho_b}$ over the entire time frame. Therefore, we define a cost function that reflects the flow delay average over the whole subframes within a timeframe, calculated as follows:

$$J(\boldsymbol{w}) = \sum_{b=1}^{B} \left(\frac{1}{w_b} \sum_{j=1}^{w_b} \frac{\rho_{b,j}^{UL}(w_b)}{1-\rho_{b,j}^{UL}(w_b)} + \frac{1}{W_f - w_b} \sum_{j=w_b+1}^{w_f} \frac{\rho_{b,j}^{DL}(w_b)}{1-\rho_{b,j}^{DL}(w_b)} \right) \tag{16}$$

Thus, we can define the following cost optimization problem:

$$\begin{aligned} & \underset{w}{\text{minimize}} J(\boldsymbol{w}) \\ \text{subject to} \quad & 0 < \rho_{b,j}^{UL}(w_b) < 1, \forall b \in B \\ & 0 < \rho_{b,j}^{DL}(w_b) < 1, \forall b \in B \end{aligned} \tag{17}$$

To solve this problem, we develop a distributed algorithm that dynamically optimizes the uplink/downlink configuration. The goal is to design a decentralized algorithm that selects a vector of switching points w that minimizes the cost function. With the lack of global network information, the algorithm must rely only on the local information available at each SCBS to optimize an individual cost function rather than the global cost. However, the cost function for each SCBS depends not only on its own traffic load but also on the interference experienced from neighboring cells. Therefore, each SCBS b should learn to estimate its cost function and use this estimated cost function to update its strategy. Here, an SCBS's strategy is essentially the selection of a switching point. In view of the interference coupling between neighboring cells, the performance of each SCBS depends not only on its choice of switching points, but on other SCBSs' choices as well. Therefore, we model this problem as a strategic noncooperative game where the set of players are the SCBSs, in which each of them selects its action $a_b^{(n_b)}$ where N_b is the number of possible actions, which corresponds to the number of switching points W_f in our problem. For each base station $b \in B$, the corresponding cost function can be expressed as follows:

$$J_b\left(a_b^{(n_b)}, \boldsymbol{a}_{-b}\right) = \frac{1}{w_b} \sum_{j=1}^{w_b} \frac{\rho_{b,j}^{UL}}{1-\rho_{b,j}^{UL}} + \frac{1}{W_f - w_b} \sum_{j=w_b+1}^{w_f} \frac{\rho_{b,j}^{DL}}{1-\rho_{b,j}^{DL}} \tag{18}$$

Each player b chooses an action following a mixed strategy profile π_b, which is a vector of probability distributions over the set of possible actions A_b. Let the strategy of choosing an action $a_b^{(n_b)}$ by player b at a time frame t be the probability that this action is selected $\pi_{b,a_b^{(n_b)}}(t) = \Pr\left(a_b(t) = a_b^{(n_b)}\right)$. Then, by randomizing the action selection following their mixed strategies, players aim at minimizing their long-term (expected) cost functions given by:

$$\bar{J}_b(\boldsymbol{\pi}_b, \boldsymbol{\pi}_{-b}) = \sum_{a \in A} J_b\left(a_b^{(n_b)}, \boldsymbol{a}_{-b}\right) \prod_{j=1}^{B} \pi_{j,a_j^{(n_j)}} \tag{19}$$

In this game, each SCBS will choose the action that can lead to minimizing its cost function J_b, given other players' actions. We propose an algorithm that captures this behaviour by

adopting the Gibbs Sampling-based probability distribution, in which the probability of playing an action $a_b^{(n_b)}$:

$$\Lambda_{b,a_b^{(n_b)}}(\boldsymbol{a}_{-b}) = \frac{\exp\left(-\beta_b J_b\left(a_b^{(n_b)}, \boldsymbol{a}_{-b}\right)\right)}{\sum_{m=1}^{N_b} \exp\left(-\beta_b J_b\left(a_b^{(m)}, \boldsymbol{a}_{-b}\right)\right)} \tag{20}$$

where β_b is a Boltzmann's temperature coefficient. In what follows, we evaluate the performance of the proposed dynamic TDD algorithm. To illustrate the gains of the proposed scheme, we compare it against two baseline schemes: 1) fixed TDD frame, in which small cells are assumed to have the same synchronous TDD frame, with equal uplink and downlink duty cycle, and 2) random TDD frame, in which the switching point is varied randomly. We consider an arbitrary number of SCBSs distributed randomly, and underlaying the macrocell coverage area. In this work, we focus only on the SCBS-to-SCBS co-channel interference scenario. The bandwidth is assumed to be shared between all SCBSs. The bandwidth is assumed to be divided equally between all UEs transmitting or receiving in a given subframe. Both SCBSs and UEs are assumed to transmit with their maximum power, and hence, no power control is considered here. We use the average packet throughput as the performance measure for different schemes, which is defined as the packet size divided by the delay encountered to complete its transmission. The motivation behind this is that it captures both packet rate and delay, which is the objective of the proposed scheme. To investigate the asymmetric uplink/downlink traffic, we conduct simulations for different mean uplink-to-downlink ratios. For example, uplink-to-downlink ratio of 0 dB means that the average rate requirement λ_b/μ_b is the same for uplink and downlink. Each SCBS uses a sequence of time frames, no more than a maximum of 200 frames to learn its load and update its uplink/downlink configuration accordingly. In general, the performed simulations are based on scenario 2.2.1 defined in [D.2.2].

In Figure 34, we compare the packet throughput performance of our scheme against the two baseline schemes for different uplink-to-downlink ratios. All SCBSs are assumed to have the same average uplink-to-downlink ratios while the instantaneous traffic is different. Figure 34 shows that the proposed scheme achieves significant gains reaching up to 200% at −20 dB compared to the random scheme in all traffic conditions. Moreover, the figure also shows that our approach outperforms the fixed scheme in case of asymmetric traffic conditions. The gain increases as the level of asymmetry increases, since the SCBSs are able to learn their uplink and downlink loads and adapt their transmissions accordingly. Figure 34 also shows that the proposed algorithm achieves up to 97% gain at −20 dB over the fixed assignments. However, the gain becomes smaller in the symmetric traffic case in which the fixed scheme is shown to achieve the same performance since it allocates equal resources to uplink and downlink and hence it is suitable for symmetric traffic.

Figure 35 shows the average packet throughput for the case in which half of the cells have opposite uplink-to-downlink ratios compared to the other half. For example, if the first half has a ratio of 10 dB, the second half has a ratio of −10 dB. This scenario is challenging in the sense that it is associated with high cross-link interference. In Figure 35, we can see that the proposed scheme achieves considerable gains over both the random and fixed schemes. Clearly, the proposed algorithm is able to find a balance between selecting the switching point that matches the SCBS load and avoiding configurations that are associated with high cross-

link interference. Figure 35 shows that the proposed approach achieves gains reaching up to 145% and 53% over the random and fixed schemes, respectively in the case of uplink-to-downlink ratio of 20 dB.

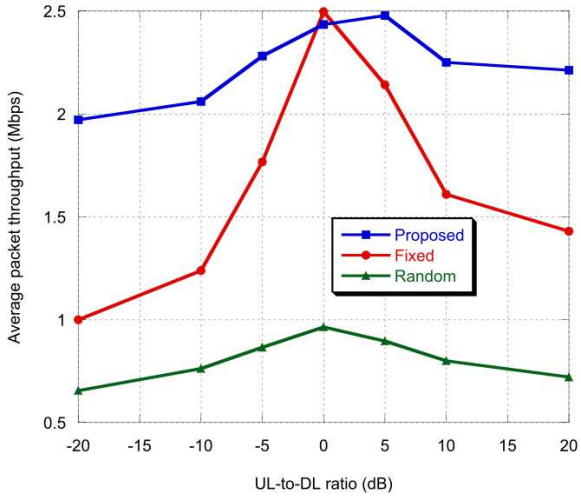

Figure 34. Packet throughput performance in case of cells having the same uplink-to-downlink ratio for a network with 4 SCBSs.

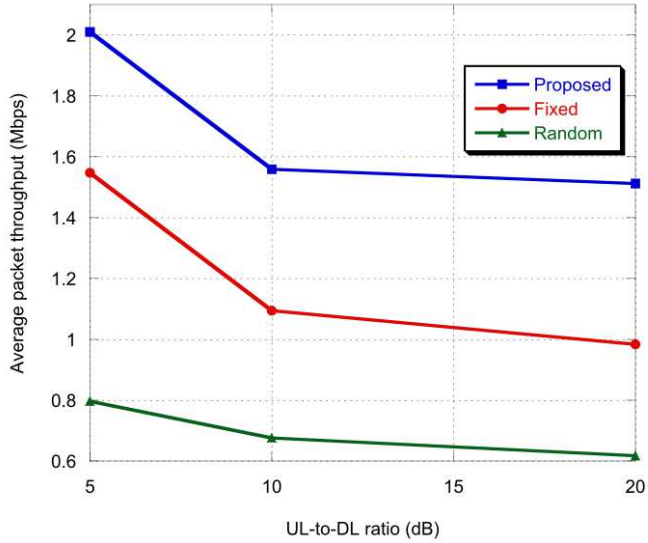

Figure 35. Packet throughput performance in case of cells having opposite uplink-to-downlink ratio for a network with 4 SCBSs.

3 MOBILITY MANAGEMENT

The introduction of heterogeneous network deployments and small cells makes some of the problems related to mobility to become worse. These problems include for example: signaling performance, data interruption during cell change, detection of small cells and coverage in border areas, especially in the unbalance zone where the macrocells have worse uplink coverage but better downlink coverage than the small cells. In order to handle this challenges, several SHARING innovations are aiming to increase the robustness of the handovers by reducing the number of handovers and by increasing the transmission and reception diversity. The following section describes such SHARING innovations and their performance evaluation.

3.1 Combined cell performance within HSPA heterogeneous network deployment

Commentaire [KH9]: *ERICSSON*

3.1.1 Introduction

The deployments of heterogeneous network with small cells in High-Speed Packet Access (HSPA) allow increasing the overall network capacity, coverage and performance. In co-channel deployment, the Low-Power Nodes (LPN) are deployed within the macrocell coverage region, where the transmission/reception points created by the low-power nodes have different cell IDs (different primary scrambling codes) as the macrocell. As shown in Figure 36, cells A, B and C have different primary scrambling codes, hence the same legacy procedure of cell selection applies for each cell and is controlled by the Radio Network Controller (RNC).

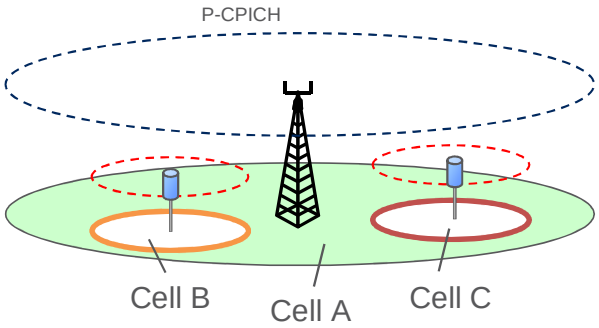

Figure 36. Low-power nodes have different cell IDs as that of the macro node in a co-channel deployment.

In a combined cell deployment, the low-power nodes are deployed within the macrocell coverage area, where the transmission/reception points created by the low-power nodes have the same cell IDs (same primary scrambling codes) as compared to the macrocell. This

deployment is also referred to as soft or shared cell. As shown in Figure 37, each node belongs to the same cell and these nodes assist the macro node.

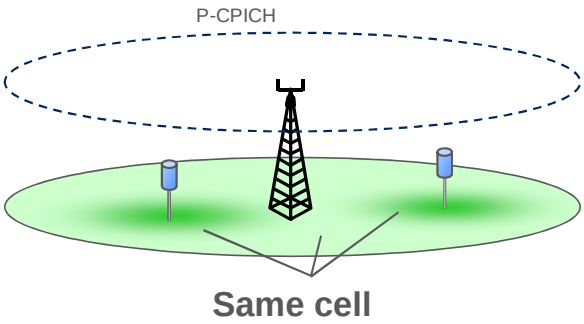

Figure 37. A combined cell deployment, where the low-power nodes are part of the macrocell, i.e., macro and low-power nodes have the same cell ID.

The co-channel deployments of small cells introduce some additional challenges that the network has to confront:

1. **Frequent Handovers and Impact on End-User Performance**: Since there are more cells in a macro node coverage area with the introduction of low-power nodes, the frequency of handovers is increased. This results in more frequent Radio Resource Control (RRC) signalling which might impact the end-user performance negatively. For example, more dropped calls due to RRC signalling delay or failure.
2. **Neighbour Cell List Size**: In a co-channel deployment, the neighbor cell list becomes too large to cover all radio positions. The required cell planning and the system capability to identify and keep the cell update subset is complex.
3. **Intercell Interference and Pilot Pollution**: With the introduction of low-power nodes, the interference structure becomes more complex than in a homogenous network. Since all the low-power nodes have to transmit the pilot signals continuously, irrespective of data transmission, the pilot pollution is more severe.
4. **Downlink/Uplink Imbalance**: The well-known problem of downlink/uplink imbalance where the UE is served by strong macro downlink and has a stronger uplink to the low-power node. This might cause problems, both for uplink and downlink control channels.
5. **Energy Consumption**: Since the pilots and certain control channels are always transmitted in a co-channel deployment (even though no UE is served by these low-power nodes), the energy associated with these channels is wasted.

The main principle of combined cell is that the UE can move seamlessly within the cell coverage area without any RNC interaction. Hence in combined cell, it can avoid active set update, serving cell change and cell selection/reselection procedures. Figure 38 shows the system architecture for the combined cell deployment; where all the nodes within a combined cell are tightly coupled by high speed data link to a central unit in the combined cell. For example this central unit can be a macro scheduling unit similar to current main unit in

main/remote base station implementations. Coupling between various nodes is not a requirement in combined cell deployment. Note that in combined cell deployment RNC connects to the central unit and is not aware of these different nodes. For example these nodes can be remote radio units (RRU). In co-channel deployment scheduling is done per each cell while in combined cell scheduling is performed per combined cell. Hence, the scheduler decides which nodes should transmit to the UE. In all, the operations performed in RNC in co-channel deployment will be performed by the central scheduler in combined cell deployment, i.e., the central scheduler tracks the UE between multiple nodes. The combined cell deployment avoids the loading of RNC, while at the same time the decisions and execution can be performed very fast (Transmission Time Interval (TTI) level), improving both the overall network performance as well as the UE performance.

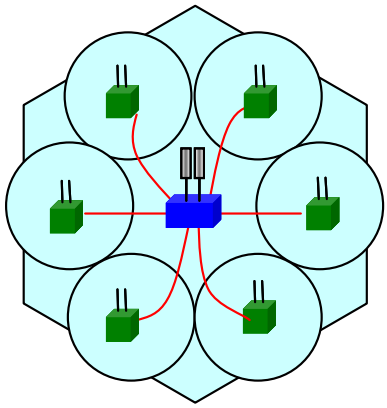

Figure 38. System architecture of combined cell deployment, where all the nodes are tightly coupled and connected to the central scheduler.

Based on the data transmission from macro and low-power nodes, we can divide the downlink transmission modes into three types:

- **Single Frequency Network (SFN) or Multicasting**. In this mode, multiple nodes (e.g. macro and low-power nodes) transmit the same data to a specific UE. Hence, the SNR of the UE can be improved. The main idea of this mode is to combine signals over the air from all nodes by means of transmitting exactly the same pilot, control channels and data channel in downlink using the same carrier frequency and spreading and scrambling codes.
- **Node Selection with Spatial Reuse**. In the SFN mode, all nodes are transmitting the same downlink signal. Hence it may not give capacity gains when the traffic load is high as SFN mode is used for coverage improvement. Since many nodes do not contribute to the performance improvement, the resources from the nodes are not used efficiently. The interference pattern in combined cell deployment is similar to that of co-channel deployment; the resources from these nodes can be utilized to schedule different UEs. In this mode, the same Primary Common Pilot Channel (P-CPICH) signal

is transmitted from all the nodes. The downlink control channel and the data traffic are scheduled to different UEs from different nodes, based in their position inside the network and the available resources (HS codes and power). Since the scheduling is done per combined cell, the central scheduler decides which nodes should transmit to the various UEs.

- **MIMO mode with spatially separated nodes**. In this mode, some of the low-power nodes act like distributed MIMO, i.e., MIMO transmission with spatially separated antennas. In this mode, MIMO gains (both diversity and multiplexing gains) can be achieved.

Since in combined cell, all the nodes are connected to the central scheduler, we envision a significant gain in uplink performance. This is due to macro diversity combining. The downlink performance might vary based on the transmission modes, but a positive impact of the reduction on mobility procedures should also be observed in the final results in realistic scenarios.

There is no impact in the legacy architecture with relation to signalling and standardized procedures. The model builds on the close network relationship between the transmitters within a cell that may be located in the same physical node or not. And for this work, the assumption is that proprietary (not standardized) signalling is used in case of any coordination between nodes is required.

3.1.2 Impact of combined cell deployments on mobility

The mobility performance of combined cell deployments has been proved to increase the robustness of the handovers [MIN14]. This is achieved because the deployment enables a reduction on the number of handovers triggered on a coverage area. Furthermore, the handover signalling failure rate is reduced compared with deployments of separated small cells, especially for challenging mobility scenarios. A challenging mobility scenario can be defined as one with high system load, several spots with low geometry and user's mobility that can reach high-speed. Some example of this scenario could be a train station or train tracks, a stadium hosting an event or a traffic light corner where low-power nodes have been deployed.

A macro-only scenario compared with a low-power node scenario would produce similar results in terms of number of handovers, but the deployment would suffer from their own capacity and coverage limitations. This means, that a combined cell deployment is expected to address also the capacity and end-user performance limitation in addition to the mobility.

3.1.3 Initial performance results for SFN mode

The SFN mode of combined cell is 100% legacy compatible and does not require any changes in the standard.

Initial simulation results are available for the scenarios 2.8.1 (macro-only) and 2.8.2 (HetNet) in [D.2.2] for FTP traffic (2 MB object) and 4 LPNs (distributed RRU's/antennas connected to macro in addition to the main antennas) per macro sector. For FTP upload, the results confirm the initial assumption that even a SFN deployment is able to increase the uplink throughput due to the macro-diversity gain of having distributed receiving antennas. As can be seen in Figure 39, by increasing the load per square kilometre, the mean user throughput is impacted

in a macro-only deployment (labelled MACRO-500m-ISD). Meanwhile, the combined cell SFN deployment shows a very low degradation (labelled CC-SFN-4LPN). Additionally, the 5%-ile user's throughput for combined cell remains virtually unchanged with the load.

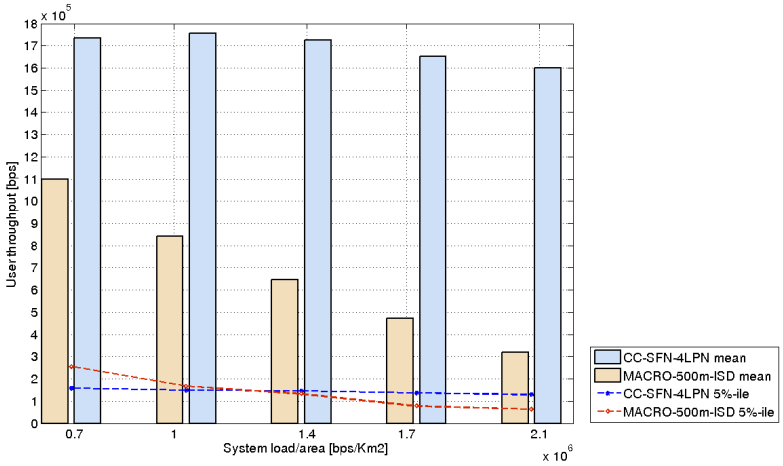

Figure 39. Comparison of uplink performance of Macro-500 m ISD deployment versus a combined cell SFN deployment with 4 additional distributed RRUs.

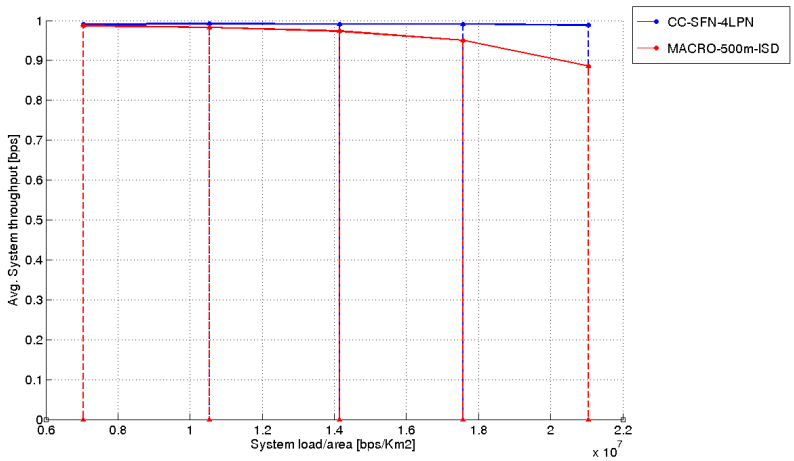

Figure 40. System throughput efficency of the simulated combined cell SFN deployment versus the macro-only with 500 m ISD.

The results indicate that the combined cell increases the area capacity. This can be visualized by looking at the system throughput efficiency, defined as the ratio between the offered load and the system throughput. If the network starts to delay packets, the output rate is reduced

with respect to the input rate meaning that the queues in the network increases and the services start to suffer. According to the results in Figure 40, the throughput efficency of the combined cell deployment for uplink is higher than the macro-only deployment for higher loads in the same area. This is an indication that more users can be served by a combined cell deployment as expected.

3.1.4 Conclusions

The deployment of combined cells is expected to improve the spatial reuse of the codes used for the transmissions. In order to do this, HSPA standardization changes are required. Also the combined cell deployments are expected to improve the receiving and transmitting diversity of the areas of coverage. This should be translated in improvements in throughput, especially for uplink transmissions. In this work, this claim is supported by the simulation results that additionally indicate an increase in the area load capacity. In addition to the diversity gain, the users benefit from a lower probability of signaling failure due to handover procedures that otherwise would be required if the same area would be covered by a heterogeneous network deployment. Additional future work will analyze the downlink impact of the deployment.

3.2 Uplink/Downlink split within a heterogeneous LTE network

Commentaire [KH10]: *ERICSSON*

3.2.1 Conclusions

Due to the nature of heterogeneous networks there is a possibility that the best cell in downlink is not the same cell as the best cell in uplink. In such situations the use of the traditional cell selection method, where the serving cell is the one with the strongest downlink signal strength may result in significantly sub-optimal performance, especially in uplink transmissions. This specific issue emerging with heterogeneous cells is called uplink/downlink imbalance. As the macro eNodeB and LPNs in heterogeneous networks have different downlink output powers and the maximum uplink transmission power of UEs is the same regardless of the serving cell, some UEs may find themselves in a uplink/downlink imbalance situation. Due to the much higher transmission power of macro eNodeB compared to LPN, the downlink cell border between macro eNodeB and LPN is pushed relatively close to the LPN, where both cells are perceived equally strong. In uplink on the other hand the maximum UE transmission power is constant regardless of serving cell, and therefore basically it makes no matter whether the receiving cell type is macro eNodeB or LPN. Therefore if only uplink would be considered, the cell border should be roughly in the middle of the two nodes where the path loss is the same to both nodes. Thus, optimal handover borders are different for uplink and downlink in heterogeneous networks.

The illustration of the uplink/downlink imbalance situation can be seen in Figure 41. In the figure, the location of the macro eNodeB and the LPN is depicted on the x-axis. The upper part of the figure shows the Reference Signal Received Power (RSRP) measurement (based on downlink received signal power) result on the y-axis while the lower part of the figure shows the path loss on the y-axis.

The RSRP measurement border can be regarded as the ideal downlink cell border since the RSRP measurements are based on downlink measurements, while the ideal uplink cell border would be the border where the path losses are equal since the UE can transmit with the same power regardless of the serving cell. As can be seen from the figure, if the downlink transmission powers of the LPN and macro node are not equal, these borders are not equal.

To improve the efficient usage of radio resources in such situations, one method is called uplink/downlink split. In case of uplink/downlink split the UE would connect both links separately to the best serving cells, in practice the downlink to the best macrocell and uplink to the closest node, whether it is the same macro eNodeB or a LPN. This would improve especially the uplink performance and the utilization of radio resources.

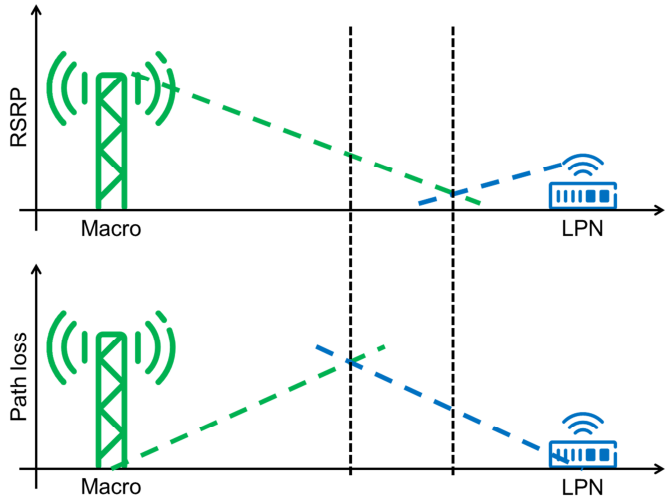

Figure 41. The Uplink/Downlink imbalance with heterogeneous networks.

As the transmission power of the UE is limited, it is beneficial to transmit to the eNodeB with the least amount of path loss, whether it is a macro eNodeB or a LPN. Transmitting to the eNodeB with least amount of path loss would increase the transmission capacity due to higher SNR. It could also decrease the interference caused to other UEs, since the users in the cell border areas would be the most probable users to activate the split mode. The power control of those users in the cell border areas still connected to the macro eNodeB in uplink adjusts the transmission power close to maximum due to the long distance and high path loss to the macro eNodeB. In co-channel case this could of course cause interference to other users in neighbouring cells. When such a user activates the uplink/downlink split and connects the uplink to the LPN, which is much closer, it can adjust the transmission power much lower and its transmissions are now scheduled together with those users it used to interfere, resulting in much less interference.

Uplink/downlink split would also help in load balancing by offloading users located within the Cell Uplink Range Expansion (CURE) area from the highly congested macrocell into the low-power cell.

The user plane split can be done on several protocol levels. In our study the uplink/downlink split is based on dual-connectivity, currently being specified in 3GPP for LTE Release-12. The separation is done at the Packet Data Convergence Protocol (PDCP) layer, as shown in Figure 42, so there would be separate Radio Link Control (RLC) and lower layers for both nodes, when the split is activated. Control signalling over X2 is used to setup and release the uplink/downlink split.

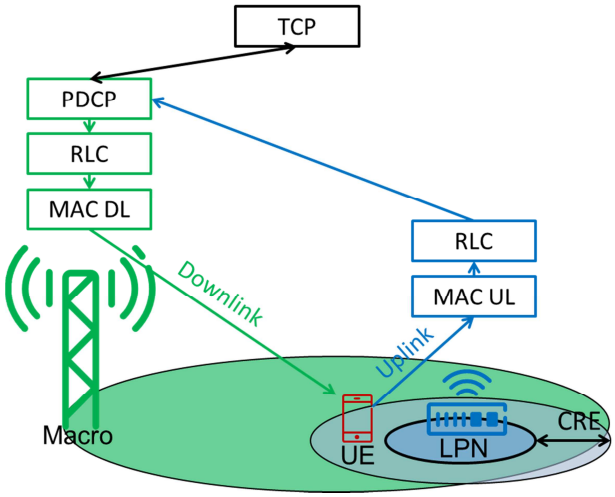

Figure 42. Realization of the uplink/downlink split.

The performance of the uplink/downlink split feature on protocol level will be evaluated by means of system-level simulations. The simulation setup is based on the 3GPP Case 1 specified in [3GPP10a] and on Scenario 2.3.5 described in [D.2.2]. The network deployment consists of 21 macrocells and 84 outdoor picocells co-located with traffic hotspots. Furthermore, the users are generated according to Poisson process with several arrival intensities, and the users are assumed to be moving with a speed of 3 km/h towards a random direction. Finally, the data traffic is mainly uplink FTP traffic with fixed packet size, but also downlink is studied. The aim of the simulations, results and the result analysis is to provide understanding about the usefulness of the uplink/downlink split in real world systems and whether or not the feature would actually provide gains especially in the uplink in heterogeneous LTE networks. The usefulness is evaluated according to the achieved gains in, for example, user throughput and delay compared to the case where no uplink/downlnk split is used.

3.2.2 Uplink simulation results

In this section the results for the gains in uplink user throughput are presented. To start with, Figure 43 presents the CDFs of user uplink throughputs in a low load case with FTP file size of 2 MB. As can be seen from the figure, the CDFs show that CURE cases get much better performance than the normal case for low user throughputs. Interestingly, the performance of especially high CURE cases seems to suffer for the users with average throughputs compared

with the normal case. With the highest throughputs, all of the CDFs seem to be quite close together. This implies that in the low load case, uplink/downlink separation provides the best gains in throughput especially for users with low throughputs. For users with average throughputs, the gains are not as high, and some of those users seem to be even suffering from the uplink/downlink separation especially with higher CUREs. This could be explained by having users with decent uplink throughput to a macrocell being transferred to a picocell with inferior uplink connection due to high CURE value resulting in performance degradation. With large throughputs the users are close to their serving base stations and experience already a very good connection and therefore the separation does not affect them much.

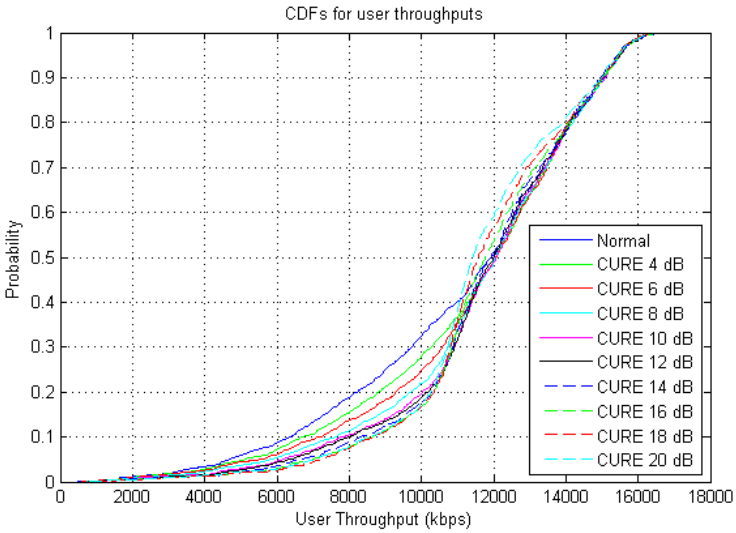

Figure 43. CDFs for user throughputs with low load, FTP file size 2 MB.

Figure 44 presents the gain in user rates on average as well as for the 5%-ile users. The 5%-ile users mean the 5% of the users who get the worst rates. This measure is generally used to indicate the users at cell-edges. As the figure clearly shows, the gains on average are quite moderate, reaching the best average gain of 5.8% with CURE of 14 dB. The 5%-ile rate gains are clearly better than the gains on average. The highest gain here is achieved with 18 dB CURE, the gain being 63%. These results support the conclusion drawn from the CDFs, that the highest gains are achieved by the users with the lowest throughputs, and users with medium throughputs may even suffer from the uplink/downlink separation, balancing the gains achieved by users with lower throughputs and resulting in quite low gains on average.

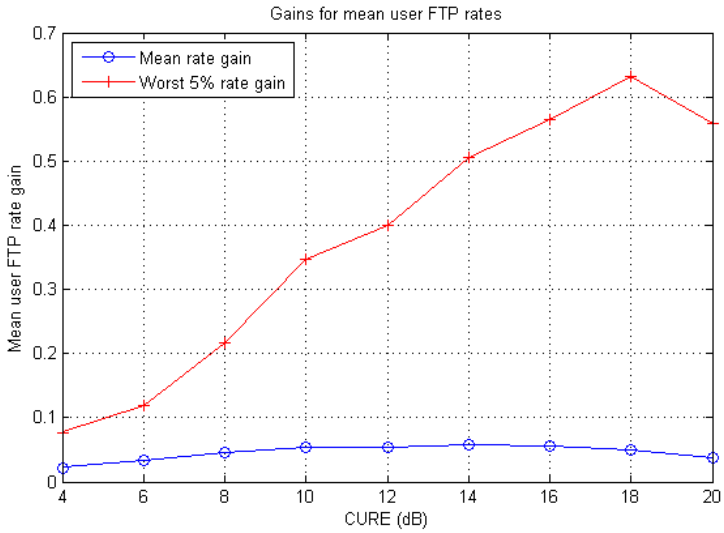

Figure 44. User rate gains with low load, FTP file size 2 MB.

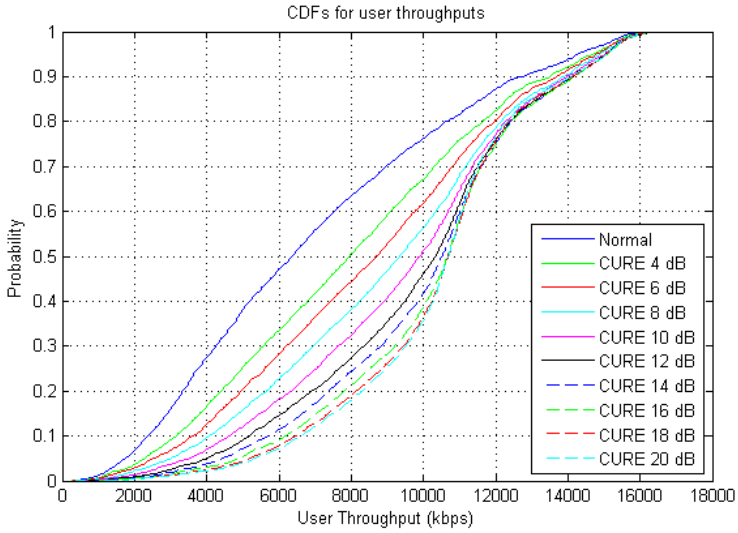

Figure 45. CDFs for user throughputs with high load, FTP file size 2 MB

In comparison, Figure 45 shows the CDFs of user uplink throughputs in a high load case with FTP file size of 2 MB. As can be seen from the figure, there is a distinctive difference between the CDF of the normal case and the CDF of already the lowest CURE case of 4 dB. This means that there are already quite considerable gains in throughput even with low CUREs, when the system is in high load. When comparing the position of the curves with the low load case, the overall throughputs in the system are now clearly smaller. It was noted that in addition to

those users, who have a lower path loss to a pico eNB and are therefore better served by it, there are highly overloaded macrocells, which benefit greatly, when traffic is offloaded from them to picocells. As the CURE is increased up to 20 dB, the gains increase, though with diminishing returns.

Finally, Figure 46 shows the user rate gains with the high load scenario, when the FTP file size is 2 MB. When compared with the low load case, it can be seen that the gains have increased and even more than tripled. Again the throughput for the 5%-ile users is higher than the average of all users reaching the gain of 218% at CURE of 20 dB. The highest average gain is achieved also at CURE 20 dB, at which the gain is 49%. These results imply that the more heavily the system is loaded the more gain from uplink/downlink separation is achieved.

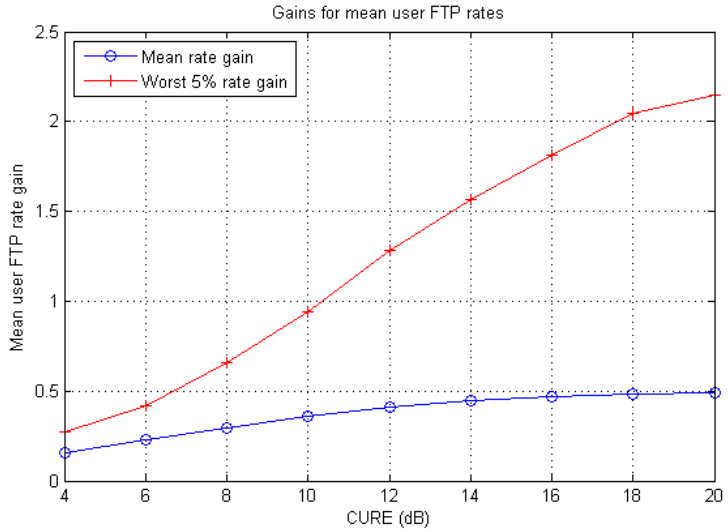

Figure 46. User rate gains with high load, FTP file size 2 MB

3.2.3 Downlink simulation results

Simulations were also performed with downlink traffic model. FTP traffic was used with FTP file size of 2 MB and similar network scenario as with uplink simulations. Looking at the downlink performance, Figure 47 shows the CDFs for user downlink throughputs with low load. As can be seen from the figure, in case of uplink/downlink separation the user throughputs seem to be lower than in the reference case. This was expected, since with downlink traffic only the higher layer signaling back to the network, such as Transmission Control Protocol (TCP) acknowledgements, goes through the picocell uplink. As the sizes of these signaling packets are small, the backhaul delay from pico to macro seems to be dominant and cause negative gains. Improvement of the bit rates in the uplink does not considerably improve the uplink transmissions of such small files in practice. On the contrary, activating uplink/downlink split will just increase the Round Trip Time (RTT) of these packets and makes especially the slow start slower thus increasing the time until TCP reaches congestion avoidance mode and is able to transmit with larger transmission window sizes. The

results were similar also with larger file sizes and higher loads, although the gains were generally not as bad when the file sizes and loads were increased, but still negative.

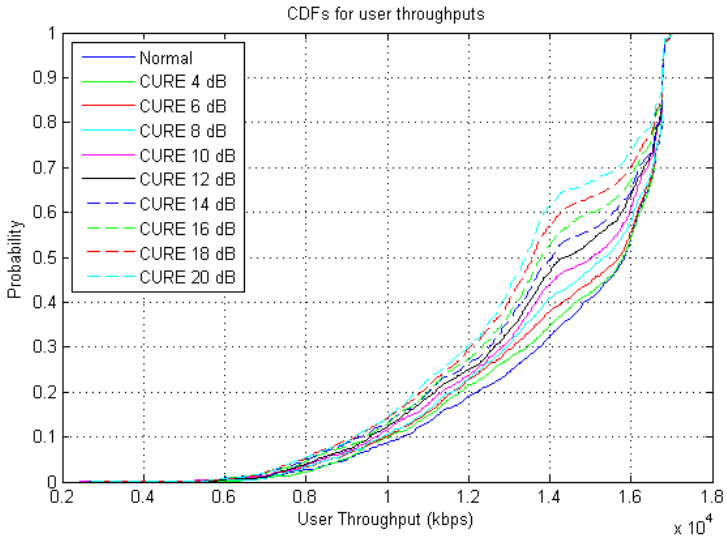

Figure 47. CDFs for user downlink throughputs with low load

3.2.4 Conclusions

The simulations show, that using uplink/downlink separation results in gains in uplink transmissions. The gains are measured from the mean FTP rates of the users both with and without uplink/downlink separation. The highest gains seem to result from a highly loaded system and relatively high CURE such as 16 – 20 dB. The highest gain for the average user FTP rate is achieved with the smaller of two file sizes, 2 MB, and the CURE value of 20 dB, where the average gain is 49%. The results show that for the worst 5%-ile of the users, FTP rate the gains are even higher than average, which suggests that users with the lowest rates benefit the most from the uplink/downlink separation. Usually, the users with the lowest rates are the users at the cell border, which makes sense in this case, since those users are now transferred from the macrocell to the picocell with the uplink/downlink separation resulting in better uplink connection. The gains seem to increase up to a certain point, when the CURE is increased, and interestingly, the higher the system load is, the larger gains are. This suggests that offloading users from highly congested macrocells to more vacant pico nodes is one of the key factors in achieved gains along with the improved uplink connection of especially the cell-edge users.

With downlink traffic, the simulations show that using UL/DL separation results in decreased performance. This is explained by downlink transmissions not benefitting from the increased capacity in uplink, since the uplink transmissions contain only small size TCP acknowledgements. On the contrary, the increased round trip time caused by the backhaul delay between the secondary eNodeB and the master eNodeB negatively affects the TCP slow start. This can be seen from the protocol simulation results where small file sizes were used.

The delay in the uplink signaling causes delay in the downlink transmissions, and therefore, decreased performance.

4 BACKHAUL MANAGEMENT

Generally speaking, each base station within a cellular network has to be connected to the core network. That connection, called e.g., a transmission or a backhaul, can be either wired (copper or fiber) or wireless (microwave link or self-backhauling). In addition, the network connection has to be able to support the required air-interface capacity and the delay requirements introduced by the desired network functionalities, such as mobility management and inter-node coordination.

Together with the network densification and the introduction of LTE-A, the topic about backhaul cost becomes increasingly important. In order to reduce the total cost of network deployment and operation, new and innovative ways to enhance the use of the backhaul connection are desired. This chapter describes the SHARING innovations within the field of backhaul management.

4.1 Backhaul offloading by proactive caching

Commentaire [KH11]: *UOULU*

4.1.1 Introduction

The rapid proliferation of smartphones has substantially enriched the mobile experience, leading to new wireless services (e.g., multimedia streaming, web-browsing applications), and content owners (Telco's, users, and Over The Top (OTT)). Currently, mobile video streaming accounts for 50% of mobile data traffic and is expected to skyrocket to a 500X increase over the next ten years. These new paradigms urge mobile operators to redesign their networks cost-effectively by deploying intelligence at the network edge. Despite these exponential traffic growths, results have shown that multiple users actually request similar contents. At the same time, dynamic content caching has recently attracted much attention and is considered as one of the most disruptive technology directions for beyond 4G networks. By harnessing recent advances in storage and computing, dynamic caching can help alleviate backhaul congestion, reduce loads at peak times and minimize latency, by pre-caching contents at strategic network edge locations. If smartly coupled with meta-data analytics, network operators can further exploit the vast amount of users' context information (location, speed, etc.) for a better predictability of future demands, to proactively cache popular contents before users actually request them.

A simplified overview of the assumed scenario is shown in Figure 48. We consider a scenario formed by M Small Base Stations (SBS) and N UEs. Each SBS m is connected to a Central Scheduler (CS) via a limited backhaul link with capacity c_m, whereas user n is connected to its serving SBS via a wireless link with capacity $c_{m;n}$. Let us assume that user n downloads contents from a library of F files with probabilities P_n. The files in the library F have lengths of L respectively, with bitrates B. Further, assume that there is R number of file requests during T time-slots. A request r is served immediately and is said to be satisfied, if the rate of delivery is higher than the file bitrate, such that: $\frac{l_r}{t'_r - t_r} \geq b_r$, where l_r is the length of the requested file, $t_r(t'_r)$ is the start (end) time of the delivery, respectively, and b_r is the bitrate of file f_r. Therefore, the file satisfaction ratio can be defined as:

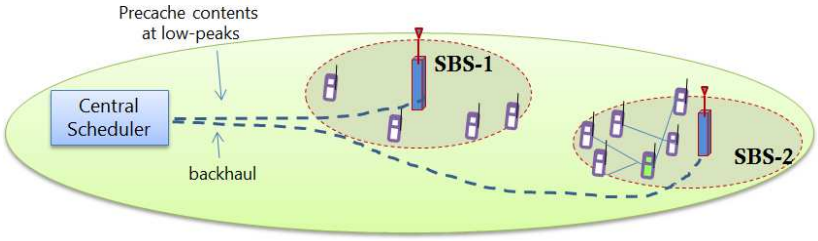

Figure 48. Illustration of backhaul offloading via caching.

$$\eta(R) = \frac{1}{R}\sum_{r} 1\left\{\frac{l_r}{t_r' - t_r} \geq b_r\right\} \tag{21}$$

The goal of the network operator is to keep this ratio above a target QoS, while reducing the backhaul delivery cost. To achieve this, we propose a proactive caching procedure.

Let us now suppose that the total backhaul link capacity is less than the total wireless link capacity between SBSs and UEs. This assumption stems from the fact that SBSs may have limited backhaul connections. Since the bottleneck is the backhaul, a smart way of minimizing the backhaul usage is to proactively cache contents at the SBSs, during low-peak demands. In other words, if the SBSs pre-cache the contents before users' actual requests arrive, corresponding UEs can immediately be served from their SBSs. Suppose that the backhaul rate during the content delivery for request r at time t is $\lambda_r(t)$. Then, the backhaul load can be defined as:

$$\rho(R) = \frac{1}{R}\sum_{r}\frac{1}{l_r}\sum_{t=t_r}\lambda_r(t) \tag{22}$$

Further, assume that SBS m has a storage capacity of s_m and the amount of storage usage at time t is $\kappa_m(t)$. Therefore, the backhaul minimization problem subject to backhaul, storage and QoS constraints is written as:

$$\begin{aligned} &\min_{t_r', r} \rho(R) \\ s.t.\quad &\lambda_r(t) \leq c_m \\ &\kappa_m(t) \leq s_m \\ &\eta(R) \geq \eta_{min} \end{aligned} \tag{23}$$

where η_{min} is the minimum target satisfaction ratio. Solving the above problem is computationally intractable, and thus a heuristic solution is used by storing popular files in the caches of SBSs. Here, each SBS m tracks, learns and builds its users' demand profiles to infer on their future requests. Let P_m denote the discrete file probabilities of users serviced by SBS m, referred to as popularity matrix where rows represent users and columns represent file popularities/ratings. A perfect knowledge of P_m would allow SBSs to precache contents, nevertheless, in practice, this matrix is not perfectly known, large and sparse. Using

supervised machine learning tools, a distributed proactive caching procedure is proposed by exploiting the correlations of the users' files to infer on the probability that user n requests file f.

The proposed caching procedure is composed of a training and prediction step. In the training step, each SBS m builds a model based on the available information of the popularity matrix P_m. This is done by solving a least square minimization problem, in order to calculate the estimated file popularity matrix $\hat{P}_m$, as follows:

$$\min_{b_n,b_f} \sum_{n,f} \left(r_{nf} - \hat{r}_{nf}\right)^2 + \lambda \left(\sum_n b_n^2 + \sum_f b_f^2 \right) \quad (24)$$

where the sum is only over the $(n;f)$ user/file pairs in the training set where user n actually rated file f (i.e., r_{nf}), and the minimization is over all the $N+F$ parameters, where N is the number of users and F the number of files in the training set. In addition, $r_f = \bar{r} + b_n + b_f$ is the baseline predictor where b_f models the quality of each file f relative to the average $\bar{r}$ and b_n models the bias of each user n relative to $\bar{r}$. Finally, the weight λ is chosen to balance between regularization and fitting training data.

4.1.2 Evaluation and results

We now turn to evaluate the performance of proactive caching and provide key insights under two different scenarios. The parameters for the numerical setup are given in Table 14. For simplification, the link and storage capacities are assumed to be equal. Three regimes of interest are considered: (i) low load, (ii) medium load, and (iii) high load. Over a time duration T, R numbers of requests are generated. The arrival times of user requests are drawn uniformly at random, and the requested files are sampled from the ZipF distribution. At $t = 0$, the popularity matrix is constructed perfectly. Out of 20% of the elements of this matrix are removed uniformly at random and the remaining elements of the matrix are used for training in Collaborative Filtering (CF). These removed entries are then predicted using the regularized Singular Value Decomposition (SVD). After the popularity matrix estimation, proactive caching is applied by storing the most popular files subject to the SBSs' storage constraints. Having these files locally in the cache of SBSs and starting from $t = 0$, the delivery is carried out by each SBS until all requests are served. Random caching is used as a baseline procedure, referred to as reactive.

Three parameters of interests are considered for the performance plots of both proactive and reactive caching approaches: (i) number of requests R, (ii) total cache size S, and (iii) ZipF distribution parameter α. To see the percentages of differences between the proactive and reactive approaches, plots are normalized. The evolution of the satisfaction ratios and backhaul loads are shown in Figure 49. Each subfigure represents the impact of one parameter for a given regime while the other parameters are kept fixed.

Table 14. Parameters for the numerical setup.

Parameter	Description	Value
T	Time slots	1024 seconds
M	Number of small cells	4
N	Number of user terminals	32
F	Number of files	128
l_f	Length of file f	1 Mbit
b_f	Bitrate of file f	1 Mbit/s
$\sum_m c_m$	Total backhaul link capacity	2 Mbit/s
$\sum_m \sum_n c_{m,n}$	Total wireless link capacity	64 Mbit/s
R	Number of requests	$0 \sim 2048$
S	Total cache size	$0 \sim l_f \times F$
α	ZipF parameter	$0 \sim 2$

1) Impact of number of requests: The satisfaction ratio decreases with the increase in users' requests. This is evident as the amount of capacity and storage resources are limited. Furthermore, the proactive caching outperforms the reactive approach in terms of satisfaction ratio. However, the reactive approach generates fewer loads on the backhaul in the case of very small number of requests. This situation can be explained by the cold start phenomenon where the CF cannot draw any inference due to non-sufficient amount of information about the popularity matrix. Therefore the random caching for a fixed library size outperforms the proposed approach at low load. However, as users' requests increase, the proactive approach minimizes the backhaul load outperforming the reactive approach, after which the gains level off.
2) Impact of cache size: It can be seen that as the total storage size of small cell base stations increases, the satisfaction ratio approaches 1 and the backhaul load tends to 0. This cannot be easily achieved in practice as it requires storing all file requests whereas SBSs have limited storage. Therefore, for reasonable values of cache size, it can be seen that the proactive caching outperforms the reactive case in terms of satisfaction ratio and backhaul load.
3) Impact of popularity distribution: As the popularity of some files increases as compared to others (i.e., α increases), the gain of the proactive caching becomes higher compared to the random approach in all regimes. Going from the low load regime to the high load regime, the gains further improve.

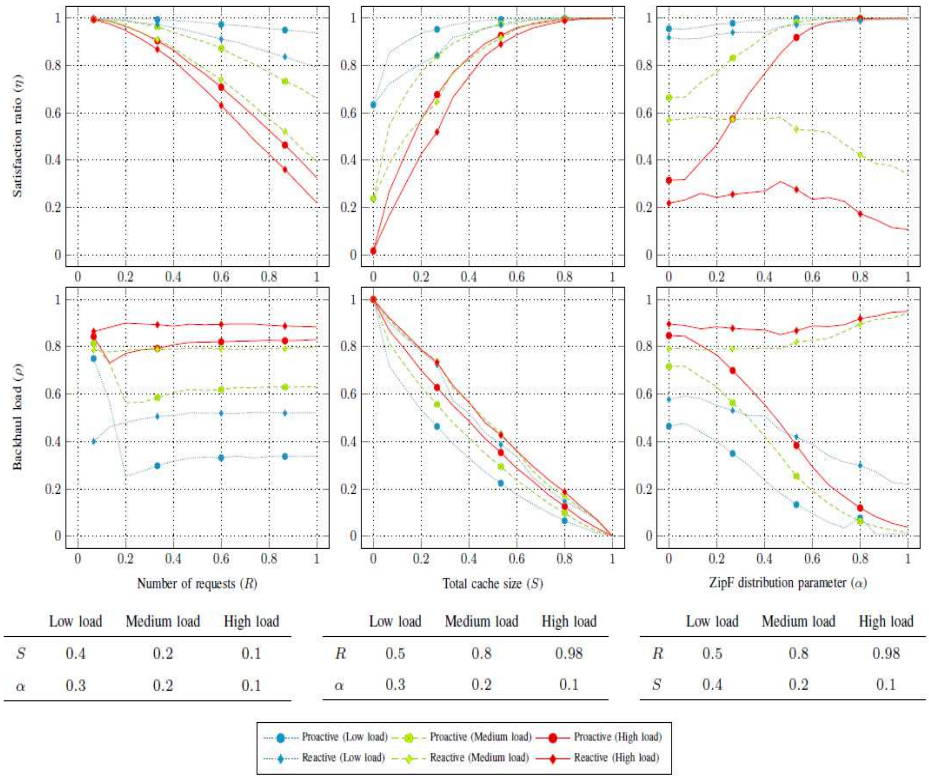

	Low load	Medium load	High load
S	0.4	0.2	0.1
α	0.3	0.2	0.1

	Low load	Medium load	High load
R	0.5	0.8	0.98
α	0.3	0.2	0.1

	Low load	Medium load	High load
R	0.5	0.8	0.98
S	0.4	0.2	0.1

Figure 49. Backhaul Offloading via Proactive Caching: Dynamics of the satisfied requests and backhaul load with respect tothe number of requests, total cache size and ZipF parameter.

5 HETEROGENEOUS NETWORK DEPLOYMENTS – PERFORMANCE AND STRATEGIES

The creation of innovations and solutions that are aimed by the SHARING project, are often based on investigations and research conducted by the partners in several areas that directly are later impacted by the innovations proposed in order to solve the problems and challenges that are observed. In this section, some of the SHARING partners describe their findings when evaluating strategies or performance of several aspects of the heterogeneous networks.

5.1 Fundamental performance limits of heterogeneous networks

Commentaire [KH12]: *SUPELEC*

The objective of this task is to investigate and analyze the performance of heterogeneous networks as a means to quantify the improvement in terms of coverage and rate by using such topologies. This will provide concrete measures on how much (and using which design/technologies) heterogeneous networks can give an answer to the data traffic "tsunami". The main challenges in performing this study are the following:

- The spatial modeling of the base station locations in a heterogeneous network remains an open topic, since little real-world information is yet available about picocell or femtocell deployments. It seems that the standard grid-based model that has been used in the past is not scalable to an accurate model of a heterogeneous multitier network. A first model, which is very tractable and allows us to derive closed-form expressions for key performance metrics, is a statistical one in which the base stations are located according to a Poisson point process in a two-dimensional plane. Such a spatial distribution for base station locations corresponds to complete randomness, and a large class of powerful results and analytical tools are available from the field of stochastic geometry. The Poisson model will be the starting point, however our performance analysis should consider other spatial models and random distributions that introduce a certain level of correlation and dependence among the base station placements.
- The issue of cell association should be taken into account and revisited as compared to traditional cellular networks. Although in existing macrocell networks, the max-power coverage regions for each base station are designed to have roughly the same amount of traffic, i.e., more base stations are deployed in areas that generate more traffic; a meaningful cell association policy should assign users to base stations that offer them the best user-perceived rate. However, optimizing the rate for all users is very complex as the rates of the users are coupled. Several relaxations and considerations should be made to be able to analyze the performance of heterogeneous networks with efficient cell association and realistic load balancing.
- A very important issue that is often neglected in the analyses is that of backhaul connection. It is often assumed that the main design challenge is the base station-mobile link and that the base station has a high-speed backhaul connection that easily handles the data flowing to and from it. In this task, the effect of backhaul connectivity and quality/robustness will be taken into account in the performance analysis of heterogeneous networks. Issues related to mobility, type of connection (wired vs. wireless) and propagation environments will play a critical role in the analysis.

This task is related to scenario 2.9.6 in [D.2.2].

5.2 Asymptotic performance analysis and design of wireless networks under heavy traffic

Commentaire [KH13]: *SUPELEC*

In this work [DES14][DES12], our main objective is to provide an asymptotic performance analysis of a wireless network composed of multiple transmitter-receiver pairs. Each transmitter is equipped with multiple transmit antennas and a coordinated beamforming is assumed to be used by the transmitters. We assume that the traffic arriving to the buffer of the transmitters is i.i.d. in time (with known mean value) and independent of the wireless channel. Furthermore, each user has an outage-based QoS metric to be achieved. In this context, the queue length of one transmitter depends also on the beamforming allocations of the other transmitters. The beamforming is performed such that the average total power is minimized and the probability that the queue size at each transmitter exceeding a threshold is bounded by a predefined threshold. We will consider the following probabilistic QoS metric for the queue length at each transmitter k

$$Pr\{q_k(t) > q_k^{thr}\} = \delta_k \tag{25}$$

which means setting a buffer outage probability in some values that can be tolerated by the application. The aforementioned QoS metric can provide better delay constraints as compared to other QoS metric based on the average queue length.

5.2.1 Interest of Heavy Traffic Modeling

Addressing the problem of coordinated beamforming under dynamic arrival traffic may not be tractable using standard optimization tools. We therefore develop our solution using the heavy traffic diffusion approximation since delay (and queue outage) is often easier to understand and analyze in this regime. Heavy traffic modeling provides an asymptotic analysis of the system where the traffic arrival is close to the boundary of the rate region. It is worth noting that delay grows to infinity if the arrivals are pushed toward the boundary of the rate region. The objective is then to design an algorithm that minimizes an asymptotic growth coefficient. It has been shown (e.g., see [BUCHE02][BUCHE05][WU06]) that developed control techniques using heavy traffic modeling performs quite well in the light/moderate traffic regime.

5.2.2 Brief description of the contribution

We tackle the coordinated beamforming and performance analysis problem by a proposing a strategy based on heavy traffic asymptotic modeling. The approach is then to divide the allocation into two parts: equilibrium and reserve beamformers. The equilibrium problem consists in allocating the beamformers according to the statistics of the channel states so that on average the transmission rate is equal to the arrival rate. This equilibrium allocation can be formulated as an optimization problem that turns out to contain some hidden convexity (one can refer to [LAK10][LAK11][LAK13] and the references therein for more details). The

transmission rate constraint can be converted using Second Order Cone Program (SOCP) into a convex problem. The main challenge lies then in the allocation of the reserve beamforming. It should be noticed that allocating the reserve beamforming using optimal control theory and Hamilton-Jacobi-Bellman (HJB) framework is very hard in this case. We therefore tackle the above reserve allocation problem as follows. We first show that the queues of the users in the heavy traffic regime can be modeled as a reflected multidimensional Stochastic Differential Equation (SDE). Then, taking advantage of the specific structure of the reflection matrix (due to the fact of having one receiver per transmitter), we propose a control policy that decouples the multidimensional SDE into several parallel SDEs and ensures that an invariant measure for each of these SDEs exists. Using results from probability theory, we can obtain a closed form expression of the stationary distribution function of the dynamics of each SDE which allows finding a relation between the reserve allocation and the overflow probability. We have noticed that the value of the reserve power allocated by our algorithm compared to the equilibrium power is very small, which implies that the sub optimality gap between our reserve allocation approach and other optimal control approach (e.g., using HJB) is small in many scenarios.

5.2.3 System Model

We consider a system of K transmitters each with L antennas serving one receiver and using bandwidth W. For notational simplicity, we index the transmitters and receivers so that transmitter k serves user k. Let $g_{ij}(t)$ denote the power gain of the channel between transmitter j and user i at time t. Each of these channel gains is assumed to evolve independently of the others as an ergodic finite state Markov chain. The matrix $\mathbf{H}(t) = \left[\mathbf{h}_{ij}(t)\right]$ of all channel gains at time t evolves then as an ergodic finite state Markov chain with, say, M_H possible states and we index the states as $S_H = \{1, \dots, M_H\}$. We shall denote the event that the channel gains are in the m-th state as $\mathbf{H}(t) = \mathbf{H}_m$. The corresponding ergodic probability distribution for each state will then be denoted as π_m, and let $\mathrm{E}_\pi\{\}$ denote the expectation over this probability distribution.

At receiver k, the interference from other transmitters is treated as Gaussian noise. When transmitter k uses beamformer $\mathbf{v}_k$, the rate $r_k\big(\mathbf{v}_1(t), \dots, \mathbf{v}_K(t), \mathbf{G}(t)\big)$ over the corresponding link will be,

$$r_k(\mathbf{v}_1, \dots, \mathbf{v}_K, \mathbf{H}) = W \log_2\left(1 + \frac{|\mathbf{v}_k^H(t)\mathbf{h}_{kk}|^2}{\sigma^2 + \sum_{i \neq k}\left|\mathbf{v}_i^H(t)\mathbf{h}_{ik}\right|^2}\right) \tag{26}$$

where W is the bandwidth and σ^2 is the noise variance. The power of transmitter k is given by $p_k(t) = \mathbf{v}_k^H(t)\mathbf{v}_k(t)$.

For each queue we suppose that the instantaneous arrivals $a_k(t)$ at time t are i.i.d., with mean λ_k and (finite) variance $\sigma_{a,k}^2$, and are independent of the arrivals at the other queues and the channel process.

In order to derive the heavy traffic asymptotic model, we assume that at a time interval Δt there will be $O(n\Delta t)$ arrivals and $O(n^\nu \Delta t)$ channel changes, for $0 < \nu < 1$. Therfore, n can be seen as the order of magnitude of the arrivals that grows highly in the heavy traffic situations

so that the network is in full load. We denote by $q_k(t)$ the queue length of transmitter k at time t, and $x_k^{(n)}(t)$ the scaled version as follows:

$$x_k^{(n)}(t) = \frac{1}{n^{\frac{\nu}{2}}} q_k(n^{\nu} t) \tag{27}$$

The heavy traffic condition in terms of arrival and departure rates will be [WU06]:

$$\lim_{n\to\infty} \left(\lambda_k^{(n)} - \mathrm{E}_{\pi}\left\{r_k\left(\mathbf{v}^{(n)}(t)\right)\right\}\right) n^{\frac{\nu}{2}} = \theta_k < 0, \ \forall k \in \{1, \dots, K\} \tag{28}$$

Under the aforementioned assumption, we have shown in [DES14] that the scaled queue can be modeled by a reflected diffusion process.

Theorem Consider K interfering links with L antennas at each transmitter. As $n \to \infty$ the vector-valued process of the scaled queue lengths is given as,

$$\mathbf{x}(t) = \mathbf{x}(0) - \int_0^t \mathbf{f}\big(\mathbf{u}(s)\big) ds + \boldsymbol{\Sigma}\mathbf{w}(t) + \mathbf{z}(t) \tag{29}$$

In the above, $\mathbf{w}(t)$ is a vector of K independent standard Wiener processes, $\mathbf{f}$ is the vector of the functions

$$f_k\big(\mathbf{u}(t)\big) = \sum_{m=1}^{M_H} \pi_m \sum_{j=1}^{LK} a_{k,j}(\mathbf{H}_m) u_j(t) \tag{30}$$

where $a_{i,j}(\mathbf{H}_m) = \frac{\partial r_i(\bar{\mathbf{v}}_a(\mathbf{H}_m))}{\partial v_j}$. The matrix $\boldsymbol{\Sigma} = [\sigma_{ij}]$ satisfies

$$\boldsymbol{\Sigma}\boldsymbol{\Sigma}^T = \boldsymbol{\Sigma}_a \boldsymbol{\Sigma}_a^T + \boldsymbol{\Sigma}_d \boldsymbol{\Sigma}_d^T \tag{31}$$

with $\boldsymbol{\Sigma}_a = diag(\sigma_{a,k})$ while the elements of the covariance matrix $\boldsymbol{\Sigma}_d \boldsymbol{\Sigma}_d^T = [s_{ij}]$ are given as

$$s_{ij} = 2\mathrm{E}\left\{\int_0^{+\infty} \hat{r}_i(0)\hat{r}_j(t) dt\right\} \tag{32}$$

where $\hat{r}_k(t) = \left(r_k\left(\bar{\mathbf{v}}(\mathbf{H}(t))\right) - \lambda_k\right)$. Finally, the elements of $\mathbf{z}(t)$ are given as

$$z_k(t) = \left[-\min_{s\le t}\left\{x_k(0) - \int_0^t f_k\big(\mathbf{u}(s)\big) ds + \sum_{j=1}^{K} \sigma_{kj} w_j(t)\right\}\right]^+ \tag{33}$$

Proof. Please refer to [DES14] for the proof.

As mentioned above, we then consider a simple/specific control policy that allows decoupling the multidimensional SDE into several parallel SDEs and ensuring that an invariant measure for each of these SDEs exists. The probabilistic QoS metric is then met by a specific choice the control vector. This is summarized in the following two results.

Lemma Consider a reserve control policy that does not depend on the channel states. Then the asymptotic model reduces to

$$d\mathbf{x}(t) = \mathbf{B}\mathbf{u}\big(\mathbf{x}(t)\big)dt + \mathbf{\Sigma}d\mathbf{w}(t) + d\mathbf{z}(t) \tag{34}$$

Lemma The overflow requirements for the asymptotic system can be satisfied by the following policy:

$$\mathbf{u}\big(\mathbf{x}(t)\big) = \mathbf{B}^{-1}\mathbf{C}\mathbf{x}(t) \tag{35}$$

with $\mathbf{C} = diag(-|c_k|)$ and $|c_k| = \frac{1}{2}\left(\frac{\sigma_{a,k}}{x_k^{thr}} erfc^{-1}(\delta_k)\right)^2$. In the above, x_k^{thr} is the corresponding threshold in the asymptotic regime.

Further discussions about the decentralized implementation of the aforementioned policy, with imperfect channel knowledge and delayed information exchange between the transmitters, can be found in [DES14].

5.2.4 Numerical Results

Finally, we provide some numerical results in a simple setting in order to show that our approach can yield desirable results in practical systems. We consider a simple scenario with 3 interfering transmitter - receiver pairs, using the same bandwidth of 5 MHz. We assume that each channel gain has only two possible values. Also, the arrivals at each transmitter are set as Poisson processes with mean rates equal to 1, 1.5 and 2 Mbps. The overflow thresholds are set to 500, 750, 1000 bits at each transmitter respectively and the overflow probability to 0.01 for all transmitters. The coherence time of the channels is set to 20 ms, modeling then slow fading channels in indoor or low mobility environments. In Figure 50, we can observe that the queue length under the proposed power control method behaves in a much more controlled manner and is below its respective threshold for most of the time. This means that our solution can be suitable for services with stringent delay constraint. In Figure 51, we can observe that the allocated reserve power is very small as compared to the equilibrium power.

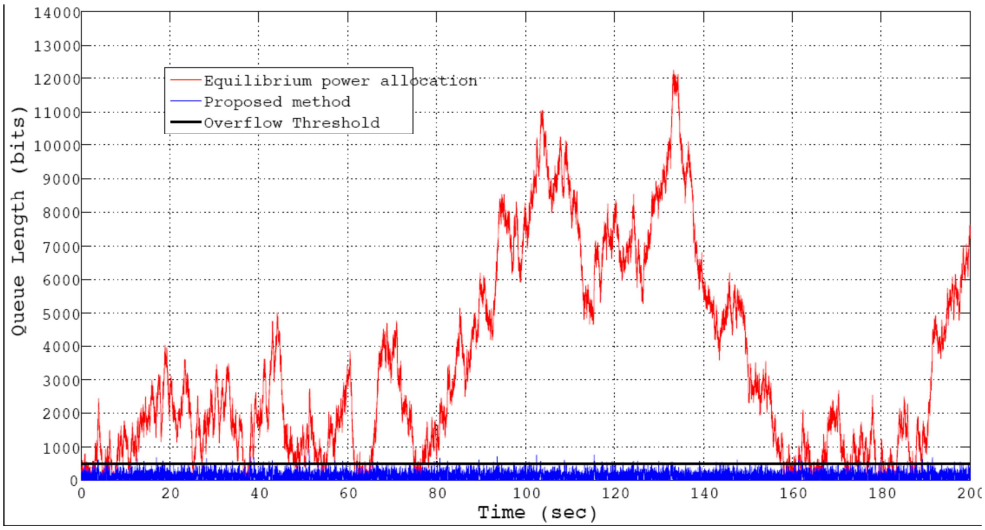

Figure 50. Evolution of the queue length

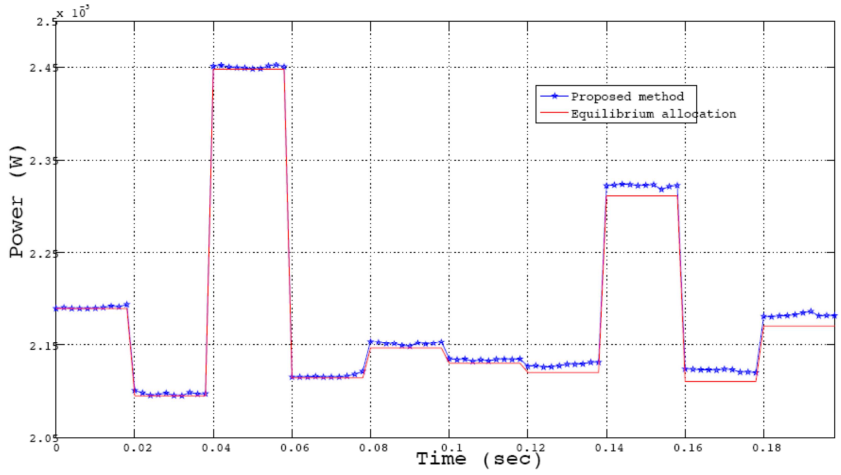

Figure 51. Evolution of the allocated power

5.2.5 Conclusion

In this section, we have studied the problem of beamforming and power allocation in a wireless network under heavy traffic limit. The objective is to keep the queue outage probability under a certain threshold while the channel evolves according to an ergodic Markov chain. For that we divide the allocation into two parts: i) equilibrium part allocated depending on the channel statistics, and ii) drift part which is function of the backlogged queues of the users at each time. Under this model, it was shown in this work that the scaled queue can be modeled as a reflected diffusion process. This allowed us to derive a closed

form expression of the allocated power and beamforming and a closed form expression of the outage probability. We have provided numerical results that corroborate our claim of improving the system performance.

5.3 Performance of heterogeneous network deployments in a large-scale real environment

Commentaire [KH14]: *SIRADEL*

In front of the huge data traffic growth [Cis14], one of the most promising answers is to densify existing macro network with small (low-power)cells [Hu11]. The reduction of interference, which is the major issue to be solved in such two-tier network, has been anticipated with the introduction of specific eICIC techniques in 3GPP LTE Release-10. Those techniques should be completed with automated network management algorithms to allow for plug-and-play installation and live optimization. Another key issue that may limit the small cell layer capacity is the backhaul network that relays the user data between the core network and the small cells. The deployment of a wired backhaul is an option, but its feasibility depends on the existing optical fiber network and on leasing costs. In many cases actually, the small cells will be deployed along with a wireless (or mixed) backhaul [SCF13]. The location of the small cells, in-street and below surrounding buildings, makes them hard to reach with traditional Line-Of-Sight (LoS) wireless backhaul which is typically used for macrocells. The selected backhaul technology must thus show strong performance even in Non-LoS (NLoS) conditions [Let14]. The links towards aggregation points, also known as hubs, which are connected to the core network, brings new challenges in the network design. In particular, the reliability of the link is of the highest importance to ensure a constant QoS to the end-user.

Densification of wireless networks with small cells usually starts with the will to enhance user QoS, and is driven by the spatial user traffic distribution, i.e., the small cell antennas are installed to increase local network capacity in relation with a local high throughput demand. But best small cell locations regarding the user QoS might not meet backhaul constraints and this could create a bottleneck in the network. The following study is thus divided in two main parts. The heterogeneous network performance under ideal backhaul assumption is first evaluated considering different small cell layer designs. Then we introduce the backhaul network on top of one of these deployments, considering different approaches, from manual to automated designs. Finally, the heterogeneous network performance is combined with backhaul capacity to characterize the impact of wireless backhaul.

5.3.1 Small cell densification design and performance evaluation under realistic traffic demand rise

The study reported in this section aims at the identification of small cell network topologies and configurations that improve QoS while minimizing energy consumption, which is a major part of the operational costs for an operator. The user QoS is characterized by the downlink/uplink service coverage outage and the user peak throughput statistics. The energy efficiency is assessed by considering the average downlink power consumed by eNodeB's transmission with respect to their traffic load according to the model published in [Kle11], which distinguishes the power consumption between macro and micro base stations (the micro model is assigned to the small cell).

The analysis of the uplink/downlink LTE-A network performance relies on an extended version of the 3D coverage simulation tool presented in [Bra12]. The user traffic is spatially distributed in 3D to take into account indoor users at different floors. Thus path loss predictions are computed at different heights based on a real 3D environment representation and the Volcano technology (site-specific ray-based propagation models [Cor09]). The framework integrates ICIC/eICIC techniques to mitigate interferences. In downlink, a static ICIC Fractional Frequency Reuse (FFR) scheme is considered for Macro eNodeB (MeNB). It is complemented with a Time-Domain eICIC to enhance the cell-edge experience of small cell users [Ped13]. Two main parameters can be tuned to modify the eICIC configuration: CRE and the ABS duty cycle, the first one being typically used to favour the attachment of users to a small cell instead of a macro eNodeB, while the second one is applied to reduce the interference of small cell edge users. In uplink, the power control relies on the conventional Open-Loop Power Control (OLPC) technique, which is driven by two cell-specific parameters: a path loss compensation factor to adjust the link quality and transmit power as a function of the path loss; and the uplink SINR target. Uplink ICIC is also enabled in case of high interference levels [Cas08].

The scenario relies on a typical macro network layout in the dense urban environment of Paris VII district, which is densified with co-channel small cells. Macro eNodeBs are deployed over a larger area, on two rings around a central three-sector site in order to take into account realistic interference patterns. Small cells are introduced into the network infrastructure to enhance the coverage and boost the capacity. They are uniformly deployed on urban furniture along the streets (at a moderate height of 6 m), leading to a quasi-constant ISD. Three different small cell deployment topologies are evaluated in the present study, respectively with ISD of 200 m, 100 m (shown in Figure 52) and 50 m. Small cells have omni-directional antennas and their maximum transmit power can take values from 100 mW to 5 W. Other main simulation parameters are summarized in Table 15

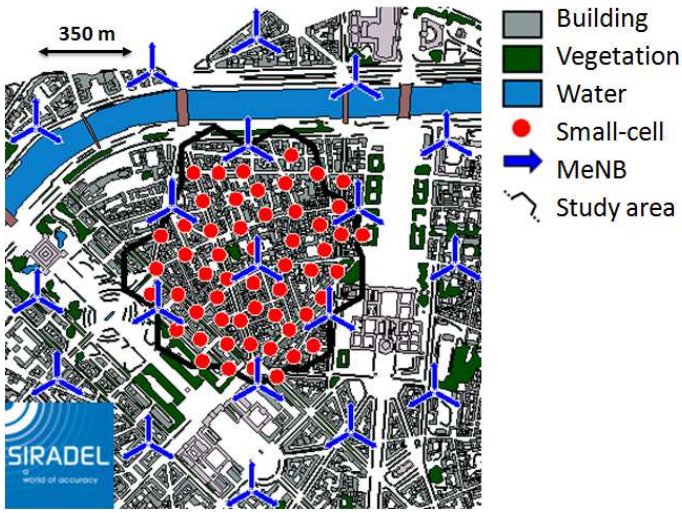

Figure 52. Simulation setup (small-cell ISD 100m).

Table 15. Simulation parameters.

System	LTE FDD 2x10 MHz. Central frequency: 2.6 GHz. Uplink/Downlink MIMO configuration: 2 x 2. Uplink path loss compensation factor: 1. Uplink SINR Target: 20.8 dB (when uplink ICIC is disabled).
Macrocell layout	Hexagonal site deployment: two rings around the central site, i.e., 19 sites corresponding to 57 cells (see Figure 52). Inter-site distance (ISD): 450 m. ICIC FFR scheme: 5% of total radio resources being allocated to each sub-band, re-use factor of 3. Average antenna height: 32 m above ground. Maximum total transmit power: 40 W. Antenna: directional, 14 dBi, 6° electric down-tilt, 32 m above ground. Uplink noise figure: 2.5 dB.
Small cell layout	Spectrum usage: co-channel. Small cell deployment: uniform with ISD from 50 m to 200 m. Maximum total transmit power: from 100 mW to 5 W. Antenna: omnidirectional, 5 dBi, 6 m above ground. Uplink noise figure: 2.5 dB.
User equipment	Uplink total transmit power: from -40 dBm to +23 dBm. Antenna: omni-directional, 0 dBi, 1.5 m above ground. Downlink noise figure: 9 dB.

In the 0.98 square km study area, active users are spread with following rules:

- 1000 active users per square km; one third is served by the considered operator.
- 20% outdoor users, uniformly distributed over the area.
- 80% indoor users, uniformly distributed in the building floors (meaning that the number of users in a building is proportional to its height).

The same throughput demand is assumed for all users. The study starts with mean throughputs of 90 kbps in downlink and 30 kbps in uplink. The downlink mean throughput has been chosen such that the interference level in the initial macro network leads to 10% of user service outage (i.e., percentage of users that cannot be served with the required throughput). Then in order to subject the network to a realistic traffic increase, we consider an annual mobile traffic growth of 47% [Cis14] during the five years following 2015. We make the assumption that the number and the distribution of active users are kept constant over the years but that their uplink/downlink throughput demands increase. The obtained evolution thus goes from 90 kbps at Y0 to 610 kbps at Y0 + 5 years (Y5) in downlink and from 30 kbps at Y0 to 205 kbps at Y5 in uplink, as illustrated in Figure 53. Note that these throughput values represent the mean user throughputs during active communications.

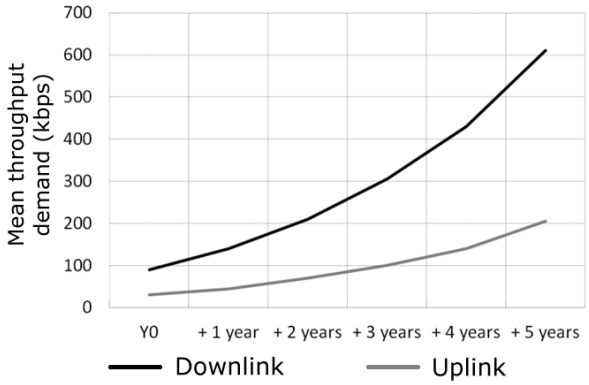

Figure 53. Mean active user downlink and uplink throughput demand growths considered in the study.

The proposed analysis involves many variable parameters related to topology, offloading, user traffic and interference management. A rough and exhaustive presentation of results would be unreadable. We made the choice to structure the results in two main scenarios, as follows:

1. The impact of the network configuration is studied with initial user traffic demand (considered as "moderate"). First, the optimal configuration (CRE and ABS) is found for each ISD. Then the different small cell densification strategies (from the three simulated ISD) are compared.
2. We go further in the evaluation by characterizing the performance of the three small cell densification strategies over a period of 5 years. Operators must indeed anticipate the evolution of the network performance over several years before starting the initial densification stage. We analyze how a heterogeneous network configuration found suitable, or even optimal, to accommodate the current network traffic at a given time may be impacted when traffic increases.

In the initial scenario, we first consider a small cell deployment with a fixed ISD and search for the optimal configuration (transmit power, CRE, ABS duty cycle) based on the joint analysis of the network capacity and energy efficiency. Simulated results for ISD equal to 100 m are presented in Figure 54. The transmit power of small cells varies along the x-axis, while the different curves correspond to different CRE values. The horizontal dotted lines give the macro-only performance as a reference. Only results with ABS duty cycle equal to 12.5% are shown.

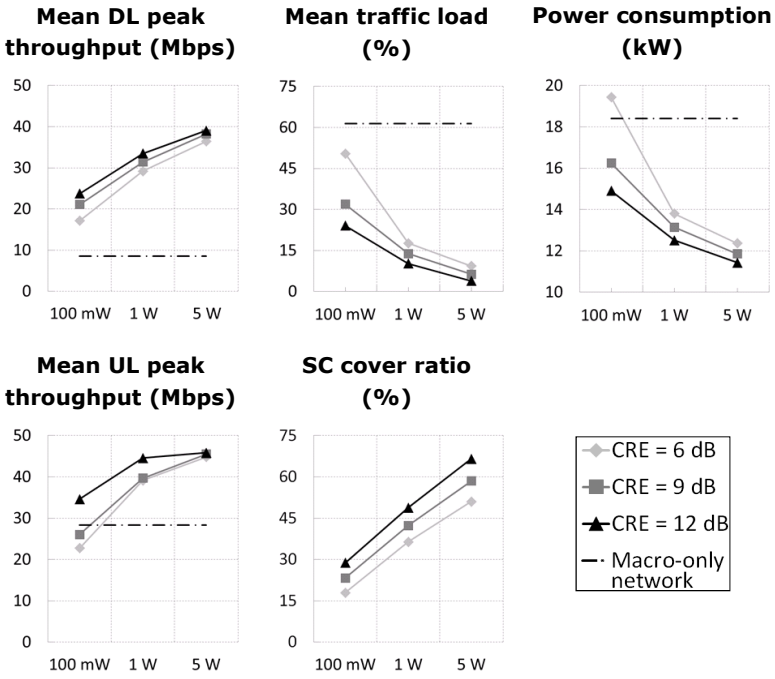

Figure 54. Network performance KPIs for various small cell (SC) transmit powers and CRE.

It is observed that all tested small cell configurations allow for full service coverage, on the contrary to the macro-only network. The small cell cover ratio shows increasing macro eNodeB offloading to the small cells when increasing small cell transmit power and CRE value. The performance is particulary increased with at least double downlink peak throughput. The uplink peak throughput is also significantly increased for a small cell transmit power higher than 1 W, making more users send data to closer eNodeBs with less path loss. Further increasing the small cell transmit power jointly enhances the QoS and reduces eNodeB downlink power consumption. These results stress the great benefits of small cell deployment. Same tendency is observed for small cell deployments with ISD equal to 200 m and 50 m, i.e., the optimal configuration is obtained when small cell transmit power and CRE are maximal.

We then compare small cell densification topologies (respectively with ISD equal to 50 m, 100 m and 200 m) based on these optimal configurations. Figure 55 shows the user downlink and uplink peak throughput obtained with these different topologies compared to the macro-only scenario. It is observed that the denser the small cell layer is, the higher is the user peak throughput. In particular, the cell-edge users seem to benefit from the network densification: the 5%-ile downlink peak throughput for ISD equal to 50 m is 43 times higher than the one of the macro-only network. Besides, the total power consumption decreases while the number of small cells increases thanks to the large decrease of the macro eNodeB traffic loads as shown in Table 16. In heterogeneous topologies, the percentage of macro eNodeB consumption decreases with ISD, while the small cell consumption strongly increases. A minimum is reached with ISD equal to 100 m. ISD equal to 200 m indeed allows for only limited macro

offloading; and ISD equal to 50 m leads to a high proportion of energy consumed by the small cell layer.

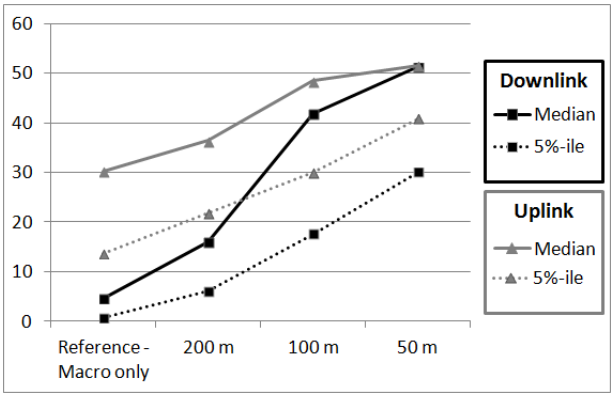

Figure 55. User peak throughput (Mbps) versus ISD.

Table 16. Network power consumption versus ISD.

ISD	Reference – Macro only	200 m	100 m	50 m
Total consumption (kW)	18.40	17.02	11.74	15.08
% from macro eNodeB	100.0	92.8	75.0	53.0

In the second scenario, we focus on the performance of the three different small cell deployment strategies against the network traffic growth over a period of five years. Figure 56 shows the downlink/uplink service outage as a function of the time. With the macro-only network, it exceeds 10% as soon as Y1 in downlink, and Y3 in uplink. The availability of radio resources is commonly the main limiting factor in downlink (overloading) whereas the service coverage is the main limiting factor in uplink (low SINR).The lowest densification (ISD equal to 200 m) is not sufficient to decrease the downlink outage under the 10% threshold, demonstrating that it is not appropriate either as a mid-term solution. On the contrary, the intermediate densification (ISD equal to 100 m) fullfils this requirement until Y3 and the highest one (ISD equal to 50 m) until Y4.

Finally, none of the tested small cell densifications allows for satisfactory user coverage in Y5. The first limiting factor for low to medium small cell densifications is the downlink network capacity. On the contrary, the highest densification undergoes first a significant loss of coverage in the uplink, due to strong interference levels. This observation highlights the importance of considering both downlink and uplink coverage-limited criteria when designing dense heterogeneous network deployments.

The analysis of user peak throughputs and energy efficiency is only relevant when the network outage remains acceptable. That is why in the following, we only compare those

metrics for scenarios having a network service outage lower than 10%. Main results are reported in Figure 57.

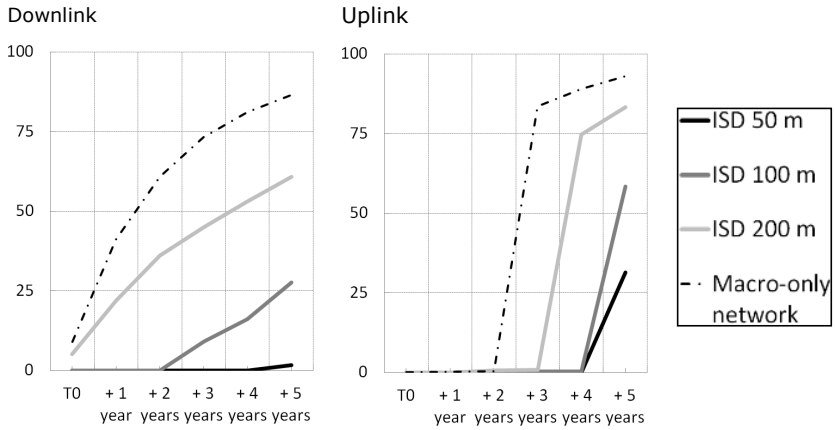

Figure 56. Service outage (%) evolution over time.

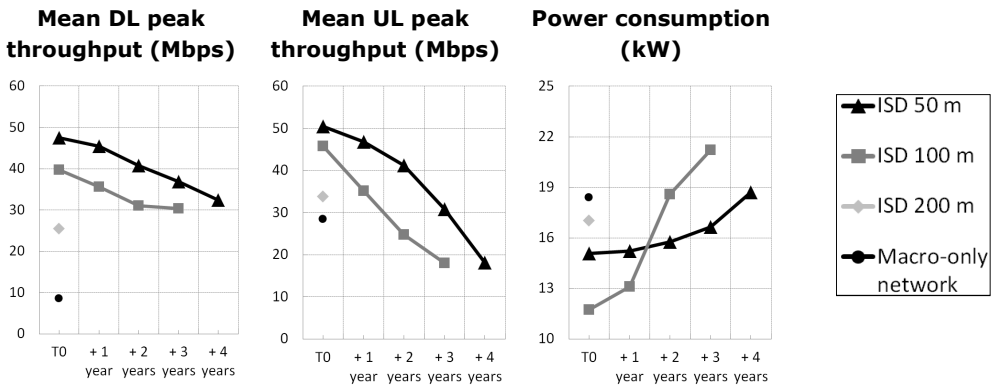

Figure 57. Network KPIs evolution over time.

The increase of user data traffic leads to significantly degraded mean downlink and uplink peak throughputs over time. For instance, they are respectively reduced by 30% and 64% at Y5 with ISD equal to 50 m. Nevertheless the densification with ISD equal to 50 m clearly remains the best option for almost all KPIs. The best energy efficiency (ratio between the downlink power consumption and downlink user traffic) is provided by ISD equal to 100 m up to Y1 and by ISD equal to 50 m in following years. As soon as the traffic load grows up in the macro layer, the total downlink power consumption significantly increases, thus the small cell deployment with maximum offloading becomes the most efficient. This demonstrates that the best strategy at Y0 (based on current traffic conditions) does not necessarily remain the best strategy in the long-term.

The current study provides input for evaluating the impact of small cell densification on network performance and base station downlink power consumption in different traffic conditions. Such analysis can help in the definition of a densification strategy over the years. Of course, when dealing with network optimization strategies, we must further consider costs (CAPEX/OPEX) as well as installation and backhauling constraints. The next section thus resumes these studies by characterizing the impact of a non-ideal backhaul design on small cell deployments and end-user experience.

5.3.2 Impact of wireless NLOS backhaul design on small cell deployments and end-user experience

As shown in the design methodology in Figure 58, the deployment of small cells is driven by the traffic distribution [Col12] so as to capture realistic user demand and optimize operational costs. Then the backhaul (wired + wireless) must be designed to feed the small cells with the requested user throughput. Both the small cell and backhaul deployments rely on radio planning techniques to select the antenna locations and other system parameters. Radio planning simulations can be done in two separate stages (without considering the backhaul constraints in the small cell design), but we illustrate in this section the interest of predicting the performance of the whole backhaul + small cell infrastructure.

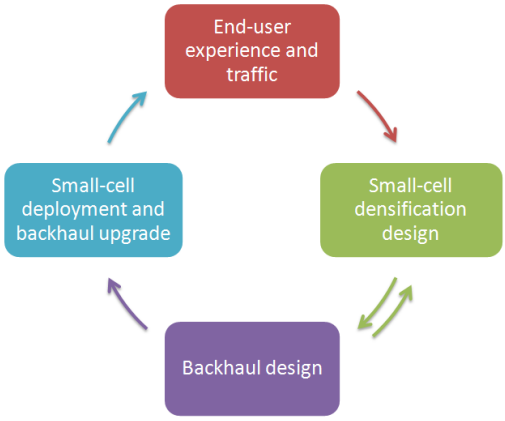

Figure 58. Small cell and backhaul joint design methodology.

One of the optimal heterogeneous network configurations obtained in the previous section is used as a reference. It is composed of a macro LTE layer which is densified with uniformly distributed small cells (average separation of 200 m) to globally increase the network capacity on the user plane. The performance reported in previous section relies on an ideal backhaul assumption. In the following, we explore different options for the backhaul deployment design in order to characterize its impact on the real network downlink capacity and make propositions on the design methodology.

The locations of the wireless backhaul hub candidates are pre-defined. Actually the hubs are assumed to be co-located with already existing macrocells. Detailed system parameters are given in Table 17.

Table 17. Backhaul system parameters.

System	LTE FDD 2x10 MHz. Central frequency: 2.6 GHz. MIMO configuration: 2 x 2.
Hubs	Hexagonal site deployment co-located with macro eNodeB (see Figure 52). Maximum total transmit power: 30 dBm per antenna. Antenna: directional (60° horizontal aperture), 12 dBi, 1 m below macro eNodeB antenna.
Small cell remotes	Small cell deployment: uniform with ISD from 200 m. Antenna: directional (60° horizontal aperture), 8 dBi, 6 m above ground. Downlink noise figure: 6 dB.

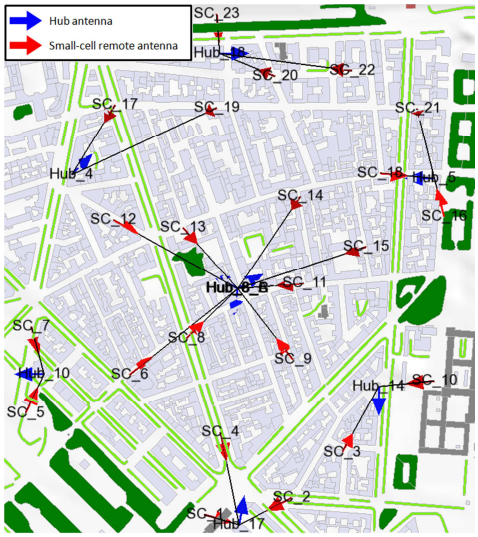

Figure 59. Basic backhaul design.

In a first study, the backhaul design is realized manually by following a basic rule: a hub is connected to a cluster of maximum three small cells located in the same area; and its directive antenna is oriented towards a median direction. The remote antennas of the small cells are oriented towards the hub they are attached to. Figure 59 shows this basic design where the 23 small cells are attached to 9 hubs (three of them being co-located at the central site).

The path loss is estimated with the same ray-based propagation model used for small cell-to-end-user predictions in the previous section. Under the assumption of an average co-channel interference of -80 dBm, all small cells show high quality links with the hubs they are attached to, and are thus served with sufficient performance to fullfil the user downlink aggregated throughput being 4.5 Mbps per small cell in average at Y5. But when predicting

the deterministic interference from all hubs with a 50% load assumption, the same backhaul design shows poor performance and introduces a bottleneck in the network. Actually, 6 hubs have very weak connections with one or more small cells and are unable to feed them with the expected throughput. These weak connections induce an overload of these hubs, which are thus unable to serve even the small cells with high SINR because of the lack of radio resources. Finally, only 7 small cells are served with the expected throughtput. In this configuration, the end-user would finally experience slower data rates than expected by the initial small cell design because of the backhaul limitation. These results show how a well deployed small cell layer can be inefficient without taking into account the backhaul constraint or without efficient backhaul design.

A second backhaul design is proposed where the selection of the hub candidates, the small cell attachments and the antenna orientations are all together optimized in an automated process to feed the small cells with requested downlink throughput at Y5. Deterministic co-channel interference is predicted and taken into account in the optimization process. Figure 60 shows three small cells that have been attached to one hub during the automated process. The impact of ray-tracing is highlighted by remote antennas being oriented towards strong indirect paths.

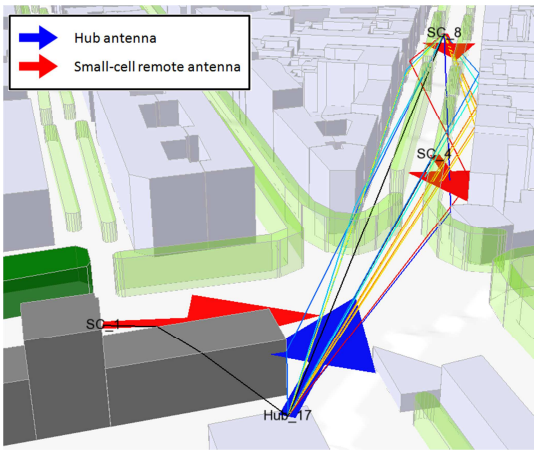

Figure 60. Attachement of three small cells to one hub.

Figure 61 shows the optimized backhaul design obtained with the automated process. With this configuration, only one hub suffers from a very weak connection and is overloaded. Actually, this small cell is interfered by a hub located on the third ring, which is not set as a candidate for attachement because the third ring is introduced only for realistic interference at the edge of the study zone. We observe that the small cell named 'SC_17' is able to attach to the distant hub named 'Hub_17', because this connection is actually found to operate in LoS thanks to the 3D capabilities of the simulator. Finally, 17 small cells are served with the required throughput and the average traffic load of the hubs is 45% when excluding the overloaded one. Large margin and low loads permit to support peak traffic and anticipate future traffic growth. These results show how an optimized process is able to provide a better wireless backhaul design in much less time.

Nevertheless, it may happen that a small cell cannot be attached to any hub because it is too obstructed or too interfered. Manual operations are then necessary, that can be for instance:

- Moving an existing hub to provide better received signal to the attached small cell.
- Adding another hub to offload the initial ones.
- Moving a small cell to try to isolate it and reduce interference from other hubs.

This latter proposition highlights the necessity for a small cell and backhaul joint design as shown in Figure 58.

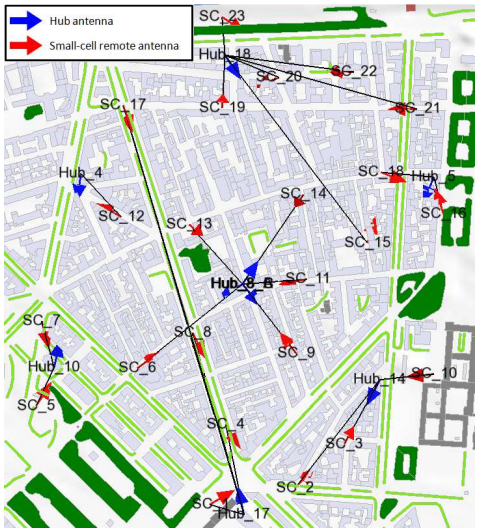

Figure 61. Optimized backhaul design from the automated process.

5.3.3 Conclusion

This section analyzes the performance of heterogeneous network deployments in a large-scale real environment, in terms of usual QoS and energy efficiency. The main objective is to identify network deployment rules that would allow achieving optimal performance from multiple key indicators taking into account a realistic and well-accepted forecast over a period of five years of wireless data traffic demand growth.

A first study under ideal backhaul assumption evaluates three different small cell deployment topologies with respectively ISD of 200 m, 100 m and 50m. For each topology, the optimal network configuration is first derived from a moderate user traffic (i.e., the one considered at Y0 by the tuning of small cell maximum transmit power, CRE and ABS duty cycle). This study relies on simulation results obtained with an innovative network coverage and analysis tool taking into account both uplink and downlink. Results show that the highest tested offloading configuration (small cell transmit power of 5 W and CRE of 12 dB) and largest tested ABS duty cycle (25%) leads to the best user QoS. The highest tested small cell densification (ISD equal to 50 m) generally gives the best coverage and highest peak throughputs; and it is the only one supporting the four-year traffic growth tested in the study (initial traffic demand x

4). All these results tend to demonstrate the interest of deploying small cell to jointly absorb expected traffic increase and reduce downlink energy consumption.

A second study focuses on the wireless backhaul design to relay the user data between the small cell layer with ISD equal to 200 m to the core network at Y5. A first basic approach that consists in a manual attachement of small cells to hubs and median antenna orientations shows very poor performance, making the wireless backhaul introduce a bottleneck in the network. A second automated approach is proposed where the selection of the hub candidates, the small cell attachments and the antenna orientations are all together optimized. It results in a much better performing wireless backhaul where 74% of the small cells can be served with the required downlink throughput, and hubs, which are co-located with macro eNodeBs, experience an average load of 45%. A perspective to this work is to illustrate the impact of the backhaul limitations on the end-user throughput statistics. The backhaul uplink performance will also be evaluated and included in the optimization process.

6 CONCLUSIONS

This deliverable has provided an initial view from SHARING Work Package 4, Task 4.1, on innovative concepts and performance evaluation related to intra-system offloading. Thus, the goal of the presented innovations is to improve the network performance, cost- or energy-efficiency by steering traffic between cells belonging to the same RAT, e.g., LTE or HSPA.

New concepts are presented within the areas of: SON-based load balancing and interference management, load balancing with the help of large scale antenna systems or middleware deployment, mobility management between macro and low-power nodes and backhaul offloading via proactive caching of data. In addition to presenting new concepts, this deliverable discusses also the performance and deployment strategies of heterogeneous network deployments within various realistic scenarios.

Based on the obtained evaluation results the proposed concepts are indeed able to improve both the user performance and the overall system capacity. Furthermore, the proposed concepts are shown to reduce the overall network energy consumption. In general, the observed performance enhancements are expected to contribute to lower CAPEX and OPEX for the operators. However, more work is still needed to investigate the real potential of the proposed concepts.

7 REFERENCES

[3GPP10a] 3GPP TR 36.814, v9.0.0 "Evolved Universal Terrestrial Radio Access (E-UTRA); Further advancements for E-UTRA physical layer aspects", March 2010.

[Bra12] M. Brau, Y. Corre and Y. Lostanlen, "Assessment of 3D network coverage performance from dense small-cell LTE", IEEE International Conference on Communications (ICC) 2012, Ottawa, June 2012.

[BUCHE02] R. Buche and H. J. Kushner, "Control of mobile communications with time-varying channels in heavy traffic," IEEE Transactions on Automatic Control, vol. 47, no. 6, pp. 992 –1003, Jun, 2002.

[BUCHE05] R. T. Buche and C. Lin, "Heavy traffic control policies for wireless systems with time-varying channels," in Proceedings of the 2005 American Control Conference, Jun. 2005, pp. 3972 – 3974 vol. 6.

[Cas08] C. U. Castellanos, F. D. Calabrese, K. I. Pedersen and C. Rosa, "Uplink interference control in UTRAN LTE based on the overload indicator", IEEE 68th Vehicular Technology Conference, May 2008.

[CHIA08] L. Chiaraviglio, D. Ciullo, M. Meo, and M. A. Marsan, "Energy-aware UMTS access networks," in The 11th International Symposium on Wireless Personal Multimedia Communications (WPMC'08), 2008.

[Cis14] Cisco, "Cisco Visual Networking Index: Global Mobile Data Traffic Forecast Update 2013-2018", February 2014.

[Col12] Coletti, C.; Hu, L.; Huan, N.; Kovács, I. Z.; Vejlgaard, B.; Irmer, R. & Scully, N. "Heterogeneous deployment to meet traffic demand in a realistic LTE urban scenario" Vehicular Technology Conference (VTC Fall), 2012 IEEE, 2012, 1-5.

[Cor09] Y. Corre and Y. Lostanlen, "Three-dimensional urban EM wave propagation model for radio network planning and optimization over large areas", IEEE Transactions on Vehicular Technology, Vol. 58, No. 7, pp. 3112-3123, Sept. 2009.

[D.2.2] Celtic-Plus SHARING, Deliverable D2.2, "Scenarios, KPIs and Evaluation Methodology for Advanced Cellular Systems", 2014.

[D.4.1] Celtic-Plus SHARING, Deliverable D4.1," New opportunities, challenges and innovative concept candidates for SON/Heterogeneous Networks", 2014.

[DES12] A. Destounis, M. Assaad, M. Debbah, B. Sayadi and A. Feki, "Heavy Traffic Approach for Queue-Aware Power Control in Interfering Wireless Links", IEEE SPAWC 2012, June 2012.

[DES14] A. Destounis, M. Assaad, M. Debbah, B. Sayadi and A. Feki, "On Queue-Aware Power Control in Interfering Wireless Links: Heavy Traffic Asymptotic Modelling and Application in QoS Provisioning ", IEEE Transactions on Mobile Computing, Vol 13 No. 10, pp. 2345-2356, 2014.

[Eri13] Ericsson, "Ericsson Mobility Report – On the Pulse of the Networked Society", November 2013.

[GATI14] A. Gati, S. Martinez Lopez, and T. En-Najjary, "Impact of traffic growth on energy consumption of LTE networks between 2010 and 2020," in Self-Organizing Networks (SONETs) Workshop in conjuction with IEEE Wireless Communications and Networking Conference (WCNC 2014), 2014.

[GDOC14] "Greentouch mobile working group architecture doc2," Internal document of GreenTouchMobile WorkingGroup, March 2013.

[GT13] GreenTouch, "Green meter research study: Reducing the net energy consumption in communications networks by up to 90% by 2020,"White paper, June 2013, available online (25 pages). [Online]. Available: http://www.greentouch.org/uploads/documents/GreenTouch Green Meter Research Study 26 June 2013.pdf

[GT14] "Green touch," http://www.greentouch.org/.

[HOY11] J. Hoydis, S. ten Brink, and M. Debbah, "Massive MIMO: How many antennas do we need?" CoRR, Sept. 2011.

[Hu11] R. Q. Hu, Y. Qian, S. Kota, and G. Giambene, "Hetnets-a new paradigm for increasing cellular capacity and coverage [guest editorial]," Wireless Communications, IEEE, vol. 18, no. 3, pp. 8-9, 2011.

[Kle11] H. Klessig, A. J. Fehske and G. P. Fettweis, "Energy efficiency gains in interference-limited heterogeneous cellular mobile radio networks with random micro site deployment", in Proc. 34th IEEE Sarnoff Symposium, Princeton, New Jersey, USA, 2011.

[LAK10] S. Lakshminarayana, J. Hoydis, M. Deabbah and M. Assaad, "Asymptotic Analysis of Distributed Multi-cell Beamforming", in proc. of IEEE PIMRC 2010, Istanbul, Turkey, Sep. 2010..

[LAK11] Subhash Lakshminarayana, M. Debbah and M. Assaad, "Asymptotic Analysis of Downlink Multi-cell Systems with Partial CSIT," IEEE International Symposium on Information Theory (ISIT 2011), July 31 – August 5, 2011, Saint Petersburg, Russia.

[LAK13] Subhash Lakshminarayana, Mohamad Assaad, Merouane Debbah, "H-Infinity Control Based Scheduler for the Deployment of Small Cell Networks", Performance Evaluation Journal, 70(7-8), pp. 513-527, 2013.

[Let14] F. Letourneux, S. Guivarch and Y. Lostanlen, "3D Propagation and Environment Modeling for NLOS Wireless Small-cell Backhaul", in Proc EuCAP'14, The Hague, April 2014.

[MAR10] T. L. Marzetta, "Noncooperative cellular wireless with unlimited numbers of base station antennas," Trans. Wireless. Comm., vol. 9, no. 11, pp. 3590–3600, Nov. 2010. [Online]. Available: http://dx.doi.org/10.1109/TWC.2010.092810.091092

[MIN14] W. Min, E. Ramos, Y.P. Wang, N. Lidian, S. Nammi, M. Curran, Evaluation of Mobility Performance and Deployment Scenarios in UMTS Heterogeneous Networks. IEEE VTC 2014 Spring; February 18, 2014

[Ped13] K.I. Pedersen, Y. Wang, S.Strzyz and F. Frederiksen, "Enhanced inter-cell interference coordination in co-channel multi-layer LTE-advanced networks", Wireless Communications, IEEE, 20.3: 120-127, June 2013.

[PLAN07] G. A. Plan, "An inefficient truth," http://globalactionplanorguk.site.securepod.com/upload/resource/-Exec-Summary.pdf, Dec. 2007.

[SCF13] Small-cell forum, Backhaul Technologies for Small-cells, February 2013.

[VER08] W. Vereecken, L. Deboosere, D. Colle, B. Vermeulen, M. Pickavet, B. Dhoedt, and P. Demeester, "Energy efficiency in telecommunication networks," in NOC2008, 2008.

[WU06] W. Wu, A. Arapostathis, and S. Shakkottai, "Optimal power allocation for a time-varying wireless channel under heavy traffic approximation," IEEE Transactions on Automatic Control, vol. 51, no. 4, pp. 580 – 594, April 2006.

GLOSSARY

ACRONYM	DEFINITION
3D	Three-Dimensional
3GPP	Third Generation Partnership Project
4G	Fourth Generation cellular system
AAS	Active Antenna Systems
ABR	Average Bit Rate
ABS	Almost Blank Subframes
ACK	Acknowledgement
AP	Access Point
BCR	Block Call Rate
BS	Base Station
BW	Bandwidth
CAPEX	Capital Expenditure
CDF	Cumulative Distribution Function
CF	Collaborative Filtering
CRE	Cell Range Extension
CS	Central Scheduler
CSI	Channel State Information
CURE	Cell Uplink Range Expansion
DCR	Drop Call rate
DL	Downlink
EARTH	Energy Aware Radio and Network Technologies
EE	Energy Efficient
eICIC	Enhanced Inter-Cell Interference Coordination
eNB	Evolved NodeB

eNodeB	Evolved NodeB
FDD	Frequency Division Duplex
FFR	Fractional Frequency Reuse
FTP	File Transfer Protocol
FTT	File Transfer Time
GBR	Guaranteed Bit Rate
HetNets	Heterogenous Networks
HJB	Hamilton-Jacobi-Bellman
HM	Handover Margin
HS	High Speed
HSPA	High Speed Packet Access
ICIC	Inter-Cell Interference Coordination
ICT	Information and Communication Technology
ID	Identity
IP	Internet Protocol
ISD	Inter-Site Distance
JPM	Joint Performance Metric
KPI	Key Perforamance Indicator
LB	Load Balancing
LHS	Latin Hypercube Sampling
LPN	Low-Power Node
LTE	3GPP Long Term Evolution
LTE-A	LTE-Advanced
LOS	Line Of Sight
LSAS	Large Scale Antenna System
MAC	Medium Access Control
MeNB	Macro eNodeB

MIMO	Multiple-Input Multiple-Output
MLB	Mobility Load Balancing
MSC	Message Sequence Chart
MU-MIMO	Multi-User MIMO
NLOS	Non-Line Of Sight
NP	Network Parameter
OLPC	Outer Loop Power Control
OMC	Operations and Maintenance Center
OPEX	Operational Expenditure
OTT	Over The Top
PA	Power Amplifier
P-CPICH	Primary Common Pilot Channel
PDCP	Packet Data Convergence Protocol
PRB	Physical Resource Block
PU	Public
QoS	Quality of Service
RAN	Radio Access Network
RAT	Radio Access Technology
RE	Range Extension
RF	Radio Frequency
RLC	Radio Link Control
RNC	Radio Network Controller
RRC	Radio Resource Control
RRH	Remote Radio Head
RRM	Radio Resource Management
RRU	Remote Radio Unit
RSRP	Reference Signal Received Power

RSSI	Received Signal Strength Indicator
RTT	Round Trip Time
SAP	Service Access Point
SBS	Small cell Base Station
SC	Small Cell
SCBS	Small Cell Base Station
SDE	Stochastic Differential Equation
SE	Spectral Efficiency
SFN	Single Frequency Network
SHARING	Self-Organized Heterogeneous Advanced Radio Networks Generation
SINR	Signal to Interference and Noise Ratio
SLA	Service-Level Agreement
SNR	Signal to Noise Ratio
SOCP	Second Order Cone Program
SON	Self Optimizing/Organizing Network
SVD	Singular Value Decomposition
TCP	Transmission Control Protocol
TDD	Time Division Duplex
TDM	Time Division Multiplexing
TTI	Transmission Time Interval
UE	User Equipment
UL	Uplink
VSC	Virtual Small Cell
WiFi	Wireless Fidelity
WP	Work Package
X2	Interface between eNodeBs